2008

New Insights into Molecular Mechanisms of Fludarabine

Alina D. Bulgar
Cleveland State University

NEW INSIGHTS INTO MOLECULAR MECHANISM OF FLUDARABINE

ALINA D. BULGAR

Pharm.D.

Victor Babes University of Medicine and Pharmacy Timisoara, Romania

September, 2002

Master of Science in Chemistry

Cleveland State University

May, 2006

submitted in partial fulfillment of requirements for the degree

DOCTOR OF PHILOSOPHY IN CLINICAL AND BIOANALYTICAL CHEMISTRY

at the

CLEVELAND STATE UNIVERSITY

December, 2008

This dissertation has been approved

for the Department of CHEMISTRY

and the College of Graduate Studies by

_____

Dissertation Committee Co-Chairperson, Dr. Yan Xu

Department of Chemistry, Cleveland State University

_____

Dissertation Committee Co-Chairperson, Dr. Stanton Gerson

Department of Hematology and Oncology, Case Comprehensive Cancer Center, Case Western Reserve University

_____

Dissertation Committee Member, Dr. Lili Liu

Department of Hematology and Oncology, Case Comprehensive Cancer Center, Case Western Reserve University

_____

Dissertation Committee Member, Dr. Lily Ng

Department of Chemistry, Cleveland State University

_____

Dissertation Committee Member, Dr. John Turner

Department of Chemistry, Cleveland State University

DEDICATION

This work is dedicated to my husband, Adrian and to my son, Marc.

NEW INSIGHTS INTO MOLECULAR MECHANISM OF FLUDARABINE

ALINA D. BULGAR

ABSTRACT

Nucleotide analogs (e.g. fludarabine) are antimetabolites used in the treatment of a wide variety of hematological malignancies and solid tumors. Upon being metabolized to their active triphosphate form, these agents are incorporated into DNA. Among other molecular targets, their incorporation may lead to activation of base excision repair (BER) pathway. The molecular mechanism of BER recognition and repair of the incorporated fludarabine has not yet been elucidated. The main focus of this research was to study the involvement of BER pathway in the response to fludarabine induced DNA damage. Also, the possibility of enhancing antineoplastic activity of fludarabine by inhibition of BER (e.g. methoxyamine) was investigated.

Firstly, capacity of uracil DNA glycosylase to recognize and excise incorporated fludarabine was established. Secondly, the formation of abasic (AP) sites after fludarabine treatment was confirmed in different human cancer cell lines. These results demonstrated that incorporated fludarabine, acting as an abnormal base in DNA, initiates BER.

The possibility to enhance fludarabine-induced damage by inhibiting BER was then considered. Exposure of cells to fludarabine and methoxyamine (MX) combined regimens caused increased apoptosis, clonogenic death, upregulation of some key BER

proteins, enhanced DNA strand breaks. It also enhanced anti-tumor effects in human xenografts. This response of cells to fludarabine plus MX was due to MX binding to the ara-AP sites formed by fludarabine, thus turning the repairable DNA damage into lethal lesions. In addition, mitochondrial DNA was found to be targeted by fludarabine and fludarabine plus MX. Apoptotic signaling from nuclear and mitochondrial DNA damage triggered mitochondrial mediated cell death during BER disruption by MX.

The modulation of fludarabine cytotoxicity by manipulating BER via MX was analyzed in a similar series of experiments using primary lymphocytes obtained from CLL patients. MX enhancement of activity of fludarabine was confirmed; the results showed that CLL cells were significantly more sensitive to the fludarabine in combination with MX as assayed by cytotoxicity, apoptosis, and levels of DNA damage.

Collectively, these results show that the combination of fludarabine plus MX represents a potential new clinical targeted therapy.

TABLE OF CONTENT

LIST OF TABLES

LIST OF FIGURES

CHAPTER I

INTRODUCTION: FLUDARABINE, BASE EXCISION REPAIR AND CELL DEATH MECHANISMS OVERVIEW

1.1. Fludarabine

1.1.1. Structure and development

The need of new therapeutic strategies in the treatment of leukemia and lymphoma led to development of the active agent, cytarabine (ara-C) and set the stage for development of other nucleoside analogues. Vidarabine (ara-A), an adenosine analog, was proven clinically ineffective due to rapid metabolic clearance by adenosine deaminase. This rapid inactivation of vidarabine by deamination suggested the need for structural modifications that will confer resistance to deamination while maintaining the antineoplastic potential. The addition of a fluorine substitute at the position 2 of adenine nucleoside renders resistance to deaminase. Montgomery and Hewson were the first ones to synthesize 9-β-D-arabinofuranosyl-2-fluoroadenine (F-ara-A) [1-3]. Because F-ara-A was relatively insoluble, its 5'-monophosphate (Fludarabine, Berlex Laboratories, Richmond, CA) had been used in clinical settings (Figure 1-1).

Figure 1-1.

Structures of Adenosine, Ara-adenosine and Fludarabine

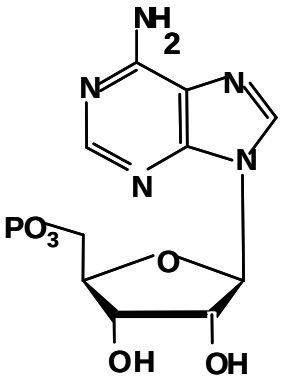

Adenosine

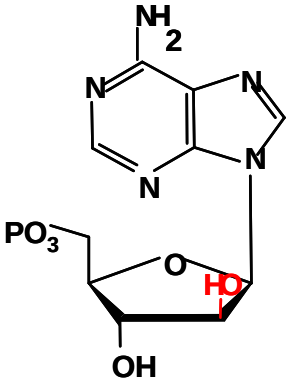

ara Adenosine

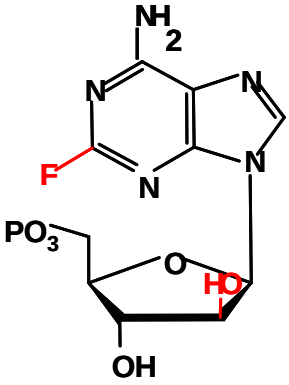

F-ara Adenosine
(Fludarabine)

The monophosphate formulation of fludarabine is rapidly and quantitative dephosphorylated to the nucleoside F-ara-A. This first pass metabolism is attributed to 5'-nucleosidase activities of erythrocytes and endothelial cells (Figure 1-2) [4]. F-ara-A is actively taken into cells by nucleoside transport systems (hENT, hCNT) [5]. Inside the cells, F-ara-A is rephosphorylated to monophosphate and subsequently to the diphosphate and triphosphate (Figure 1-2). It has been shown that deoxycytidine kinase is the major kinase for phosphorylation to the monophosphate [6], while adenylate kinase and nucleoside diphosphate kinase are the enzymes responsible for the subsequent phosphorylation steps. The triphosphate, F-ara-ATP is the main metabolite of fludarabine and the only known to have cytotoxic activity.

Figure 1-2

Transport and metabolism of Fludarabine

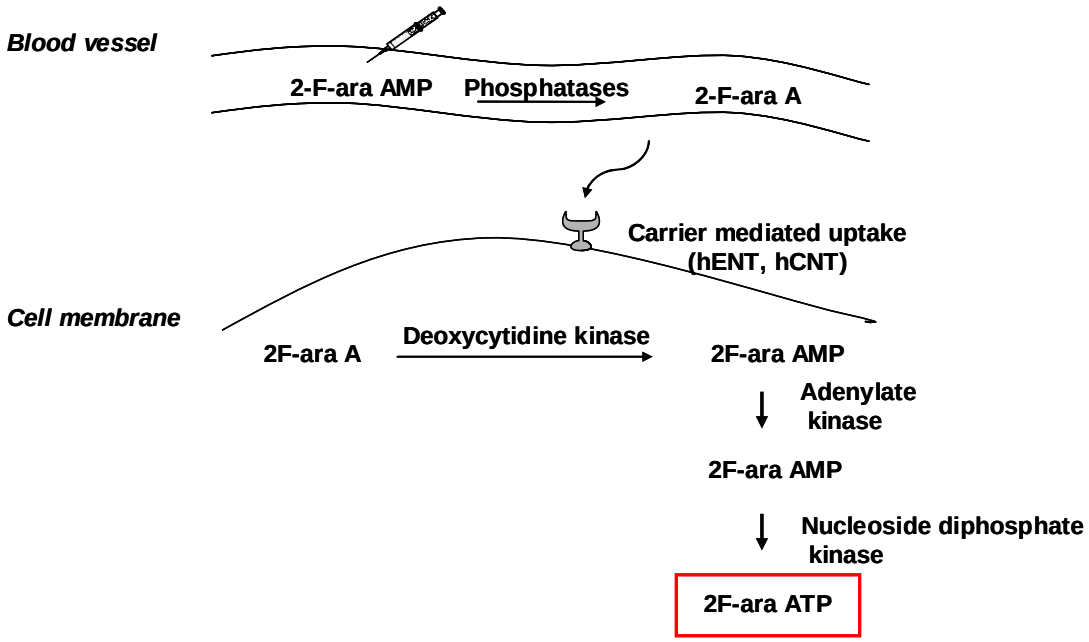
Blood vessel
2-F-ara AMP
Phosphatases
2-F-ara A
Carrier mediated uptake
(hENT, hCNT)
Cell membrane
2F-ara A
Deoxycytidine kinase
2F-ara AMP
Adenylate
kinase
2F-ara AMP
Nucleoside diphosphate
kinase
2F-ara ATP

1.1.2. Mechanisms of action

1.1.2.1. Target: DNA polymerase

The principal pharmacodynamic effect of fludarabine is inhibition of DNA synthesis, by targeting multiple enzymes at different steps in this process. The central component of the DNA synthesis machinery is the DNA polymerase. Early reports demonstrate that DNA polymerases are targets for the action of F-ara-ATP. F-ara-ATP does not directly inhibit the enzymes, but its inhibitory properties are achieved after incorporation into DNA [7]. The presence of a thymidylate in the template strand leads to incorporation of F-ara-ATP competitively with dATP. When one F-ara-A was incorporated into DNA strand , the DNA polymerases are inhibited or forced to pause at that specific site in the DNA strand. This inhibitory property makes fludarabine a chain terminator. Studies using cell-free systems have shown that significant percentage of F-ara-AMP was at the terminal position in DNA extracted from cells incubated with [^{3}H]F-ara-A [8]. Human DNA polymerase α, β, γ and ε are the main polymerases that are sensitive to inhibition by F-ara-ATP [9,10].

In addition, the stability of F-ara-AMP at the 3' end suggests that it is resistant to the proof-reading activities of DNA polymerases. DNA polymerase ε has been studied for its associated 3' to 5' exonuclease activities. DNA polymerase ε has a 35 fold greater affinity for F-ara-AMP-terminated DNA than for DNA terminated by deoxyadenosine monophosphate. Removal of F-ara-AMP was slow and the excision of the subsequent nucleotide was not observed. The velocity of the excision reactions was lower when compared with the rate of deoxyadenosine monophosphate [11]. Thus, the polymerization

and the proof reading activities associated with DNA polymerases are inhibited by the presence of F-ara-A in the DNA strand.

1.1.2.2. Target: Ribonucleotide reductase

Ribonucleotide reductase is the central and rate-limiting enzyme involved in the synthesis of deoxyribonucleotides, the building blocks for DNA synthesis. Incubation of cells with F-ara-A leads to reduction in cellular concentrations of deoxynucleotides and DNA synthesis concomitant with increase in F-ara-ATP levels [12-14]. Fludarabine is an allosteric inhibitor of ribonucleotide reductase resulting in reduction of the cellular concentrations of deoxycytidine triphosphate (dCTP), deoxyadenosine triphosphate (dATP) and deoxyguanosine triphosphate (dGTP) except for the concentrations of deoxythymidine triphosphate (dTTP). Incubation of purified ribonucleotide reductase with F-ara-ATP led to decreased enzymatic activity due to interaction with global allosteric inhibitory site of the enzyme [7,9].

F-ara-ATP competes with dATP for incorporation into DNA strand, thus reduction in dATP levels results in self-potentiation. Furthermore, fludarabine is also involved in a different metabolic self-potentiation mechanism involving deoxycitidine kinase. This enzyme is regulated by the levels of deoxynucleotides, mainly dCTP. Due to decrease in the dCTP levels, the activity of deoxycytidine kinase is enhanced that will result in increased phosphorylation rate of F-ara-A [15,16]. This is the rate limiting step in accumulation of the cytotoxic metabolite, F-ara-ATP.

1.1.2.3. Target: Inhibition of DNA primase

DNA replication is a fundamental process using different mechanism of synthesis for each DNA strand, involving separate set of enzymes. Replication of the leading strand

(5’ to 3’ direction) is a continuous process that uses either polymerase δ or ε. In contrast, the replication of the lagging strand (3’ to 5’ direction) occurs discontinuously by the sequential joining of the Okazaki fragments (200 nucleotides). Along the lagging strand's template, DNA primase builds RNA primers in short bursts. DNA polymerases α are then able to use the free 3' OH groups of the RNA primers to synthesize DNA in the 5'→3' direction. Once the Okazaki fragments are completed, the RNA fragments are then removed (different mechanisms are used in eukaryotes and prokaryotes). DNA ligase then joins the deoxyribonucleotides together, completing the synthesis of the lagging strand. It was previously reported that F-Ara-ATP inhibits the function of DNA primase. More specifically, F-ara-ATP is a better substrate for this enzyme that the natural substrate, adenosine triphosphate, leading to termination of RNA primer. Additonally, DNA polymerase α is unable to add deoxynucleotides to the RNA primers terminated by F-ara-AMP [17-19].

1.1.2.4. Target: Inhibition of DNA ligase I

DNA ligase I has a role in both replication and repair of DNA. DNA ligase I seal a single-stranded nick in a double-stranded DNA by catalyzing the formation of phosphodiester bond between the 3’-hydroxyl of one piece of DNA with the 5’-phosphate of an adjacent DNA. The enzymatic activity involves several steps. First, DNA ligase I interacts with ATP to form a ligase-AMP complex with the release of pyrophosphate. In the next step, nicked DNA interacts with the ligase-AMP complex to form a DNA-AMP complex in which AMP is linked to the 5’-terminus of the nick. In the third step, a phosphodiester bond is formed across the nick and AMP is released from the enzyme. Fludarabine inhibits this process at two steps. Firstly, F-ara-ATP interacts directly with

DNA ligase I to form a complex. This inhibition persisted even after removal of free F-ara-ATP from treated enzyme. Secondly, the enzymatic activity of the DNA ligase I was inhibited by the reaction with a DNA strand terminated in F-ara-AMP. The rate of the ligation, using this substrate was 10 % of that of normal DNA. This data indicate that the DNA strand with F-ara-AMP is a poor substrate for DNA ligase I [20].

1.1.2.5. Inhibition of RNA synthesis

Fludarabine is been shown to incorporate not only in DNA, but also in RNA, as a consequence is inhibitory to RNA synthesis. The inhibition of RNA synthesis is dependent on concentration of F-ara-ATP [21]. RNA synthesis is enzymatically achieved by RNA polymerase I, II and III. Incubation of human lymphoblast with fludarabine resulted in incorporation of F-ara-A preferentially into poly (A+) RNA fraction. This incorporation into RNA resulted in premature termination of RNA transcript and subsequently impaired the protein synthesis.

1.1.3. Fludarabine in CLL: rationale for combination therapies

Fludarabine monotherapy is an established regimen for treatment of chronic lymphocytic leukemia (CLL) achieving superior remission rate compared with older treatment regimens containing alkylating agents or corticosteroid [22,23]. CLL is the most common hematological malignancy in western world. CLL arises from a malignant clone of B cells with a characteristic phenotype. The disease encompasses a diversity of clinical symptoms which translate into variable prognosis and survival. Complete response rates with fludarabine as single agents are 15-20 % in previously treated patients and 40-50 % in newly diagnosed ones. However, this response rates are low and usually transient, with all patients eventually experience a relapse [24,25]. Because fludarabine is

not curative when used as monotherapy, efforts are made to improve fludarabine efficacy by establishing a rational basis for combination with other drugs. Both biochemical and biological modulation have been studied. Biochemical modulation of cytarabine metabolism by fludarabine through up-regulation of deoxycytidine kinase activity led to promising results [26]. In addition, by biological modulation, the remission rate of patients treated with combined therapy, fludarabine plus granulocyte colony stimulating factor (G-CSF), was greater (63 %) than therapy with fludarabine alone (41 %) [27]. Several other combined regimens were extensively studied.

1.1.3.1. Combinations with DNA-damaging agents

The overall concept of combining DNA damaging agents with fludarabine relays on the hypothesis that fludarabine inhibits the nucleotide excision repair process (NER) induced by the damaging agents and thus enhances the cytotoxicity of these compounds.

Cyclophosphamide. Combination of fludarabine with cyclophosphamide has been examined in 10 clinical trials. For example, in a phase III comparative trial, 207 treatment-naive patients with advanced CLL were treated with either fludarabine or in combination with cyclophosphamide. The combination regimens resulted in significantly higher overall response (OR) (94 versus 85 % with fludarabine alone) and complete response (CR) (21 versus 9 % respectively) [28]. The main disadvantage associated with this combination was the myelosuppression (neutropenia, thrombocytopenia and anemia).

Chlorambucil. Fludarabine plus chlorambucil was evaluated in four clinical trials, two phase I/II trials and two large phase III trials. Collectively, the results from these studies suggest that the combination does not produce a significant improvement in response rate

or survival compared with fludarabine alone. Furthermore, the combined regimen was associated with severe adverse effects [29,30].

Cyclophosphamide and mitoxantrone. The combination of fludarabine with cyclophosphamide and mitoxantrone was assed in one clinical trial. The OR was 78 %, including 50 % CR and 28 % PR, but the incidences of myelosuppression and infection were significantly higher.

Prednisone. Two studies of CLL patients were used to evaluate the efficacy of fludarabine plus prednisone. The results show that the combination resulted in an OR of 80 %, no significant different from fludarabine alone (80 %). CR rate for fludarabine plus prednisone was 23 %, significantly lower than for fludarabine alone (38 %). Together, these results showed that fludarabine plus prednisone is no more effective than fludarabine alone [31].

Other chemotherapeutic agents. Seven trials have investigated fludarabine in combination with six other chemotherapeutic agents. Fludarabine plus mitoxantrone did not markedly increase the response rate compared to fludarabine alone (OR was 77 % and CR was 20 %) [32]. Fludarabine plus doxorubicin demonstrated no therapeutic benefits and increased rates of opportunistic infections [33]. In contrary, a higher response rate was achieved in a phase II study with fludarabine and epirubicin. (OR of 92 % and CR of 40 %). Also, adverse effects associated with this combined treatments were relatively mild. These results were also confirmed in a phase III randomized trial (OR of 89% and CR of 26 %) [34]. There are three other fludarabine combination regimens which have proved to be less effective than monotherapy with fludarabine: cytarabine, cisplatin and dexamethasone [35-37].

Collectively, these studies demonstrated that when fludarabine is given as a component of combination therapies, clinical relevant effects are sometimes observed, but also show that there is a need for further, more effective combinatory regimens.

1.2. Base excision repair pathway

1.2.1. Overview

Base excision repair is the major system responsible for removal of damaged DNA bases and repair of DNA single strand breaks generated spontaneously or induced by exogenous DNA damaging factors such as ionizing radiation and alkylating agents [38]. In brief, BER involves: (i) damaged base excision, (ii) incision at the resulting abasic (AP) site, (iii) replacement of missing nucleotide, and (iv) sealing of the resulting nick. Excision repair of the damaged base is initiated by a specific DNA glycosylase, the enzyme responsible for the recognition and removal of damaged base by hydrolyzing the glycosylic bond (the bound linking the base residue to the DNA sugar phosphate backbone). Further, the AP site is recognize by AP endonuclease (APE) that will cleave the phosphodiester bond 5' to the AP site generating an single strand break containing a 5'-sugar phosphate. Several proteins are involved in processing of the modified 3'and 5'-ends: DNA polymerase β (pol β), polynucleotide kinase (PNK), APE and aprataxin. After restoring conventional 3'-hydroxyl and 5'-phosphate strand breaks ends, repair is accomplished by either short or long -patch pathway. In the major BER pathway, short-patch repair, pol β adds one nucleotide to the 3'-OH end of the strand break, thus filling one nucleotide gap created during repair. The DNA ligase IIIα-XRCC1 heterodimer seals the DNA end and completes the repair process (Figure 1-3) [39,40]. The minor BER

pathway, long-patch acts to repair AP sites that have the sugar residue modified, e.g. oxidized or reduced [41]. To initiate this pathway, pol β first adds one nucleotide to the 3' end of the nick and than pol δ and ε add a few more nucleotides to generate part of a single-stranded flap structure containing a 5' sugar phosphate. This flap structure is recognized and excised by flap endonuclease 1 (FEN1) and the DNA is finally ligated by DNA ligase I. FEN1 activity is stimulated by proliferating cell nuclear antigen (PCNA) [42]. Alternately, the repair process can be catalyzed by pol δ plus PCNA [41].

Figure 1-3

The base excision repair pathway [39]

The proteins believed to be responsible for various reaction steps are shown. The detailed mechanism is described in text. Short-patch BER is responsible for a single nucleotide repair, whereas in long-patch BER, two to ten nucleotides are replaced.

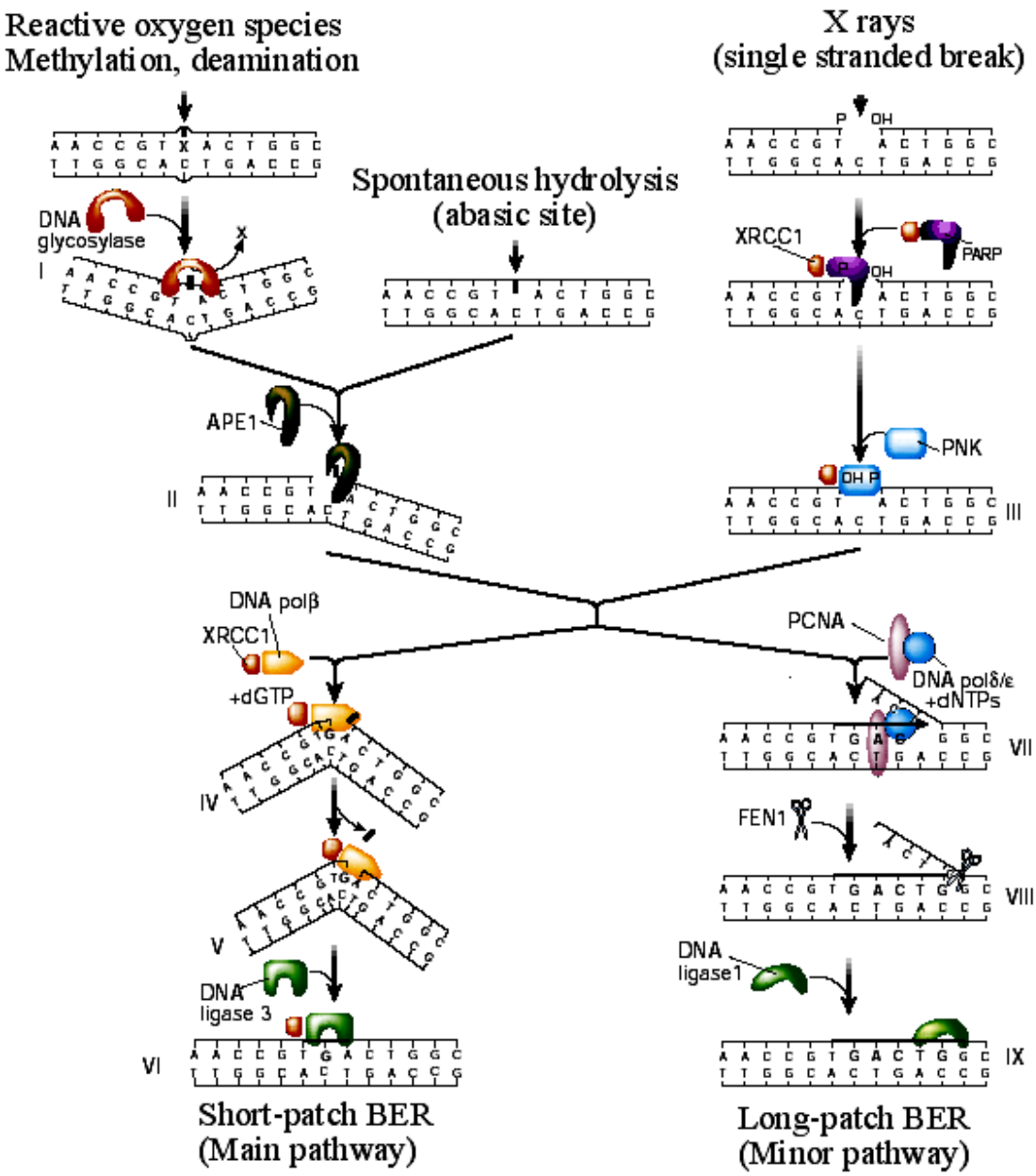
Reactive oxygen species
Methylation, deamination
X rays
(single stranded break)
Spontaneous hydrolysis
(abasic site)
DNA
glycosylase
APE1
XRCC1
PARP
PNK
DNA polβ
XRCC1
+dGTP
PCNA
DNA polδ/ε
+dNTPs
FEN1
DNA
ligase 3
DNA
ligase1
I
II
III
IV
V
VI
VII
VIII
IX
Short-patch BER
(Main pathway)
Long-patch BER
(Minor pathway)

Base excision repair proteins:

DNA glycosylases. DNA glycosylases are responsible for initiating BER by catalyzing hydrolysis of the C1'-N glycosylic bond to the damaged base and by removing the base, generating an AP site. Ten glycosylases have been identified to have a role in mammalian BER and their specificities are summarized in Tabel 1-I. DNA glycosylases can be divided in two classes based on their mechanistic activity: mono-functional (i.e. glycosylase activity only) such as UDG and bi-functional (i.e. glycosylase and β-lyase activities) such as hOGG1 [43].

TABLE 1-I. Mammalian DNA Glycosylases and their substrates

Glycosylases	Bifunctional ?	Substrates
UNG2	No	U, 5FU.
Smug1	No	U, OHMeU
TDG	No	U:G, T:G, ethenoC
MBD4	No	U:G, T:G in CpG sites
OGG1	Yes	8oxoG:C, FapyA, FapyG
MYH	No	A:8oxoG
NTH1	Yes	Oxidised and fragmented pyrimidines (e.g. Tg, DHU) Fapy
AAG (MPG)	No	3-meA, 7-meG, ethenoA, ethenoG, hypoxanthine
NEIL 1	Yes	FapyA, FapyG, dihydrouracil, thymine glycol, 8-oxoG (low)
NEIl2	Yes	cytosine oxidation products (5-OHU, DHU)

The crystal structures of many of the DNA glycosylases have been elucidated. They show some similarities which suggests a common mode of action. The glycosylases gently pinch the DNA while scanning it resulting in bending of DNA at the site of instability caused by mismatching. This DNA bending combined with pushing from the enzyme makes mismatch base to flip out of the DNA and to enter the binding site of the enzyme. While in the binding site, the base bond to the sugar is cleaved by the enzyme. In Figure 1-4 is presented the enzymatic mechanism of UDG [44].

Figure 1-4

Proposed mechanism for UDG cleavage of N-glycosyl bond [44]

The uracil base dissociates leading to an oxocarbenium cation intermediate (1 → 2). Subsequent attack by water produces an apurinic/apyrimidinic (AP) site (2 → 3).

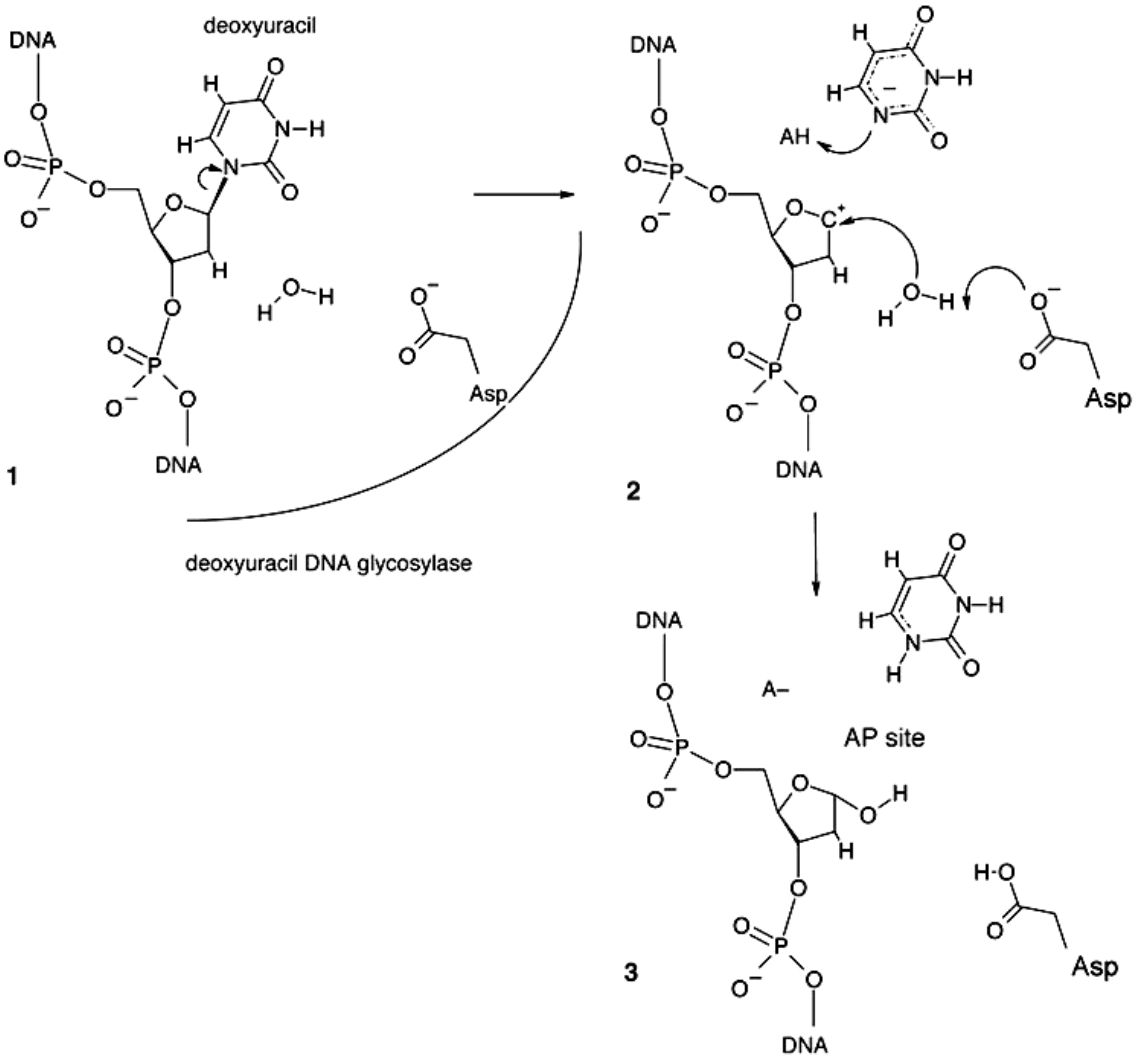
DNA
deoxyuracil
1
deoxyuracil DNA glycosylase
AH
2
Asp
A–
AP site
3

AP endonucleases. An important step in BER pathway involves the cleavage of the AP site by APE. APE is a multifunctional enzyme that is not involved only in BER, but also functions as a reduction-oxidation factor to maintain transcription factors in an active state. Extensive studies showed that mice nullzygous for APE gene are embryonic lethal [45] and downregulation of APE levels in human cells using RNAi leads to accumulation of AP sites, inhibiting DNA replication and generating apoptosis [46]. APE cleaves the phosphodiester bonds in an Mg^{2+}-dependent manner, leaving a 3'-hydroxyl group and a 5'-deoxyribose phosphate (dRP) group flanking the nucleotide gap.

BER DNA polymerases. The presence of an intermediate containing a 3'-hydroxyl group acts as a substrate for DNA polymerase. In the short-patch BER pathway, DNA synthesis is carried out by pol β [47,48]. Pol β contains two domains: a C-terminal polymerase domain and an N-terminal dRP domain. Both domains are required for short-patch BER. Processing of the single-strand breaks resulted by dRP lyase activity of pol β is carried out through catalysis of a β-elimination reaction. This reaction is followed by a polymerase activity to fill the nucleotide missing [49]. Pol β lacks any intrinsic proof-reading activities. Pol β is ubiquitinously express in all tissues. It is also expressed constitutively and without demonstrable cell-cycle dependence. The importance of this enzyme for the cells was demonstrated using studies in mice. They showed that mice nullizygous for pol β are non-viable and die early in embryogenesis [50].

DNA ligases. DNA ligase I and DNA ligase III are the main ligases involved in BER. DNA ligase III exists as two isoforms: DNA ligase IIIα and DNA ligase IIIβ [51]. The enzymatic activity of DNA ligase IIIα is dependent on interaction with XRCC1. DNA ligase I is involved in long-patch BER pathway, but also plays a role in DNA replication

[51]. Human cells containing DNA ligase I show hypersensitivity to DNA-damaging agents [52].

XRCC1. XRCC1 is a multi-domain protein with an N-terminal DNA binding domain and two BRCT (BRCA1 C-terminus) motifs. BRCT I contains the site of interaction with PARP1 and BRCT II is involved in interaction with DNA ligase IIIα [53]. The nick-binding N-terminal domain of XRCC1 interacts with pol β, forming a tertiary complex with the polymerase and nicked DNA. Cells deficient in XRCC1 show partial defect in BER efficiency when compared to wild type. The importance of the XRCC1 gene for cellular functioning is underlined by the fact its targeted knockout results in embryonic lethality [54]. XRCC1 interacts also with PARP1, APE and PCNA.

Poly(ADP-ribose)polymerase, Polynucleotide kinase, Aprataxin. The role of PARP1 in BER is to bind to incised AP sites before any other repair proteins. In vitro repair reactions carried out on absence of PARP1 result in increased nucleolytic degradation of BER intermediates, thus it suggests that PARP1 functions to protect strand breaks and repair intermediates from degradation or recombination [55]. Additionally, it has been reported that the genome of PARP1 null mice shows an increased incidence of deletion mutations upon DNA damage.

Polynucleotide kinase (PNK) in an enzyme involved in the processing of 5'-phosphate and 3'-hydroxyl ends at single strand breaks. As part of the repair pathway, PNK interacts with XRCC1, DNA ligase IIIα and pol β [56].

Aprataxin is a member of the HIT superfamily of nucleotide hydrolases/transferases. Aprataxin interacts with XRCC1 and it is involved in the resolution of abortive DNA

ligation intermediates by catalyzing the release of adenylate groups covalently linked to 5'-phosphate termini at single strand nicks [57].

1.2.2. Targeting BER to overcome drug resistance

Most chemotherapeutic agents cause cell death by damaging DNA. Some of this agents, initially effective, develop resistance through repair capacities of the cancer cells. Various preclinical studies suggest that BER represents an important target for anticancer therapy as its inhibition has been shown to sensitizes cells to cytotoxic effects of different alkylating agents. Several approaches have been developed. One direction was focused on inhibiting BER by targeting APE. Up to date, two chemical compounds were isolated (CRT0044876 and lucanthone) and shown to have APE inhibitory characteristics. By combining these compounds with alkylating agents or methylating agents, significant increase in cytotoxic activity against ovarian cancer cells has been measured [58,59]. A second direction was focused on PARP1 inhibition. Even though the role of PARP1 in BER is not fully understood, inhibition of PARP1 leads to inhibition of DNA repair and promotes apoptosis in cancer cells. Currently, several PARP1 inhibitors are evaluated in clinical trials in combination with certain anticancers agents (Tabel 1-II). One example of this combined therapy is TMZ plus PARP1 inhibitor. It has been shown that when PARP1 is inhibited, it remains bound to the SSB created by TMZ which triggers apoptosis [60]. PAPR1 inhibitors enhance the cytotoxicity of DNA topoisomerase I inhibitors, irinotecan and topotecan. They also enhance the cytotoxic effect of radiotherapy, both *in vitro* and *in vivo* [61]. Several other combination strategies for PARP1 inhibitors are under investigation.

TABLE 1-II. PARP inhibitors currently in clinical trials

PARP inhibitor	Phase of trial	Subject group
AG-014699	I, II	Patients with malignant melanoma
KU 59436	I	Patients with advanced solid tumors
INO-1001	IB	Patients with advanced solid tumors
INO-1001	I	Patients with glioblastoma multiforme
BSI-201	I	Patients with advanced solid tumors
GPI 21016	I	Patients with advanced solid tumors
ABT-888	Pilot study	Patients with advanced solid tumors and lymphoid malignacies

A more promising strategy to enhance cytotoxic effect of chemotherapeutic agents by targeting BER is the use of a small molecule, methoxyamine (MX) and its derivatives.

1.3. Methoxyamine

1.3.1. Mechanism of action

Methoxyamine (MX) has been extensively studied as an inhibitor of BER. The action of MX in inhibiting BER has been demonstrated (Figure 1-5): (a) MX binds to the aldehyde group of the tautomeric open ring form of deoxyribose generated after removal of the abnormal base by DNA glycosylase; (b) the reaction of MX with AP sites is faster than APE reaction with the same site; (c) MX-bound AP sites reduce the APE cleavage of the DNA backbone by more than 300-fold compared with the cleavage of the normal AP site [62-65]. Chemotherapeutic agents such as temozolomide (TMZ) and 1,3-bis-(2-chloroethyl)1-nitrosurea (BCNU) form AP sites due to removal of the drug-induced

methylated purine by DNA glycosylase. BCNU alkylates DNA predominantly (>90 %) at N^7 position of guanine. Repair of these lesions involves formammidopyrimidine-DNA glycosylase (FPG) and 8-oxoguanine-DNA glycosylase (OGG1). Temozolomide treatments result in methylation of N^7 position of guanine (70 %) and of N^3 position of adenine (4 %). These lesions are removed from DNA by methylpurine glycosylase (MPG) leading to formation of AP sites. Blocking the repair of these AP sites with MX leads to accumulation of these cytotoxic sites (MX-bound AP-sites) in DNA [65]. MX has been shown to augment the cytotoxicity of several DNA damaging agents *in vitro* and also in xenograft studies [66,67]. MX is able to potentiate cytotoxicity in both MMR-proficient and MMR-deficient cells [60]. MX is also able to overcome other resistance factors such as the loss of p53 tumor suppressor function [65]. An example of effective enhancement of cytotoxicity by MX is the combination with TMZ. This combined treatment regimen was extensively studied *in vitro* and *in vivo*. In vivo, MX enhanced antitumor effect of TMZ in several colon cancer cell lines that was associated with significant apoptotic cell death and severe chromosomal aberrations (sister chromatin exchange, DNA breakage and aneuploidity) [66]. *In vitro*, MX binds to the AP sites formed by TMZ treatments to form MX-bound AP-sites. These sites cannot be repaired by APE leading to apoptotic cell death. One molecular mechanism of cell death mediated by MX-bound AP-MX is conversion of topoisomerase II into biotoxin, resulting in enzyme-mediated DNA scission and cell death. [68]. MX was also shown to enhance cytotoxicity of 5-iodo-2'deoxyuridine (IdUrd), a halogenated thymidine analog. [69]. Such results led to BER modulation to augment clinical response of cytotoxic agents

currently used in the clinic. A Phase I clinical trial of MX in combination with TMZ is currently in progress.

Figure 1-5

Methoxyamine binds to the AP site and blocks APE cleavage [65]

Methoxyamine reacts with the aldehyde moiety of the open-ring form of the AP site generated after removal of the damaged base by a DNA glycosylase. The MX-bound AP sites formed are refractory to cleavage by APE.

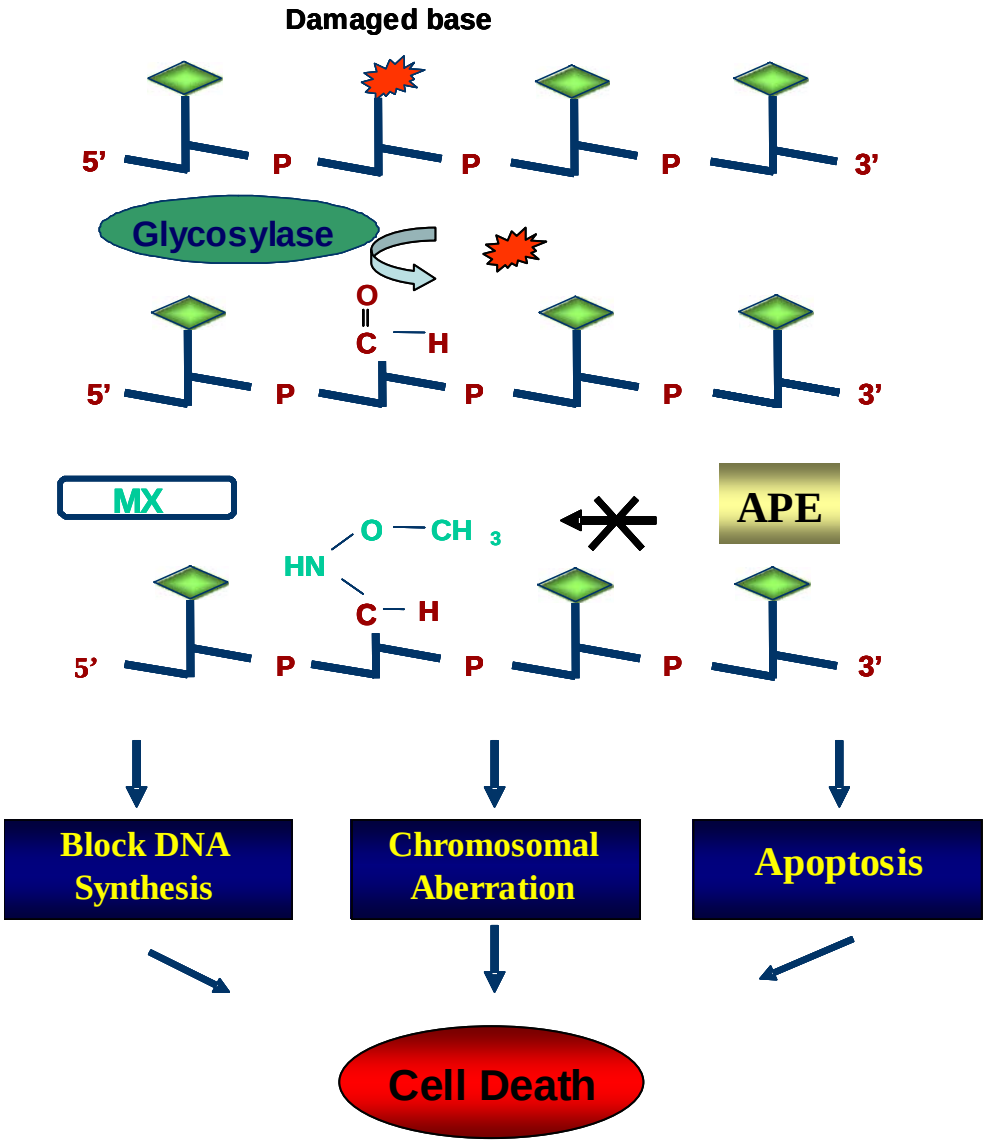
Damaged base
5'
P
P
P
3'
Glycosylase
O
C
H
MX
O
CH 3
HN
C
H
APE
Block DNA Synthesis
Chromosomal Aberration
Apoptosis
Cell Death

1.4. Apoptotic cell death pathways

Apoptosis is in general characterized by distinct features and energy-dependent biochemical mechanisms. Apoptosis is considered a vital component of normal cell turnover, proper development and function of immune system, hormone-dependent atrophy, embryonic development and chemical-induced cell death. The ability to modulate the death of a cell it is recognized for its tremendous therapeutic potential. To date, numerous studies have shown that there are two main apoptotic pathways: the extrinsic or death receptor pathway and the intrinsic or mitochondrial pathway. These pathways converge on the same terminal, execution pathway [70].

1.4.1. Extrinsic (death receptor) pathway

The extrinsic pathway is characterized by transmembrane-receptor-mediated interactions. The key players are the death receptors that are members of the tumor necrosis factor (TNF) receptor gene superfamily. All members share a similar cytoplasmatic domain called the "death domain" which plays an important role in transferring the death signaling from the surface to intracellular signaling. Several ligands and corresponding death receptors have been studied: FasL/FasR, TNFα/TNFR1, Apo3L/DR, Apo2L/DR4 and Apo2L/DR5 [71,72]. Upon ligand binding, cytoplasmatic adaptor proteins are recruited and will bind the receptor. These adaptor proteins will associate with procaspase-8 through dimerization of the death effector domain. Following this association, death-inducing signaling complex (DISC) is formed, resulting in auto-catalytic activation of procaspase-8 [73]. Once caspase 8 is activated, the execution phase of apoptosis is triggered (Figure 1-6).

Figure 1-6

The extrinsic apoptotic pathway [74]

The extrinsic pathway begins outside the cell through the activation of specific pro-apoptotic receptors on the cell surface by specific molecules known as pro-apoptotic ligands. The intracellular domains of these receptors, known as the 'death domains', bind to the adaptor protein Fas-associated death domain (FADD), leading to the assembly of the death-inducing signaling complex, or DISC, and recruitment and assembly of initiator caspases 8 and 10. Caspases 8 and 10 are stimulated and undergo self processing, releasing active enzyme molecules into the cytosol, where they activate caspases 3, 6, and 7, thereby converging on the intrinsic pathway.

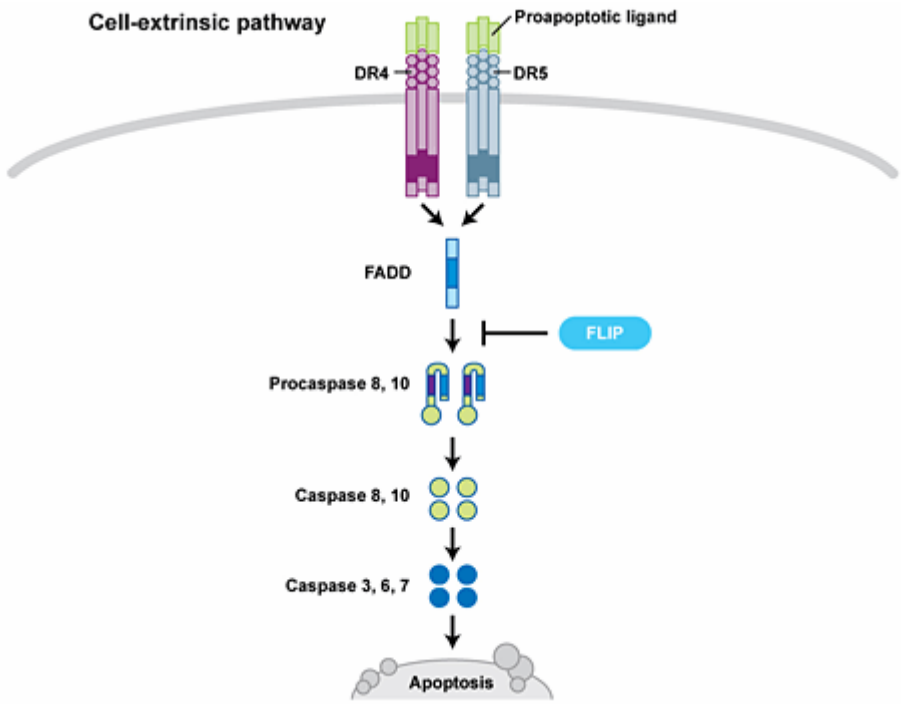
Cell-extrinsic pathway
Proapoptotic ligand
DR4
DR5
FADD
FLIP
Procaspase 8, 10
Caspase 8, 10
Caspase 3, 6, 7
Apoptosis

1.4.2. Intrinsic (mitochondrial) pathway

The intrinsic signaling pathway involves a variety of stimuli that result in intracellular signals that act directly on targets within the cell and are mitochondrial-initiated events. These stimuli cause changes in the inner mitochondrial membrane that will lead to opening of the mitochondrial permeability transition (MPT) pore, loss of the mitochondrial transmembrane potential and release of the two groups of sequestered pro-apoptotic proteins from the intermembrane space to the cytosol [75]. The first group contains cytochrome C, Smac/Diablo and a serine protease Htr2/Omi. Cytochrome c binds and activates Apaf-1 and procaspase-9, forming a complex called "apoptosome" (Figure 1-7) [76]. This complex formation leads to caspase-9 activation. Additionally, Smac/Diablo and Htr2/Omi promote apoptosis by inhibiting IAP (inhibitors of apoptosis proteins). The second group of pro-apoptotic proteins, AIF, endonuclease G and Caspase-activated DNase (CAD), are release late from mitochondria, after the cell has committed to die. AIF translocated to nucleus and cause DNA fragmentation into 50-300 kb pieces and condensation of peripheral nuclear chromatin, known as stage I condensation [77]. Endonuclease G translocates to nucleus as well where it cleaves nuclear chromatin to produce oligonucleosomal DNA fragments [78]. CAD translocates to nucleus where leads to DNA fragmentation and a more advanced chromatin condensation. The control and regulation of these mitochondrial events occurs through members of Bcl-2 family proteins. These proteins can be either pro-apoptotic or antiapoptotic. To date, 25 genes have been identified. The antiapoptotic proteins include Bcl-2, Bcl-xl, BAG, Bcl-xs. The pro-apoptotic proteins include Bcl-10, Bax, Bad, Bim, Bik [79].

Figure 1-7

The intrinsic (mitochondrial) apoptotic pathway [74]

The intrinsic pathway is initiated from within the cell. This is usually in response to cellular signals resulting from DNA damage. This pathway involves release from the mitochondria of pro-apoptotic proteins that activate caspase enzymes, which ultimately trigger apoptosis.

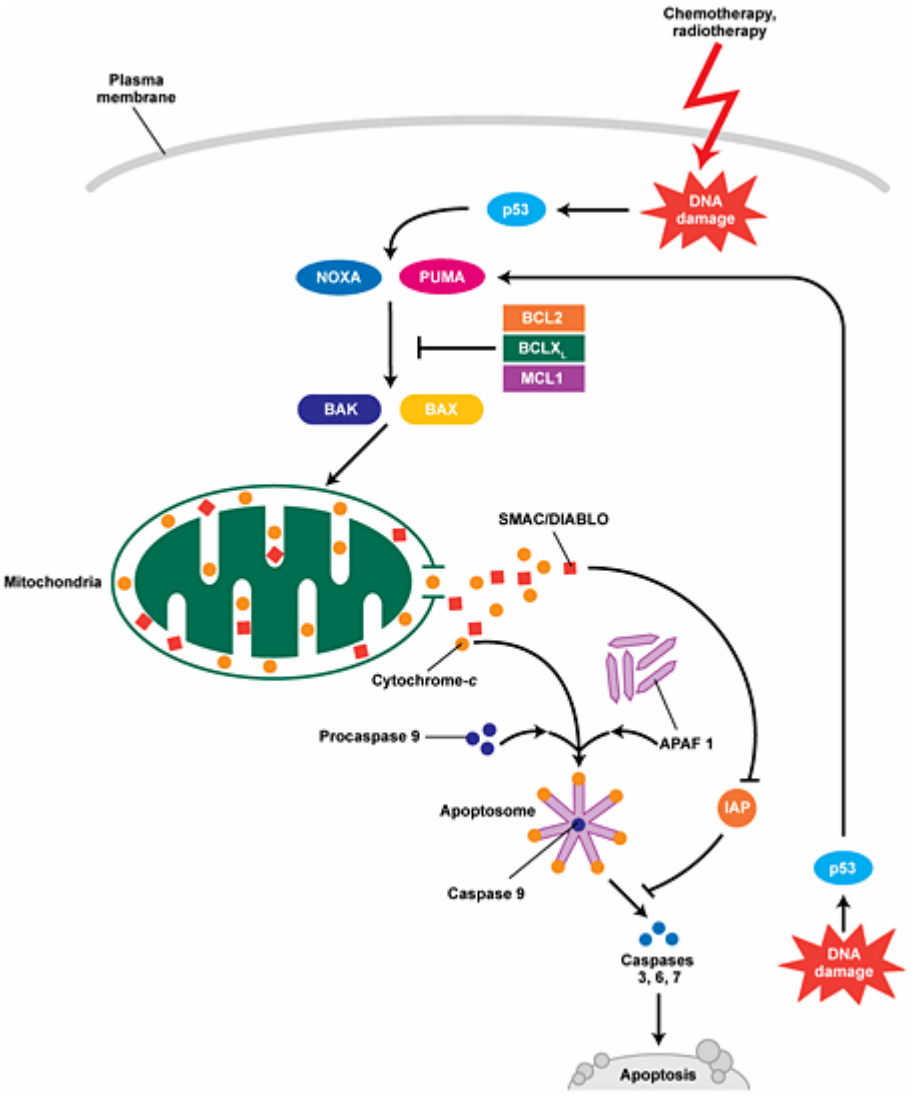
Chemotherapy, radiotherapy
Plasma membrane
p53
DNA damage
NOXA
PUMA
BCL2
BCLXL
MCL1
BAK
BAX
Mitochondria
SMAC/DIABLO
Cytochrome-c
Procaspase 9
APAF 1
Apoptosome
IAP
Caspase 9
Caspases 3, 6, 7
Apoptosis
p53
DNA damage

The intrinsic and extrinsic pathways converge to execution phase. This phase is represented by the activation of execution caspases. Execution caspases activate cyoplasmic endonuclease which degrades nuclear material, and protease that degrade the nuclear and cytoskeletal proteins. Executioner caspases are: caspase-3, caspase-6 and caspase-7. These caspases cleave various substrates such as PARP, cytokeratins, the plasma membrane cytoskeletal protein alpha fodrin, and other, that cause the morphological and biochemical changes in apoptotic cells [80].

1.4.2.1. Mitochondrial DNA damage

Mitochondrial DNA (mtDNA) is a circular double-stranded genome, consists of 15,000-17,000 base pairs (bp) that codes for 13 subunits of the oxidative phosphorylation system, 2 ribosomal RNAs (rRNAs), and 22 transfer RNAs (tRNAs) (Figure 1-8) [81]. It is present in 100-10,000 copies per cells. MtDNA consists of predominantly of coding DNA with exception of an 1100 bp long region that has mainly regulatory functions. The DNA polymerase gamma (pol γ) is used for the replication of mtDNA. The replication is in a D-loop mode due to different origins of replication on the two strands. One strand begins to replicate first, displacing the other strand. This process continues until replication reaches the origin of replication of the other strand, at which point the other strand begins to replicate in the opposite direction.

Figure 1-8

Mitochondrial DNA [81]

Human mtDNA encodes 13 polypeptides: 7 subunits - ND1, ND2, ND3, ND4, ND4L, ND5, and ND6 - of Complex I (NADH-Coenzyme Q oxidoreductase); 1 subunit - cytochrome b - of Complex III (CoQ-cytochrome c oxidoreductase), 3 subunits - COX I, COX II, and COX III - of Complex IV (cytochrome c oxidase, or COX), and 2 subunits - ATPase 6 and ATPase 8 - of Complex V (ATP synthase). It also encodes 2 rRNAs (in green) and 22 tRNAs (in blue).

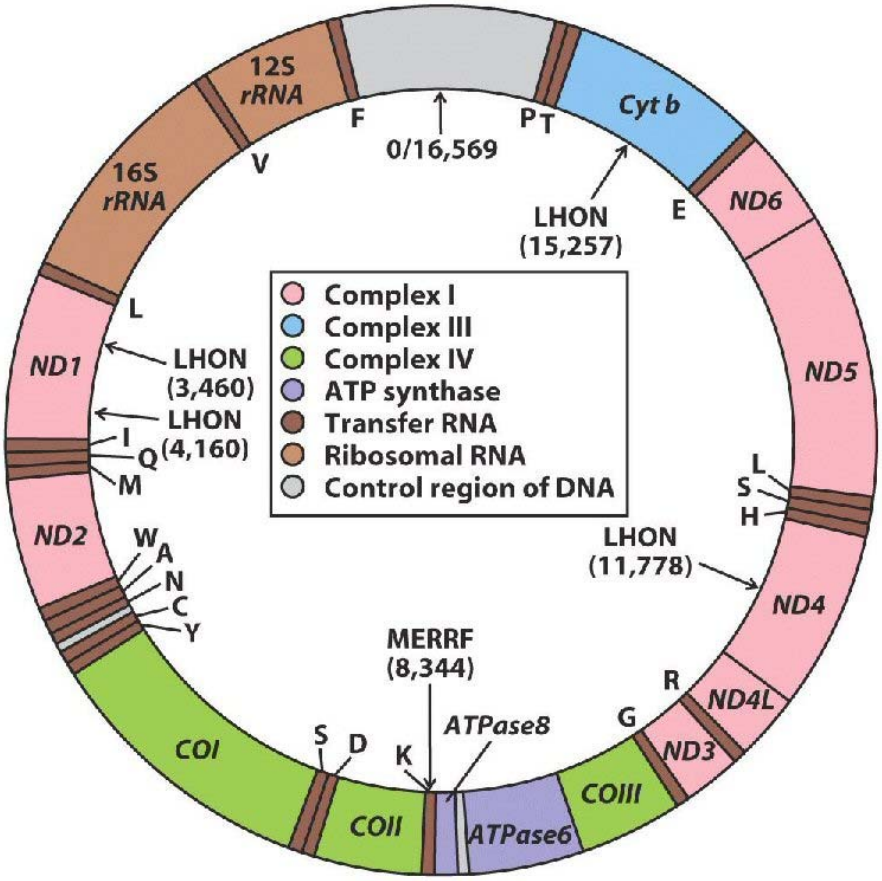
12S rRNA
16S rRNA
F
V
0/16,569
PT
Cyt b
ND6
E
LHON (15,257)
L
ND1
LHON (3,460)
LHON (4,160)
I
Q
M
ND2
W
A
N
C
Y
Complex I
Complex III
Complex IV
ATP synthase
Transfer RNA
Ribosomal RNA
Control region of DNA
ND5
L
S
H
LHON (11,778)
ND4
R
ND4L
G
ND3
COIII
ATPase6
ATPase8
MERRF (8,344)
K
S
D
COI
COII

Mitochondrial DNA transcription involves mtRNA polymerase, mitochondrial transcription factor A and mitochondrial transcription factors B1 and B2. The proteins assemble at the mitochondrial promoters and begin transcription. MtDNA has three promoters, H1, H2 and L (heavy strand 1, heavy strand 2 and light strand promoters. The H1 promoter transcribes the entire heavy strand, the L promoter transcribes the entire light strand, while H2 promoter causes transcription of the two mitochondrial rRNAs.

MtDNA is very susceptible to damage from various sources such as free radicals and chemotherapeutic agents which will lead to deletions, rearrangements, other mutations or activation of apoptosis. Recent evidence suggests that mitochondria contain DNA repair mechanisms. There is evidence for base excision repair (BER), direct damage reversal, mismatch repair, and recombinational repair mechanisms in mitochondria, while nucleotide excision repair (NER), as we know it from nuclear repair, is not present [82].

1.4.2.2. Mitochondrial DNA base excision repair pathway

A simplified BER in mitochondria has been established but has not been extensively characterized. Several BER enzymes such as uracil DNA glycosylase [83] and AP endonuclease [84] have been detected in mitochondria (Figure 1-9). The replication polymerase in mitochondria is γ (pol γ), and it has been demonstrated that purified pol γ can also serve as a repair polymerase in mitochondria [85-87]. The ligase involved in mitochondrial BER is believed to be an alternate splice variant of nuclear DNA ligase III [84]. The pathway includes four distinct steps: lesion removal by a glycosylase, abasic site processing by an AP endonuclease, insertion of a new nucleotide by polymerase γ and ligation of the broken strand by DNA ligase.

Figure 1-9

The short-patch mitochondrial BER [87]

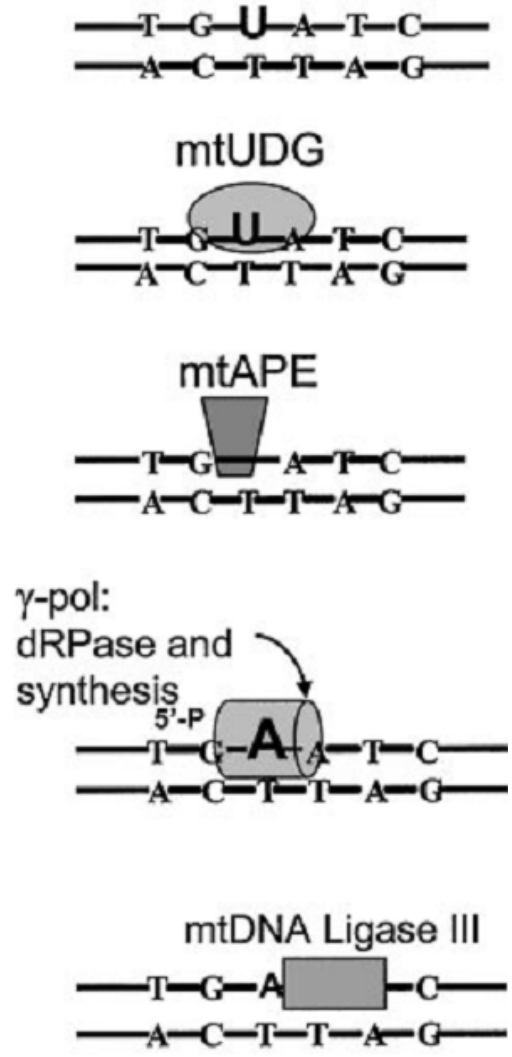
T G U A T C
A C T T A G
mtUDG
mtAPE
γ-pol:
dRPase and
synthesis
5'-P
mtDNA Ligase III

1.5. References

1. Montgomery JA, Hewson K. Synthesis of potential anticancer agents X: 2-fluoroadenine. J Am Chem Soc; 79: 4559-63, 1957.

2. Frederickson S. Specificity of adenosine deaminase toward adenosine and 2'-deoxyadenosine analogues. Arch Biochem Biophys, 113: 383-9, 1966

3. Skipper HE, Montgomery JA, Thompson JR, et al. Structure-activity relationship and cross-resistance observed on evaluation of a series of purine analogs against experimental neoplasm. Cancer Res, 19: 425- 37, 1959.

4. Danhauser L, Plunkett W, Keating M, et al. 9-β-D-Arabinofuranosyl-2-fluoroadenine 5'monophospahte pharmacokinetics in plasma and tumor cells of patients with relapsed leukemia and lymphoma, Cancer Chemother Pharmacol, 18: 145-52, 1996.

5. Barrueco JR, Jacobsen DM, Chang CH, et al. Proposed mechanism of therapeutic selectivity of the 9-β-D-Arabinofuranosyl-2-fluoroadenine against murine leukemia based upon lower capacities for transport and phosphorylation in proliferative intestinal epithelium compared to tumor cells. Cancer Res, 47: 700-6, 1987.

6. Carson DA, Wasson DB, Kaye J, et al. Deoxycytidine kinase-mediated toxicity of deoxyadenosine analogs toward human lymphoblasts in vitro and toward human lymphoblast in vitro and toward murine L1210 leukemia in vivo. Proc Natl Acad Sci USA, 77: 6865-9, 1980.

7. Parker WB, Bapat AR, Sgen J-X, et al. Interaction of 2-halogenated dATP analogs (F, Cl, and Br) with human DNA polymerases, DNA primases, and ribonucleotide reductase. Mol Pharmacolog 34: 485-491, 1988.

8. Huang P, Chubb S, Plunkett W. Termination of DNA synthesis by 9-β-D-arabinofuranosyl-2-fluoroadenine: A mechanism for cytotoxicity. J Biol Chem. 265: 16617-166625, 1990.

9. Tseng WC, Derse D, Cheng YC, et al. In vivo activity of 9-β-D-arabinofuranosyl-2-fluoroadenine and the biochemical actions of its triphosphate on DNA polymerase and ribonucleotide reductase from HeLa cells. Mol Pharmacol. 21: 474-7, 1982.

10. Gandhi V, Huang P, Chapman A et al. Incorporation of fludarabine and arabinosylcytosine 5'-triphosphates by DNA polymerase α: affinity, interaction, and consequences. Clin Cancer Res. 3: 1347-55, 1997.

11. Kamiya K, Huang P, Plunkett W. Excision of incorporated fludarabine from DNA by human DNA polymerase ε. Proc Am Assoc Cancer Res, 34: 349, 1993.

12. Reichard P. Interactions between deoxyribonucleotide and DNA synthesis. Ann Rev Biochem 57: 349-374, 1988.

13. Plunkett W, Chubb S, Alexander L, et al. Comparison of the toxicity and metabolism of 9-β-D-arabinofuranosyl-2-fluoroadenine and 9-β-D-arabinofuranosyladenine in human lymphoblastoid cells. Cancer Res 40: 2349-2355, 1980.

14. Gandhi V, Plunkett W. Modulation of arabinosylnucleoside metabolism by arabinosylnucleotides in human leukemia cells. Cancer Res 48: 329-34, 1988.

15. Chang CH, Desre D, Cheng YC, et al. Self potentiation mechanism of action for 9-β-D-arabinofuranosyl-2-fluoroadenine. Fed Proc 98: 2497, 1981

16. Gandhi V, Plunkett W. Interaction of arabinosyl nucleotides in K562 human leukemia cells. Biochem Pharmacol, 38: 3551-3558, 1989.

17. Parker W, Cheng YC. Inhibition of DNA primase by nucleoside triphosphate and their arabinosyl analogs. Mol Pharmacol, 31: 146-151. 1987.

18. Catapano CV, Chandler KB, Fernades DJ. Inhibition of primer RNA formation in CCRF-CEM leukemia cells by fludarabine triphosphate. Cancer Res, 51: 1829-1935, 1991.

19. Catapano CV, Perrino FW, Fernades DJ. Primer RNA chain termination induced by 9-β-D-arabinofuranosyl-2-fluoroadenine 5'triphosphate. A mechanism of DNA synthesis inhibition. J Biol Chem 268: 7179-7185, 1993.

20. Yang SW, Huang P, Plunkett W, et al. Dual mode of inhibition of purified DNA ligase I from human cells by 9-β-D-arabinofuranosyl-2-fluoroadenine triphosphate. J Biol Chem 267: 2345-2349, 1991.

21. Huang P, Plunkett W. Action of 9-β-D-arabinofuranosyl-2-fluoroadenine on RNA metabolism, Mol Pharmacol, 39: 449-455, 1991.

22. Keating M, O'Brien S, Lerner S, Kolle C, Beran M, Robertson LE et al. Long –term follow-up of patients with chronic lymphocytoc leukemia (CLL) receiving fludarabine regimens as initial therapy. Blood 92: 1165-1171, 1998.

23. Rai KR, Peterson BL, Appelbaum FR, Kolits J, Elias L, Shepherd L et al. Fludarabine compared with chlorambucil as primary therapy for chronic lymphocytic leukemia. N Engl J med; 343: 1750-1757, 2000.

24. Zinzai PL, Lauria F, Rondelli D, Benfenati D et al. Fludarabine in patients with advanced and/or resistant B-chronic lymphocytic leukemia. Eur J Haematolog 51: 93-97, 1998.

25. Sorensen JM, Vena DA< Fallavollita A, Chun HG, Chenson BD. Treatment of refractory chronic lymphocytic leukemia with fludarabine phosphate via the group C protocol mechanism of the National Cancer Institute : five years follow-up report. J Clin Oncol 15: 458-465, 1997.

26. Gandhi V, Kemena A, Keating MJ, et al. Fludarabine infusion potentiates arabinosylcytosine metabolism in lymphocytes of patients with chronic lymphocytic leukemia. Cancer Res 52: 897-903, 1992.

27. Estey E, Gandhi V, Keating MJ et al. G0CSF potentiates clinical and pharmacokinetic response to fludarabine and ara-C in AML and MDS. Porc Am Soc Clin Onc 12, 301, 1993.

28. Eichhorst BF, Hopfinger G, Pasold R, Hensel M, Zsoling U, Siehl S, et al. Fludarabine plus cyclophosphamide (FC) induces higher remission rates and longer progression free survival (PFS) than fludarabine (F) alone in first line therapy of advanced chronic lymphocytic leukemia (CLL): results of a phase III study (CLL4 protocol) of the German CLL study Group (GCLLSG). Blood 102:243a, 2003.

29. Rai KR, Peterson BL, Appelbaum FR, Kolitz J, Shepherd L et al. Fludarabine compared with chlorambucil as primary therapy for chronic lymphocytic leukemia. N Engl J Med, 343: 1750-1757, 2000.

30. Elias L, Stock-Novack D, Head DR, Grever MR, Weick JK, Champan RA et al. A phase I trial of combination fludarabine monophosphate and chlorambucil in chronic lymphocytic leukemia: a Southwest Oncology Group study. Leukemia 7: 36-365, 1993.

31. O'Brien S, Kantarjan H, Bean M, Smith T, Koller C, Estery E et al. Results from fludarabine and prednisone therapy in 264 patients with chronic lymphocytic leukemia with multivariate analysis-derived prognostic model for response to treatment. Blood, 82: 1695-1700, 1993.

32. O'Brien S, Kantarjian H, Beran C, Robertson IE, Freireich E, Kornblau S et al. Fludarabine (FAMP) and mitoxantrone therapy in chronic lymphocytic leukemia. Blood, 88: 588a, 1996.

33. Robertson LE, O'Brien S, Kantarjian H, Koller C, Beran M, Andreff Met al. Fludarabine plus doxorubicin in previously treated chronic lymphocytic leukemia. Leukemia, 9: 943-945, 1995.

34. Rummel MJ, Stilgenbauer S, Gamm H, Rost A, Doehner H, Hoelzer D et al. Fludarabine versus fludarabine plus epirubicin in the treatment of chronic lymphocytic leukemia (CLL)- preliminary results of a randomizes phase III multicenter study. Blood 100: 384a, 2002.

35. Gandhi V, Robertson LE, Keating MJ, Plunkett. Combination of fludarabine and arabinosylcytosine for treatment of chronic lymphocytic leukemia: clinical efficacy and modulation of arabinosylcytosyne pharmacology. Cancer Chemother Pharmacol, 34: 30-36, 1994.

36. Giles FJ, O'Brien SM, Snatini V, Gandhi V, Plunkett W, Seymaor JF et al. Sequential cis-platinum and fludarabine with or without arabinosyl cytosine in patients failing prior fludarabine therapy for chronic lymphocytic leukemia: a phase II study. Leuk Lymphoma, 36: 57-65, 1999.

37. Mauro FR, Foa R, Meloni G, Gentile M, Giammartini E et al. Fludarabine, ara-C, novotrone and dexa,ethasone (FAND) in previously treated chronic lymphocytic leukemia patients. Haematologica, 87: 926-933, 2002.

38. Srivastava DK, Berg BJV, Prasad R, et al. Mammalian abasic site base excision repair. J Biol Chem 1998; 273:21203-9

39. Hoeijmakers. Genome maintenance mechanisms for preventing cancer. JNJ Nature 2001; 411:366-74.

40. Matray T and Kool ET. A specific partner for abasic damage in DNA. Nature 1999; 399: 704-7.

41. Klungland A, Lindahl T. Second pathway for completion oh human DNA base excision repair: reconstitution with purified proteins and requirement for DNase IV (FEN1). EMBO J. 16, 3341-3348, 1997.

42. Podlutsky AJ, Dianova II, Podust VN, Bohr VA, Dianov GL. Human DNA polymeraseβ initiates DNA synthesis during long-patch repair of reduced AP sites in DNA. EMBO J, 20, 1477-1482, 2001

43. Fortini P, Parlanti E, Sidorkina OM, Laval J, Dogliotti E. The type of DNA glycosylase determines the base excision repair pathway in mammalian cells. J Biol Chem; 274:15230-6, 1999.

44. www..courses.biology.utah.edu/.../11_glycosylase.html

45. Xanthoudakis S, Smeyene RJ, Wallace JD, Curran T. The redox /DNA repair protein, Ref1, is essential for early embryonic development in mice. Proc Natl Acad Sci USA. 93: 8919-8923, 1996.

46. Fung H, Demple B. A vital role for ape1/ref1 protein in repairing spontaneous DNA damage in human cells. Mol Cell 17: 463-470. 2005.

47. Dianov GL, Price A, Lindahl T. Generation of single-nucleotide repair patches following excision of uracil residues from DNA. Mol Cell Biol. 12, 1605-1612, 1992.

48. Sobol RW, Horton JK, Kuhn R, Gu H, Singhal RK, Prasad R, Rajewsky K, Wilson SH. Requirement of mammalian DNA-polymerase β in base excision repair. Nature 379, 183-186. 1996.

49. Matsumoto Y, Kim R. Excision of deoxyribose phosphate residues by DNA polymerase β during DNA repair. Science. 269, 699-702, 1995.

50. Gu H, Marth JD, Orban PC, Mossmann H, Rajewsky K. Deletion of a DNA-polymerase-beta gene segment in T-cells using cell-type-specific gene targeting. Science, 265, 103-106, 1994.

51. Tomkinson AE, Mackey ZB. Structure and function of mammalian DNA ligase. Mut Res, 407, 1-9. 1998.

52. Barnes DE, Tomkinson AE, Lehmann AR, Webster HDB, Lindahl T. Mutations in the DNA ligase I gene of an individual with immunodeficiency and cellular hypersensitivity. Cell 68, 495-504, 1992.

53. Nash RA, Caldecott KW, Barnes DE, Lindahl T. XRCC1 protein interacts with one of two distinct forms of DNA ligase III. Biochemistry 36, 5207-5211, 1997.

54. Tebbs RS, Flannery ML, Meness JJ, Hartmann A, tucker JD, Thompson LH, Cleaver JE, Pedersen RA. Requirement for the XRCC1 DNA base excision repair gene during early mouse development. Dev Biol, 208, 513-529, 1999.

55. Parson JL, Dianova II, Allison SL, Dianov GL. Poly(ADP-ribose)polymerase 1 protects excessive DNA strand breaks from deterioration during repair in human cell extracts. FEBS J. 272, 2012-2021, 2005.

56. Whitehouse CJ, Taylor RM, Thistlethwaite A, Zhang H, Karimi-Busheri F et al. XRCC1 stimulates human PNK activity at damaged DNA termini and accelerates DNA single –strand break repair. Cell 104, 107-117, 2001.

57. Kijas AW, Harris JL, Harris JM, Lavin MF. Aprataxin forms a discrete branch in HIT superfamily of proteins with both DNA/RNA binding and nucleotide hydrolase activities. J Biol Chem 281, 1393-13948, 2006.

58. Madhusudan S, Smart F et al. Isolation of small molecule inhibitor of DNA base excision repair. Nucleic Acid Res, 33, 4711-24, 2005.

59. Luo M, Caldwell D, Xu Y et al. Inhibition of human apurinic/apyrimidinic endonuclease DNA base excision repair enzyme/redox factor (APE1/Ref1) using small

molecule redox and repair inhibitors: Therapeutics implications. Proc Amer Assoc Cancer Res., 45, 3042, 2004.

60. Liu L, Taverna P, Whitacre CM, Chatterjee S, Gerson SL. Pharmacological disruption of base excision repair sensitizes mismatch repair deficient and proficient colon cancer cells to methylating agents. Clin Cancer Res 1999; 5:2908-17.

61. Calabrese KW, Almassy R, Barton S, et al. Anticancer chemosensitization and radiosensitization by the novel poly(ADP-ribose)polymerase -1 inhibitor AG14361. J Natl. Cancer Inst. 96, 56-67, 2004.

62. Liuzzi M, Talpeart-Borle, M. A new approach to study of the base excision repair pathway using methoxyamine. J Biolg Chem 1985; 260:5252-58.

63. Nakamura J, Walker VE, Upton PB, Chiang SY, Kow YW, Swenberg JA. Highly sensitive apurinic/apyrimidinic site assay can detect spontaneous and chemically induced depurination under physiological conditions. Cancer Res 1998; 58:222-5.

64. Atamna H, Cheung I, Ames BN. A method for detecting abasic sites in living cells: age-dependent changes in base excision repair. Proc Natl Acad Sci USA 2000; 97:686-92.

65. Liu L, Gerson SL. Therapeutic impact of methoxyamine: Blocking repair of abasic sites in the base excision repair pathway. Current Opinion in investigational Drug; 5:623-7, 2004.

66. Liu L, Nakatsuru Y, Gerson SL. Base excision repair as a therapeutic target in colon cancer. Clin Cancer Res; 8:2985-91, 2002.

67. Liu L, Yan L, Donze JR, Gerson SL. Blockage of abasic site repair enhances antitumor efficacy of 1,3-bis-(2-chloroethyl)-1-nitrosourea in colon tumor xenografts. Mol Cancer Ther; 2:1061-6,2003.

68. Ling Y, Bulgar A, Miao YL, et al. Combined treatment with temozolomide and methoxyamine: blocking apurinic/pyrimidinic site repair coupled with targeting topoisomerase IIα. Clin Cancer Res 2007; 13:1532-9.

69. Taverna P, Hwang HS, Schupp JE, et al. Inhibition of base excision repair potentiates iododeoxyuridine cytotoxicity and radiosensitization. Cancer Res 2003; 63:838-46.

70. Elmore S. Apoptosis: A review of programmed cell death. Toxicol Pathol, 35: 495-516, 2007.

71. Ashkenazi A, Dixit VM. Death receptors: signaling and modulation. Science, 281:1305-8, 1998.

72. Suliman A, Lam A, Datta R, Srivastava RK. Intracellular mechanism of TRAIL: apoptosis through mitochondrial-dependent and –independent pathways. Oncogene, 20: 2122-33, 2001.

73. Kischkel KL, Hellbardt S, Berhman I, Germer M, et al. Cytotoxicity-dependent APO-1 (FAs/CD95)-associated proteins from a death –inducing signaling complex (DUSC) with the receptor. EMBO J, 14: 5579-88, 1995.

74. Ashkenazi A. Targeting death and decoy receptors of the tumor-necrosis factor superfamily. Nat Rev Cancer 2002;2:420–430.

75. Saelens X, Festjens N, Vandle Walle L, van Gurp M, van Loo G, Vandenebeele P. Toxic proteins released from mitochondria in cell death. Oncogene, 23: 2861-74, 2004.

76. Chinnaiyan AM. The apoptosome: heart and soul of the cell death machine. Neoplasia, 1:5-15, 1999.

77. Joza N, Susin SA, Daugas E, Stanford WL, Cho SK, Li CY, et al. Essential role of the mitochondrial apoptosis-inducing factor in programmed cell death. Nature, 410:549-54, 2001.

78. Li LY, Luo X, Wang X. Endonuclease G is an apoptotic DNase when released from mitochondria. Nature, 412:95-9, 2001.

79. Schler M, Green DR. Mechanism of p53-dependent apoptosis. Biochem Soc Trans, 19:684-8, 2001.

80. Slee EA, Adrain C, Martin SJ. Executioner caspase-3, -6, and -7 perform distinct, non-redundant roles during the demolition phase of apoptosis, J Biol Chem 276: 7320-6, 2001.

81. www.greentiger.com/mtdna.htm

82. Scheffler, Immo E. (2000) Review Article: A Century of Mitochondrial Research: Achievements and Perspectives. Elsevier Science B. V. and Mitochondrial Research Society. (dl November 2004).

83. Nilsen, H., Otterlei, M., Haug, T., Solum, K., Nagelhus, T. A., Skorpen, F., and Krokan, H. E. Nuclear and mitochondrial uracil-DNA glycosylases are generated by

alternative splicing and transcription from different positions in the UNG gene. Nucleic Acids Res., *25:* 750–755, 1997.

84. Tomkinson, A. E., Bonk, R. T., and Linn, S. Mitochondrial endonuclease activities specific for apurinic/apyrimidinic sites in DNA from mouse cells. J. Biol. Chem., *263:* 12532–12537, 1988.

85. Pinz, K. G., and Bogenhagen, D. F. Efficient repair of abasic sites in DNA by mitochondrial enzymes. Mol. Cell. Biol., *18:* 1257–1265, 1998.

86. Longley, M. J., Prasad, R., Srivastava, D. K., Wilson, S. H., and Copeland, W. C. Identification of 5_-deoxyribose phosphate lyase activity in human DNA polymerase γ and its role in mitochondrial base excision repair *in vitro*. Proc. Natl. Acad. Sci. USA, *95:* 12244–12248, 1998.

87. Fishel ML, Seo YR, Smith ML, Kelley MR. Imbalancing the DNA base excision repair pathway in the mitochondria; targeting and overexpressing N-methylpurine DNA glycosylase in mitochondria leads to enhanced cell killing. Cancer Res. 2003;63(3):608-15.

CHAPTER II

STATEMENT OF OBJECTIVES

Fludarabine is a widely used anti-tumor agent for the treatment of indolent lymphoproliferative disorders. The inhibition of DNA replication via incorporation of F-ara-ATP into DNA and subsequent chain termination is thought to be a significant mechanism leading to fludarabine-induced cell death. However, the molecular aspects of the cytotoxic action of fludarabine are not completely understood.

This work aims to expand the knowledge on the biochemical mechanisms of fludarabine-induced cytotoxic effects. Fludarabine, a purine base analog, incorporates into DNA and possibly acts as an abnormal base, triggering the activation of base excision repair (BER) system. BER entails the combined effort of several repair proteins (DNA glycosylases) that recognize and excise specific DNA damages, converting diverse base lesions into a common intermediate, apurinic/apyrimidinic (AP) sites. Eventually the damaged moiety is replaced with a normal nucleotide and DNA is restored back to its original state. The potential involvement of BER (essential for both, nuclear and mitochondrial DNA) in processing incorporated fludarabine was not previously documented or explored. Moreover, once initiated BER could account for resistance to fludarabine, since a functional active BER should be able to recognize and repair the

specific DNA damage induced by the incorporated drug. It would be then only reasonable to predict that BER inhibitors – e.g. methoxyamine (MX) – could enhance antineoplastic activity of fludarabine and thus, a combination of fludarabine plus MX might represent a new and effective therapeutic strategy. To test this series of suppositions, the following specific aims were devised:

1. To demonstrate that BER enzymes are capable to recognize and initiate removal of fludarabine incorporated into DNA (Chapter 3)

The working hypothesis for this aim is that *at least one of the members of DNA glycosylase family can recognize and excise incorporated fludarabine.* An *in vitro* screening for DNA glycosylase activity, employing various purified enzymes or whole cell extracts and a synthesized 40-mer oligonucleotide substrate that contains fludarabine, is performed. Subsequent kinetic studies to characterize the enzymatic activity of selected glycosylase are carried out.

Identifying the glycosylase potentially implicated in fludarabine recognition is significant for two main reasons: (i) it sustains the possibility that BER is involved in processing incorporated fludarabine and (ii) it is critical for the subsequent molecular studies, since more targeted experiments can be devised to investigate the eventual role of BER in modulating fludarabine action.

2. To demonstrate BER involvement in fludarabine-induced damage and to investigate the effect of MX on blocking the repair process (Chapter 4)

Based on the structural similarities with the normal base and the primary action of fludarabine to incorporate into DNA, the tested hypothesis is that *incorporated fludarabine, acting as an abnormal base in DNA, initiates BER.* This hypothesis is verified in cancer cell lines that are expressing or not the glycosylase identified in specific aim 1. The experimental approach involves (i) a correlation of AP site formation with concentrations of fludarabine (first step in BER) and (ii) an examination of expression of key BER proteins in a strategy of treatments with fludarabine alone.

Additionally, a new possibility to enhance fludarabine-induced damage by using MX in combination with fludarabine is proposed. Hypothesis that *MX is able to bind to fludarabine-induced AP sites, thus further blocking the repair pathway* is tested in human tumor cell lines with different repair status and in several human tumor xenografts, by assessing the toxicity induced by fludarabine alone or in combination with MX.

Two important findings are aimed here: (i) a first demonstration that in cells BER can process incorporated fludarabine and (ii) insights into a new and promising drug combination (fludarabine plus MX).

3. To delineate the contribution of mitochondrial apoptotic pathway in cell death after fludarabine and MX exposure (Chapter 5)

The working hypothesis is that *mitochondrial DNA is a target for fludarabine and MX and thus, mitochondrial DNA damage mediates the apoptotic cell death.*

Mitochondrial DNA damage – and more specifically AP site formation in mitochondrial DNA – is characterized in fludarabine alone or fludarabine plus MX treatments. Mitochondrial DNA damage is then correlated with known markers of

programmed cell death to demonstrate that fludarabine targets the mitochondria and promotes release of cytochrome c and other pro-apoptotic proteins, eventually triggering caspase activation and the apoptotic process.

Valuable information suggesting a mitochondrial mediated apoptotic death after fludarabine and MX treatments is obtained, which could place the mitochondrial apoptotic pathway in the focus of future studies on the mechanisms of cell killing by fludarabine.

4. To examine whether the combination of fludarabine and the BER inhibitor MX can represent a new therapeutic strategy for improving the treatment of chronic lymphocytic leukemia (CLL)

To confirm the hypothesis that *combination treatment of fludarabine and MX has greater antineoplastic activity when compared with single agents*, modulation of fludarabine activity by manipulating BER via MX is analyzed in a series of experiments employing CLL patient samples. The MX enhancement of activity of fludarabine is confirmed, since CLL cells are significantly more sensitive to the fludarabine in combination with MX as assayed by cytotoxicity, apoptosis, and levels of DNA damage.

These studies show that through manipulation of the BER pathway, an increase in response to fludarabine is achieved in CLL lymphocytes. The combination of fludarabine plus MX represents a potential new clinical targeted therapy with lower toxicity to normal cells.

CHAPTER III

UDG IS A MAJOR DNA GLYCOSYLASE HAVING ACTIVITY ON F:T MISPAIRS: IDENTIFYING A NEW TARGET FOR FLUDARABINE

Abstract

Fludarabine primary cytotoxic mechanism of action is mediated by the incorporation of F-ara-ATP into DNA leading to subsequent inhibition of DNA replication. We hypothesized that the incorporation of F-ara-adenosine as an abnormal base initiates the sequential repair cascade to produce AP sites through a DNA glycosylase, the first step in BER. However, the molecular mechanism of BER to process incorporated fludarabine is not known. In this *in vitro* study, using oligonucleotide substrates containing F-ara-adenosine: thymidine mispairs (F:T), we examined the cleavage activity of five purified DNA glycosylases. Our results showed that only UDG can recognize F:T mispairs and excise 2-fluoroadenine from DNA,

displaying a time- and concentration-dependent cleavage. Analysis of products of the enzymatic reaction, as performed by LC-ESI-mass spectrometry revealed 2-fluoroadenine as the cleaved product after reaction. Similarly, cleaved products of the UDG enzymatic reaction were seen when the F-ara-A oligonucleotide substrate was incubated with cell extracts from HL60 or Jurkat cells, as observed by electrophoresis on denaturing acrylamide gels. To evaluate the relative substrate specificity of UDG, the kinetics of excision of F-ara-A were compared with uracil in a double-stranded oligonucleotide. The results show that, although the specificity of UDG for F-ara-A residues is ~20-fold lower compared to uracil, F-ara-A is also a substrate for UDG. Moreover, the cleavage activity of UDG in purified form or in cell extracts can be abolished or reduced by UDG specific antibody or uracil glycosylase inhibitor, respectively. Our results indicate that BER can process incorporated fludarabine through the recognition and removal of 2-fluoroadenine in DNA by UDG.

3.1. Introduction

Most chemotherapeutic agents currently used in the treatment of cancer, directly or indirectly damage DNA causing direct base damage, misincorporation of analogs, formation of single or double-strand breaks or interfering with DNA-interacting proteins. The cellular response to these lesions is orchestrated in such way that the detection of the damage leads to either repair or induction of cell death (1). The repair activity of the cell plays an important role in cell sensitivity to anticancer agents (2,3). Thus, understanding the repair machinery has provided the rationale for the development of new therapeutic strategies to optimize the current ones. Among all the repair mechanisms that cells have

developed, the most important one in removing non-bulky damaged nucleotides is base excision repair pathway (BER) (4).

The BER pathway involves a series of sequential steps. These steps are: (1) cleavage of the N-glycosidic bond by a DNA glycosylase resulting in the formation of abasic site (AP site); (2) cleavage of the DNA backbone at the abasic site by apurinic/ apyrimidinic (AP) endonuclease; (3) polymerase insertion of a templated nucleotide at the position of the abasic sites by DNA polymerase; (4) ligation of the nicked DNA by DNA ligase (Figure 3-1.) (5-9) DNA glycosylases family, the enzymes that catalyze the first step in BER has been extensively studied. Cells have many different DNA glycosylases with different but sometimes overlapping specificities. Human cells at present, have eleven distinct DNA glycosylases (UDG, SMUG1, TDG, MBD4, OGG1, MYH, NTH1, MPG, NEL1, NEL2 (10,11). Two mechanistic classes of DNA glycosylase are recognized: mono-functional (glycosylase activity only) such as UDG and bi-functional (glycosylase and β-lyase activity) such as OGG1 (12,13).

Figure 3-1

Base excision repair pathway

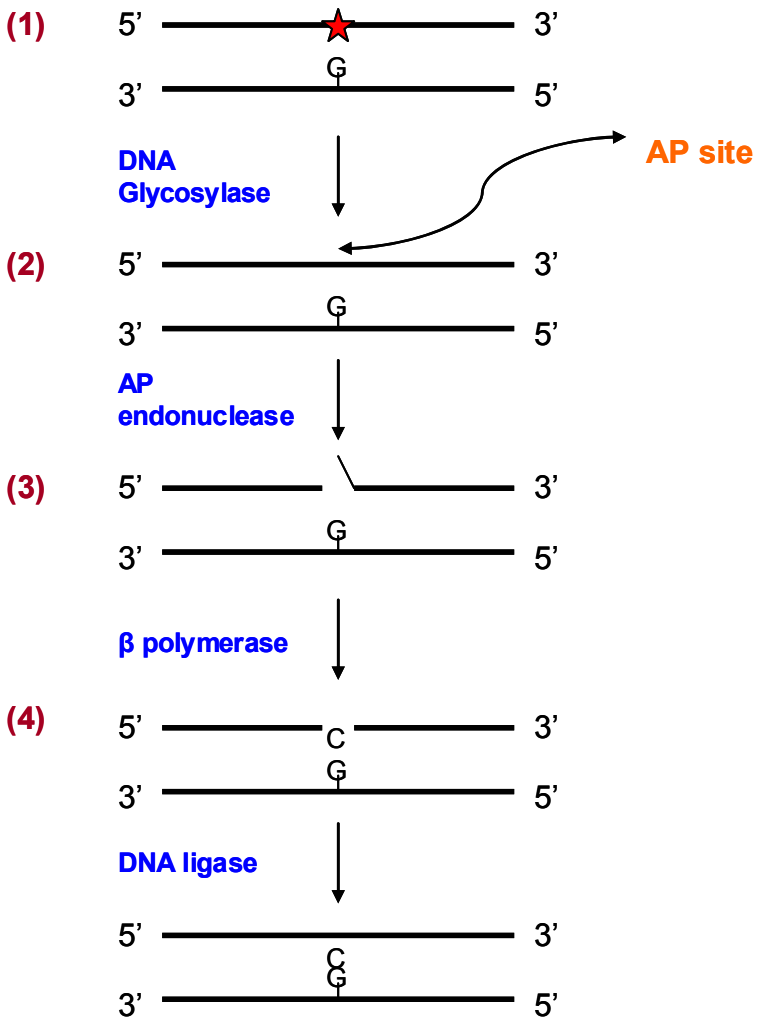

One structurally well-characterized DNA glycosylase and a prototype for other DNA glycosylases that used base flipping mechanism is uracil DNA glycosylase (UDG). The primary function of UDG is to remove mainly uracil from U/G mispairs. Other substrates for this enzyme have been identified: 5-fluorouracil, isodialuric acid, 5-hydroxyluracil and alloxan (14-17). There are two isoforms of this enzyme, a nuclear form (UNG2, 313 amino acids) and a mitochondrial form (UNG1, 304 amino acids), generated from UNG gene by alternative splicing and alternative transcription start point (18). The two isoforms have identical catalytic domains. UDG crystal structure revealed that the enzyme has a single α/β domain containing eight α-helices and a central four-stranded parallel and twisted β-sheet (Figure 3-2. A) (19,20). The catalytic mechanism of action has been elucidated: DNA binds along a positively charged groove in the enzyme, but the tight-fitting uracil-binding pocket located at the base of this groove is too deep and narrow to allow binding of DNA-uracil unless it is 'flipped out' of DNA helix. While the enzyme scans the minor-groove, it "pushes" the dUMP residue from the dsDNA base stack via the major groove. This is associated with a compression of the DNA backbone flanking the uracil and specific recognition of the 5'phosphate, deoxyribose and uracil by UDG active-site residue which stabilizes the extra helical nucleotide confirmation. It promotes condensation of the surrounding catalytic residue to form a productive complex specific for uracil cleavage. In the UDG-DNA complex, both uracil and the deoxyribose phosphate are rotated by nearly 180 ° from their normal positions. The mechanism is described as nucleotide flipping (Figure 3-2. B) (21).

Figure 3-2

UDG enzymatic mechanism [19,20,21]

A. UDG-DNA complex. ***B*** Backbone compression forced by three Ser–Pro-rich loops. The loops of the Ser–Pro pinch (green) compress the uracil-containing DNA strand at the phosphates 5' and 3' of the uracil nucleotide in the directions indicated by the arrows. ***C,*** The UDG Ser–Pro pinch for initial damage detection. The initial UDG–DNA complex is recreated by superimposing straight B-DNA (white) onto the kinked DNA seen in the co-crystal structures (orange), and the structure of uncomplexed wtUDG (stippled magenta ribbons) onto the DNA-bound enzyme.

A

B

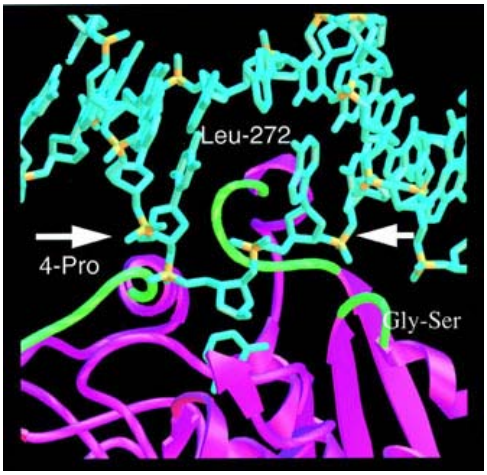

C

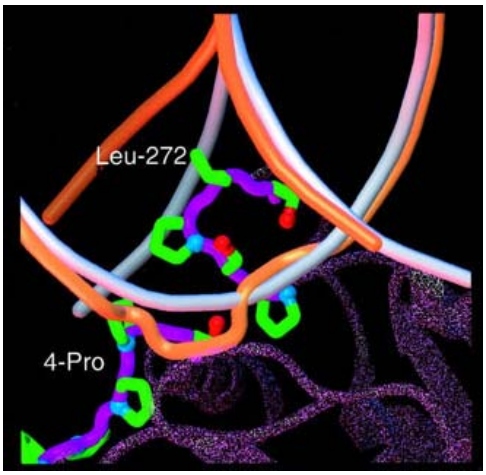

Nucleotide analogs are a class of therapeutic agents that target DNA. Fludarabine, an adenosine analog, is used for the treatment of hematological malignancies (22). Upon being metabolized to its active triphosphate form, fludarabine is incorporated into DNA (23). Among other molecular targets such as DNA polymerase and ribonucleotide reductase (24-27), its incorporation may lead to activation of BER pathway. The molecular mechanism of BER recognition and repair of the incorporated fludarabine has not yet been elucidated.

3.1.1. Hypothesis and Rationale

Research focus: To demonstrate that BER enzymes are capable to recognize and initiate removal of fludarabine incorporated into DNA.

Given that the fludarabine mechanism of action is mediated by the incorporation into DNA and the structural characteristics between fludarabine and adenosine (the normal nucleotide) are similar but still different , we hypothesized that at least one of the members of DNA glycosylase family, as part of BER pathway, can recognize and excise incorporated fludarabine.

We examined *in vitro* the enzymatic requirements for removal of incorporated fludarabine. Identifying the glycosylase potentially implicated in fludarabine recognition is important for proving the possibility that BER process is involved in processing of fludarabine induced-damage. It also set the stage for future, combinatory regimens.

3.2. Materials and Methods

3.2.1. Cells and reagents

Human tumor cell lines, Jurkat (lymphoblastic), HL60 (myelocitic leukemic), U937 (myelononocytic), were obtained from the American Type Culture Collection (Rockville, MD) and cultured in proper mediums. Methoxyamine (MX) and 2-fluoroadenine were purchased from Sigma Chemical Co (St. Louis, MO).

3.2.2. Oligonucleotides and enzymes

The fluorescent HEX labeled 17-mer oligonucleotide 5'-[HEX]GTAAAACGAC GGCCAGT-3', the 21-mer 5'-ATTCGAGCTCGGTACCCGGGG-3', the Cy5-labeled 40 mer oligonucleotide, 5'-[Cy5]CCCCGGGTACCGAGCTCGAATTCACTGGCCGTCGT TTTAC-3' were purchased from Operon Biotechnologies (Huntsville, Alabama). Complementary single-stranded oligonucleotides for U:G, U:T and G:T mispairs were purchased from the same company:

5'[HEX]GTAAAACGACGGCCAGTG**U**ATTCGAGCTCGGTACCCGGGG-3';

5'-[Cy5]CCCCGGGTACCGAGCTCGAATGCACTGGC CGTCGTTTTAC-3' for U:G;

5'-[HEX]GTAAAACGACGGCCAGTG**U**ATTCGAGCTCGGTACCCGGGG-3';

5'-[Cy5]CCCCGGGTACCGAGCTCGAATTCACTGGCCGTCGTTTTAC-3' for U:T and 5'-[HEX]GTAAAACGACGGCCAGTG**G**ATTCGAGCTCGGTACCCGGGG-3', 5'-[Cy5]CCCCGGGTACCGAGCTCGAATTCACTGGCCGTCGTTTTAC-3' for G:T mispairs. The duplex oligonucleotides were made by annealing the two complementary strands in a reaction buffer containing 10 mM Tris-HCl, 50 mM KCl, 1 mm EDTA, by heating at 95 ºC for 5 min and slowly cool it down at room temperature for 1 hour.

The T4 polynucleotide kinase and T4 ligase were purchased from Invitrogen (Carlband, CA). Human DNA polymerase β, E. Coli Uracil DNA glycosylase (UDG), mouse 3-methyladenine DNA glycosylase (Aag), human 8-oxoGuanine DNA glycosylase (OGG1), E. Coli Mut Y DNA glycosylase (Mut Y), Thymidine DNA glycosylase (TDG) and human AP endonuclease were purchased from Trevigen (Gaithersburg, MD).

3.2.3. Preparation of oligonucleotide substrates containing fludarabine

The procedure to construct oligonucleotide substrate containing an insertion of F-ara-A was performed as described by Yang *et al* (8) with modifications. A fluorescent HEX-labeled oligonucleotide, 5'-[HEX]GTAAAACGACGGCCAGT-3' (17-mer) and an oligonucleotide of 5'-ATTCGAGCTCGGTACCCGGGG-3' (21-mer) were annealed to a complementary Cy5-labeled oligonucleotide (Operon Biotechnologies, Huntsville, Alabama),

5'-[Cy5]CCCCGGGTACCGAGCTCGAATTCACTGGCCGTCGTTTTAC-3'(40-mer).

The double stranded oligonucleotides with a gap of two nucleotides at position 18 and 19 were generated:

5' [HEX] GTAAAACGACGGCCAGT--ATTCGAGCTCGGTACCCGGGG

3' CATTTTGCTGCCGGTCACTTAAGCTCGAGCCATGGGCCCC [Cy5]

The oligonucleotides were incubated with dGTP and DNA polymerase β, and either dATP or F-ara-ATP (Trevigen, Gaithersburg, MD) for 1 hr at 37 °C. After precipitation, the reactants were then incubated with T4 DNA ligase (Invitrogen, Carlband, CA) in a reaction buffer containing 50 mM Tris-HCl, pH 7.6, 10 mM $MgCl_2$, 1 mM ATP, 1mM

DTT at 14 ºC for 18 hrs, producing a 40-mer oligonucleotide substrate containing either a normal adenine (A) or a fludarabine (B) at position 19:

A. 5’ [HEX]GTAAAACGACGGCCAGTG**A**ATTCGAGCTCGGTACCCGGGG
3’CATTTTGCTGCCGGTCACTTAAGCTCGAGCCATGGGCCCC[Cy5]

B. 5’ [HEX]GTAAAACGACGGCCAGTG**F**ATTCGAGCTCGGTACCCGGGG
3’ CATTTTGCTGCCGGTCACTTAAGCTCGAGCCATGGGCCCC[Cy5]

Given that uracil base in DNA *in vitro* efficiently activates UDG excision-activity (32), the oligonucleotide substrates containing either uracil to thymine (U:T) or uracil to guanine (U:G) base pair at position 19 were constructed as well. These oligonuleotides were used as the control substrates to standardize UDG activity and specificity *in vitro* assay.

3.2.4. DNA glycosylase/APE assay

The assay mixture for DNA glycosylase activity contained various Units (from 0-20 Units) of purified enzymes and 4 pmol of the fluorescent labeled oligonucleotide duplex in 20 µl reaction buffer containing 1 mM EDTA, 1 mM dithiothreitol (DTT), and 20 mM Tris-HCl (pH 8.0). DNA glycosylase reaction was stopped at 95°C for 5 min after excising 2’-fluoroadenine (F-Ade) from oligonucleotide, resultant abasic sites were incised by 1 Unit of APE1 treatment at 37 °C for 30 min. Reaction products were resolved by electrophoresis through 20 % denaturing polyacrylamide gels (7 M urea, 1x Tris-borate-EDTA) and visualized by using a Typhoon 9200 fluorescent Imager (Amersham BioScience, Piscarawat, NJ). Fluorescent density was quantified using ImageQuant software.

3.2.5. Enzyme kinetic assays

To calculate enzyme kinetics parameters UDG was incubated with substrates (F:T, U:G and U:T) concentrations ranging from 10 to 600 nM, in the presence of APE1 (1unit) for 30 min at 37 °C, in a volume of 100 μL. Kinetics parameters were determined using Michaelis-Menten fit and Lineweaver –Burk plots based on the levels of products produced by the reaction of oligonucleotide with UDG/APE1.

3.2.6. Detection and quantification of 2-fluoroadenine using LC-ESI mass spectrometer

The 2-fluoroadenine standard solutions were prepared by serial dilution of 2-fluoroadenine stock solution (1 mg 2-fluoroadenine per mL of 1 M HCl) in the enzyme reaction buffer (containing 29 mM Tris-HCl, 1.8 mM EDTA, 1.1 mM DTT, 42 mM NaCl, 3.3 mM KCl, 0.013 mg/mL BSA, and 3.3% glycerol, at pH 8.0). The mobile phase was an aqueous solution 20% methanol and 0.1% formic acid. UDG glycosylase reaction product sample (obtained as describe above, by incubating B oligonucleotide substrate with purified UDG) and 2-fluoroadenine standards were pretreated by solid-phase extraction using Waters Oasis® HLB cartridges (3 cc). Prior to the sample loading, the cartridge was equilibrated with 3.0 mL of methanol, followed by 3.0 mL of 0.1 M phosphate buffer (pH 8.0). 0.6 mL of sample or standard was diluted with equal volume of 0.1 M phosphate buffer (pH 8.0) and loaded to the cartridge. The cartridge was washed with 4.0 mL of deionized water and the retained 2-fluoroadenine was eluted with 10% formic acid in methanol. The eluent was evaporated to dryness in a ThermoSavant DNA 120 SpeedVac®. Both the sample and the standards were six times concentrated by

reconstitution in 100 µL deionized water.

An Agilent™ 1100 series HPLC system and a Bruker™ esquire HCT® ESI-ion-trap mass spectrometer were used for this work. During an analysis, 20-µL sample was injected into the system. The analytical separation was carried out on a Waters YMC-AQ® Column (2.0×50 mm, 5 µm) by isocratic elution with the mobile phase at a flow rate of 0.1 mL/min. The mass spectrometer was operated under the following conditions: positive ionization mode; scan range, m/z = 140-158; scan speed, 8,100 m/z s^{-1}; nebulizer flow, 18.0 psi; drying gas flow, 5.0 L/min; drying temperature, 350°C; capillary, 4.0 kV; skimmer, 40.0 V; ion charge control (ICC) target, 6,000; maximum accumulation time, 100.00 ms; spectra averages, 10; rolling averages, 1. The protonated 2-fluoroadenine ion at m/z of 154 was used for the detection of 2-fluoroadenine.

3.2.7. AP site assay

The AP sites were measured using ARP (aldehyde reactive probe) reagent. The assay was performed as previously described with minor modifications (28-30). DNA (10 µg) was incubated with 15 µl of 1 mM ARP (Dojindo Laboratories, Kumamoto, Japan) in 150 µl PBS solution at 37 ºC for 15 min. DNA was then precipitated with 400 µl ice-cold ethanol (100%) at -20 ºC for 20 min and washed with 70% ethanol. DNA was dried at room temperature for 30 min and then resuspended in TE buffer to achieve a final concentration of 0.3 µg/100 µl. The ARP-labeled DNA was then heat-denatured at 100 ºC for 5 min, quickly chilled on ice and mixed with an equal amount of 2 M ammonium acetate. The DNA was then immobilized on BA-S 85 nitrocellulose membrane (Schleicher and Schuell, Dassel, Germany) using a minifold II vacuum filter device

(Schleicher and Schuell, Dassel, Germany). The membrane was baked at 80 ºC for 1 hr and incubated with 0.25% BSA/PBS containing streptavidin-conjugated horseradish peroxidase (BioGenex, SanRamon, CA) at room temperature for 40 min with gentle shaking. ARP-labeled AP sites were visualized by chemiluminescence (Amersham Corp, Piscataway, NJ) followed by quantitative densitometry using NIH ImageJ software.

3.3. Results

3.3.1. UDG is a DNA glycosylase having activity on F:T mispairs

In order to examine whether incorporation of fludarabine residue into DNA can be recognized and removed by BER mechanism, we constructed oligonucleotide substrates containing a F-ara-A:T base pair (Figure 3-3. A) and examined the activity of five purified DNA glycosylases, including UDG, AAG, TDG, OGG and Mut Y, excising F-ara-A from oligonucleotide substrates (Figure 3-3.B), which is the first step of BER pathway. Results revealed that among these glycosylases, only UDG displayed the glycosylase activity to excise 2-fluoroadenine (F-Ade), producing a small fragment (~18 mer) after incubation with APE1 to incise the DNA backbone. No cleavage was seen as expected, when UDG was incubated with oligonucleotide containing a normal base-pair of A to T at position 19. To further confirm the specific role of UDG in recognition and removal of F-Ade, several experiments were performed. First, dose and time dependent assessment of UDG activity excising F-Ade from oligonucleotide duplex were examined and showed that the increased levels of cleaved fragments were proportionally correlated with both the concentrations of UDG and the duration of enzymatic reaction (Figure 3-3.C). Second, to clarify that UDG excised F-Ade as an abnormal base and this excision

was not due to the molecules of arabinose, an ara-Adenine-ATP was inserted into oligonucleotide at position 19 instead of F-ara-A, and then UDG cleavage activity was examined with this substrate. Results clearly showed that UDG had no activity to remove ara-Adenine, leaving entire 40-mer oligonucleotide substrates (Figure 3-3.C). The results indicated that the molecule of arabinose sugar could not stimulate the UDG excision activity. Third, to verify that UDG removed base was 2-fluoroadenine (F-Ade), mass spectro-analysis for F-Ade released from F:T oligonucleotide substrates after UDG reaction was developed. After the reaction of UDG with F:T oligonucleotide substrates, reaction products were collected and extracted with Waters Oasis® HLB solid-phase extraction cartridge (3 ml) and concentrated for 6 times. F-Ade standards were prepared by spiking F-Ade in the reaction buffer, and extracted and concentrated with the same procedures used to prepare samples of UDG reaction. Analytical separation was carried out on Waters YMC-AQ® Column (2.0×50 mm, 5 μm particle size with 120 Å pore size) by isocratic elution with the mobile phase (*i.e.*, 20 % methanol with 0.1 % formic acid) at a flow rate of 0.1 ml/min. As shown in Figure 3-2. D, F-Ade in UDG reaction buffer was detected by ESI-IT mass spectrometer (c), which was confirmed by standards of 2-fluoroadenine (a, b). Samples containing F:T substrate but without UDG showed no detectable F-Ade (d).

Figure 3-3

Double-stranded DNA oligonucleotide containing

F:T mispairs is a substrate for UDG

A, Schematic diagram represents the preparation of oligonucleotide substrates containing F:T mispairs and the products of reaction of DNA glycosylase/APE with the oligonucleotide substrates. ***B***, Oligonucleotide duplex containing F-ara A (F:T) was incubated with 5 DNA glycosylases (UDG, OGG, TDG, AAG and MutY) at 37 ºC for 1 hr and followed by incubation with APE1 at 37 ºC for 30 min. Reaction products were resolved by electrophoresis through denaturing 20 % polyacrylamine gels. ***C,*** UDG has the activity excising F-Ade in a dose and time dependent fashion, but it has no activity to cleave the substrates containing either A:T or ara-A:T. ***D,*** Identification of reaction product of UDG on F:T substrate by HPLC-ESI-mass spectrometer. Schematic diagram of the enzymatic reaction with the hydrolysis of the N-glycosydic bound between arabinose and 2-fluoroadenine residue. UDG reaction samples were analyzed after incubation of F:T substrate with UDG for 3 hrs.

A

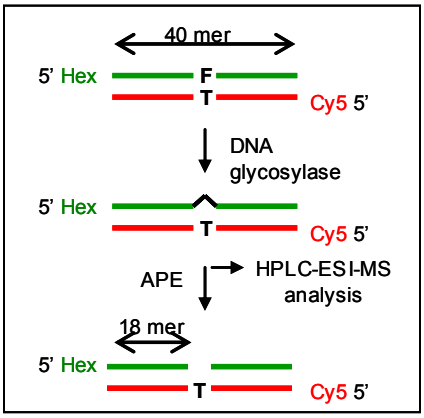
40 mer
5' Hex
F
T
Cy5 5'
DNA
glycosylase
5' Hex
T
Cy5 5'
APE
HPLC-ESI-MS
analysis
18 mer
5' Hex
T
Cy5 5'

B

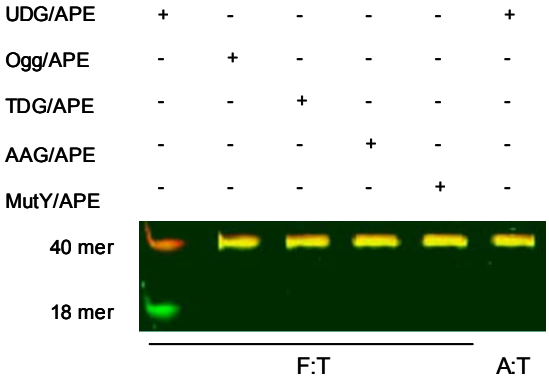
UDG/APE + - - - - +
Ogg/APE - + - - - -
TDG/APE - - + - - -
AAG/APE - - - + - -
MutY/APE - - - - + -
40 mer
18 mer
F:T
A:T

C

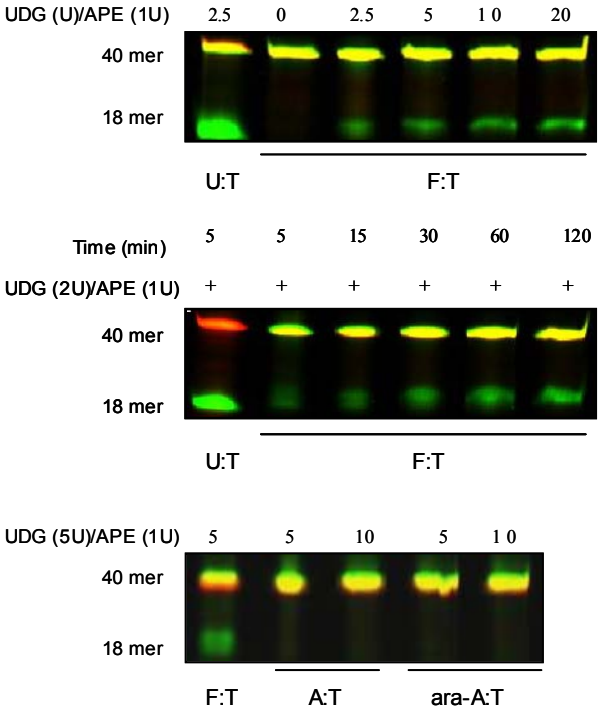
UDG (U)/APE (1U) 2.5 0 2.5 5 10 20
40 mer
18 mer
U:T
F:T
Time (min) 5 5 15 30 60 120
UDG (2U)/APE (1U) + + + + + +
40 mer
18 mer
U:T
F:T
UDG (5U)/APE (1U) 5 5 10 5 10
40 mer
18 mer
F:T
A:T
ara-A:T

D

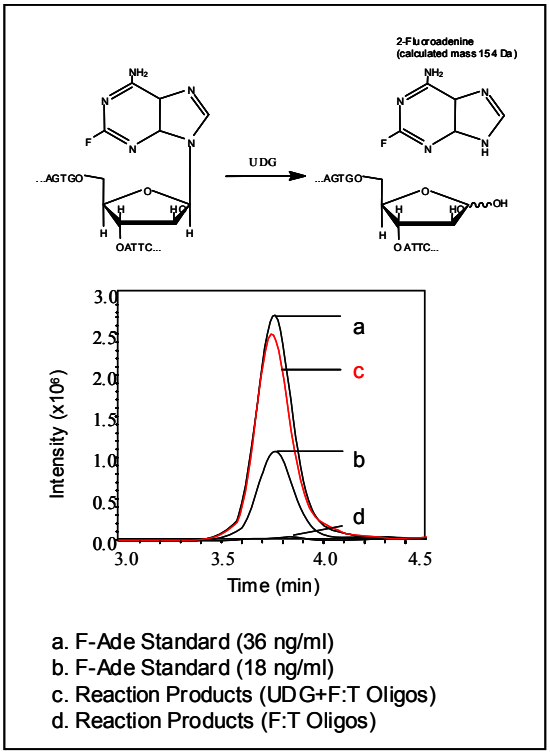
2-Fluoroadenine
(calculated mass 154 Da)
UDG
Intensity (x10⁶)
Time (min)
a
c
b
d
a. F-Ade Standard (36 ng/ml)
b. F-Ade Standard (18 ng/ml)
c. Reaction Products (UDG+F:T Oligos)
d. Reaction Products (F:T Oligos)

3.3.2. Enzymatic kinetics of UDG activity excising 2-fluoroadenine from double stranded oligonucleotide

To characterize UDG activity excising F-Ade, kinetic analysis was performed using a 40-base oligonucleotide duplex containing either F:T or U:G, or U:T base pairs. In this assay U:G oligonucleotide as the specific substrate of UDG was used to standardize enzymatic activity. U:T substrates were used as controls to examine whether T in an opposite strand affects UDG activity in comparison with U:G. Given that the removal of the target base from 40-mer double-stranded oligonucleotide generated an AP site that was incised by APE1, resulting in a fragment (~18 mer), the UDG activity was measured based on the levels of cleaved products (Figure 3-3.C). As shown in Figure 3-4.A, when 5 units of purified UDG and 4 pmol of either F:T or U:G substrates were used for reaction, enzyme-catalyzed reactions were saturable, their rate of catalysis does not show a linear response to increasing substrate. UDG produced products at a linear initial rate followed by a slower rate at later time points. In comparison with uracil substrates, the rate of UDG excising F-Ade was much slower, Vmax was 0.51 nM/min compared to 3.62 and 6.31 nM/min for U:G and U:T substrates respectively (Table 3-I). The products of F-Ade were much lower than uracil excised by UDG, even after increased concentrations of UDG (up to 20 units, Figure 3-4. B) and prolonged reaction time (60 min, Figure 3-4. C). The kinetic parameters of excision of uracil or F-Ade from oligonucleotide substrates using purified UDG were shown in Table 3-I. It was noted that the rate of turnover (K_{cat}) of UDG against U:G or U:T was high, about 7-12-fold faster than that against F:T. The specificity constant (K_{cat}/Km) of UDG for F-Ade was 19-fold lower than for uracil excised from either U:T or U:G oligonucleotide substrates. Data indicate that F-ara-A is the substrate of UDG, but with low enzymatic specificity.

Figure 3-4

Enzymatic kinetics of UDG activity to excise 2-fluororadenine or uracil from oligonucleotides containing F:T, U:T and U:G mispairs

A, The UDG catalyzed reaction: relation between the concentration of substrate and rate. UDG was incubated with increasing concentrations of F:T or U:G substrate (10-600 nM) for 30 min at 37 ºC in the presence of APE1 (1U). The cleavage products were analyzed by 20 % denaturing polyacrylamide gel electrophoresis. The velocities of the reactions were plotted against the substrates concentrations using Michaelis-Menten fit. Each point represents the mean value from at least three independent experiments. ***B***, Left panel: Enzymatic activity of UDG was measured as a function of enzyme concentration (0-20 units) and the substrates (4 pmols) at 37 ºC for 1 hr. Right panel: Enzymatic activity of UDG (5 units) was measured as a function of reaction time (0-60 min). Results are representative of at least three independent experiments.

A

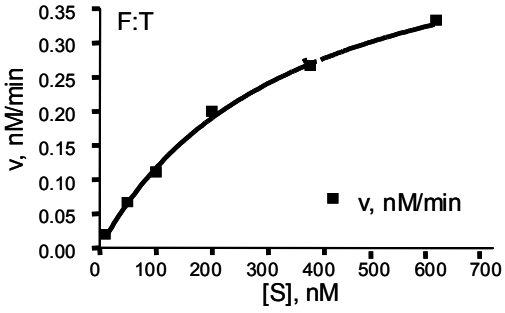
F:T
v, nM/min
[S], nM
0.35
0.30
0.25
0.20
0.15
0.10
0.05
0.00
0
100
200
300
400
500
600
700

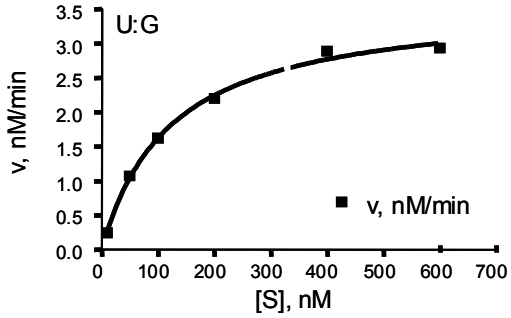
U:G
v, nM/min
[S], nM
3.5
3.0
2.5
2.0
1.5
1.0
0.5
0.0
0
100
200
300
400
500
600
700

B

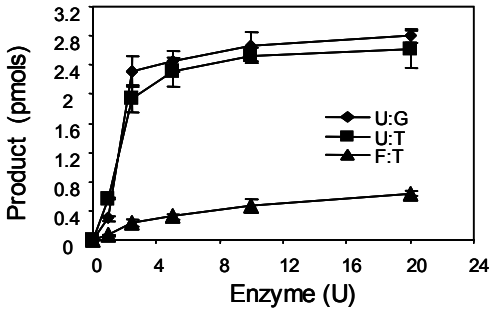
Product (pmols)
Enzyme (U)
U:G
U:T
F:T
3.2
2.8
2.4
2
1.6
1.2
0.8
0.4
0
0
4
8
12
16
20
24

C

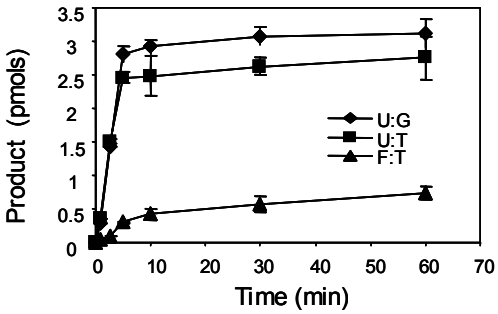
Product (pmols)
Time (min)
U:G
U:T
F:T
3.5
3
2.5
2
1.5
1
0.5
0
0
10
20
30
40
50
60
70

Table 3-I: The kinetic parameters of uracil or F-Ade excision from oligonucleotide substrates using purified UDG

substrate	*Km* (nM)	Vmax (nM/min)	K_{cat} (min^{-1})	K_{cat}/Km ($x10^{-3}$ min^{-1} nM^{-1})
U:G	122 ± 43	3.617 ± 0.11	0.723 ± 0.11	5.92 ± 1.23
U:T	221 ± 19	6.314 ± 0.50	1.260 ± 0.07	5.70 ± 0.29
F:T	340 ± 89	0.514 ± 0.03	0.102 ± 0.02	0.30 ± 0.01

3.3.3. Characterization of UDG glycosylase activity in cell extracts for excising F:T mismatch

We next examined the ability of DNA glycosylases in cell to recognize and excise F-ara-A from the oligonucleotide substrates. As shown in Figure 3-5. A and B, oligonucleotide duplex containing F:T base pair was fragmented and the cleaved products were increased proportionally with the concentrations of cell extracts from HL60 leukemia or Jurkat lymphoma cells (Figure 3-5. A, B). To further clarify the UDG cleavage activity of F-Ade in cells, the Uracil Glycosylase Inhibitor (Ugi, NewEngland Biolabs, Ipswich, MA) was used to inhibit UDG from cell extract. Ugi has been shown to bind and form a tight complex with UDG (E. Coli or human), thus inhibiting UDG activity (31,32).

As illustrated in Figure 3-5. C, the glycosylase activity of UDG both purified and cellular enzyme on F-Ade from oligonucleotide substrates was completely inhibited after pre-incubated with Ugi. Similarly, the UDG antibody was added in cell extracts from HL60 cells prior to the reaction with substrates in order to specifically reduce UDG activity, the reduction of UDG activity was seen by the decrease in cleaved products which was correlated to the increase in the concentration of UDG antibodies. The UDG antibody at concentrations of 10 - 20 μg/ml resulted in 80-90 % reduction of the cleaved fragments compared to that produced by cell extracts containing entire UDG activity (Figure 3-5. D). In contrast, cell extracts efficiently and completely excised uracil from inserted strand of oligonucleotide (U:T), even at low protein concentrations (2.5 μg), showing the cleaved fragments with strong density of green fluorescence and a intact complemented oligonucleotide (40-mer) labeled with Cy5 (red). Reduced activity of

UDG for excision of uracil was only seen when UDG-antibody was used up to high concentrations (20 μg/ml). These results indicate that in human cells, uracil is the common substrate for UDG. UDG antibody did not completely abolish UDG activity in cell extracts, suggesting that in cell UDG is not a sole glycosylase to remove uracil from DNA.

Figure 3-5

Cleavage of oligonucleotide containing F:T by UDG

in cell extracts from HL60 and Jurkat cells

Oligonucleotide duplex containing F:T or U:T base-pair was incubated with various concentrations of cell extracts (2.5- 40 μg) at 37 ºC for 30 min. The products of reaction were analyzed by electrophoresis on 20 % denaturating polyacrylamide gel. ***A,*** HL-60 cells ***B***, Jurkat cell ***C***, UDG activity in cell extracts was inhibited by Ugi (Ugi was pre-incubated with cell extracts at 37 ºC for 30 min). ***D***, UDG activity in cell extracts from HL-60 cells was reduced by UDG specific antibody. Results are representative of at least three independent experiments.

A

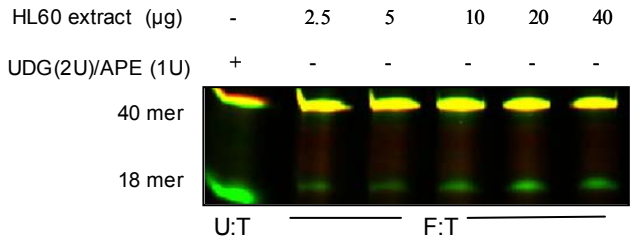
HL60 extract (μg) - 2.5 5 10 20 40
UDG(2U)/APE (1U) + - - - - -
40 mer
18 mer
U:T
F:T

B

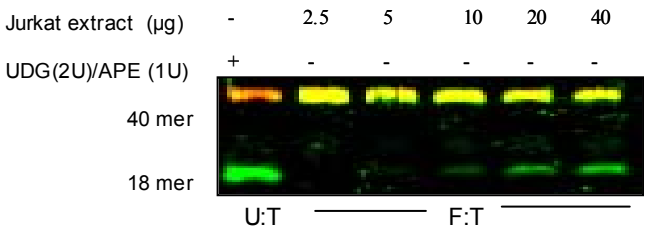
Jurkat extract (μg) - 2.5 5 10 20 40
UDG(2U)/APE (1U) + - - - - -
40 mer
18 mer
U:T
F:T

C

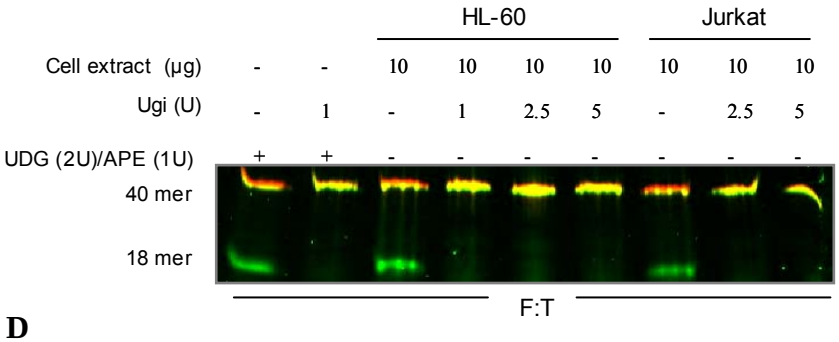
HL-60
Jurkat
Cell extract (μg) - - 10 10 10 10 10 10 10
Ugi (U) - 1 - 1 2.5 5 - 2.5 5
UDG (2U)/APE (1U) + + - - - - - - -
40 mer
18 mer
F:T

D

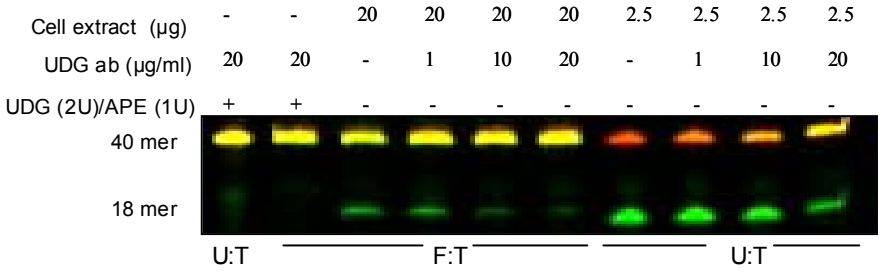
Cell extract (μg) - - 20 20 20 20 2.5 2.5 2.5 2.5
UDG ab (μg/ml) 20 20 - 1 10 20 - 1 10 20
UDG (2U)/APE (1U) + + - - - - - - - -
40 mer
18 mer
U:T
F:T
U:T

3.3.4. The formation of abasic sites of arabinosyl nucleotides (ara-AP site) after UDG cleavage of 2-fluoroadenine

Studies *in vitro* and *ex vivo* using oligonucleotide demonstrated that F-ara-A residues in DNA were recognized and removed by UDG. However, it is not clear whether the BER process of fludarabine occurs in cells. Thus, to detect the formation of ara-AP sites is like confirming the initial step of BER in process of incorporated fludarabine in DNA. We have measured AP sites using an aldehyde reactive probe reagent (ARP). ARP has been demonstrated to bind to an aldehyde group in an AP site of the natural deoxyribosyl sugar. However, we do not know whether the AP site of an arabinosyl sugar can be detected by ARP. Therefore, in this study, ARP was the first time used to measure ara-AP sites induced by fludarabine. A 40 mer oligonucleotide containing either F:T mispair, A:T normal base pairing or U:T mispairs were reacted with purified UDG for 30 min, at 37 °C. The reaction was stopped and the DNA was extracted using ethanol. The extract DNA duplex was labeled with ARP and the ara-AP sites were quantitated. As shown in the Figure 3-6. when the normal, A:T oligonucleotide was reacted with UDG, no AP sites were detected due to lack of enzymatic cleavage by UDG. In contrast, when 40 mer double stranded oligo containing F:T mispairs was incubated with UDG and labeled, we detected AP sites. The levels of AP sites formed were lower that those obtained using U:T substrate, as the control substrate.

Figure 3-6

Ara-AP sites formed by UDG using substrate containing F:T mispairs

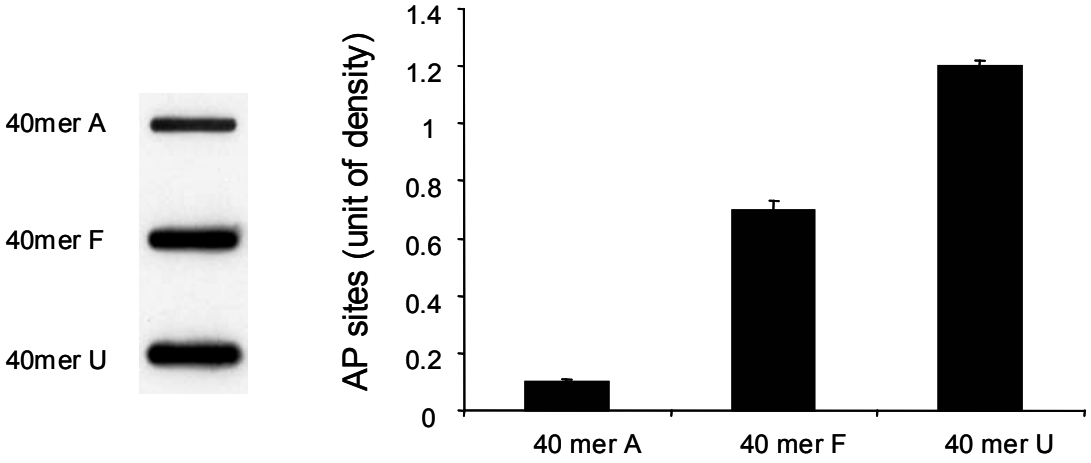
40mer A
40mer F
40mer U
AP sites (unit of density)
1.4
1.2
1
0.8
0.6
0.4
0.2
0
40 mer A
40 mer F
40 mer U

3.4. Discussion

In the present chapter we have demonstrated that: (i) among the five purified DNA glycosylases tested, UDG was identified as the enzyme responsible for recognition and removal of fludarabine incorporated in a synthesized 40-mer double stranded oligonucleotide, (ii) kinetic studies have shown that F-ara-A is a substrate for UDG with a lower specificity of the enzyme for this substrate and (iii) UDG was also responsible for cleavage of fludarabine when whole tumor cell extracts were used.

DNA glycosylases remove a large number of cytotoxic bases from DNA. Some of the enzymes have narrow specificities, whereas most can remove a large variety of structural different bases. Noteworthy, some glycosylases have overlapping substrate specificities which serve as a backup function (11). Using oligonucleotide substrates containing F-ara-A residues, we demonstrated that *in vitro* and *ex vivo* purified UDG excised incorporated F-ara-A from DNA, showing a direct relationship between the UDG activity and the levels of excision of incorporated F-ara-A. By determining the enzyme kinetic parameters, we confirmed that UDG is active against F-ara-A, but with a 19-folds lower catalytic efficiency when compared with the UDG specific substrate, uracil. Furthermore, using human cell extracts that were either depleted of the enzyme, either with UDG activity altered with a specific inhibitor (31,32), we confirmed that the cleavage of the F-ara-A is initiated by UDG.

Furthermore, the available evidence (J. Biol. Chem. 265: 16617-16625, 1990) demonstrated that following its incorporation into the 3' terminus, the fludarabine nucleotide is a poor substrate for addition of a subsequent nucleotide. Thus, evaluating the activity of UDG against a substrate that contains the analogues at the 3’ position

would model the other portion of the lesions that occur in whole cells. Even though this question was not answered *in vitro*, our *in vivo* experimental approach and results presented in Chapter 4 confirmed the role of UDG in removal of incorporated fludarabine, regardless of possible locations of incorporated fludarabine.

Previous research has characterized the details of the chemical mechanism by which UDG catalysis the removal of uracil residues from the DNA strand. The catalytic unit of the enzyme gains access to the glycosidic bond by flipping the target nucleotide out of the DNA helix. The very specific interaction between the active site of the enzyme and the target lesion weaken the glycosidic bond, allowing rapid hydrolysis (11,20). One could assume that UDG catalysis fludarabine-base removal by a similar mechanism.

In the case of fludarabine molecule both the sugar moiety and the base are modified when compared with common nucleotide structure. The sugar moiety of fludarabine is arabinose, while the base part contains a fluorine substitute in the second position of the adenine ring. Considering these differences, we decided to test the eventual involvement of the sugar. Thus, we synthesized a 40 mer oligonucleotide (AraA:T) containing the sugar moiety of fludarabine attached to the adenine, the common unmodified base (of adenosine). Studies using AraA:T substrate and purified UDG have demonstrated that the sugar moiety of the fludarabine molecule does not participate in UDG catalytic mechanism.

The base contained in fludarabine molecule is not the typical pyrimidinic substrate for UDG. Still, we believe that the presence of fluorine substitute at the second position of the adenine ring is a key structural feature for UDG activity on fludarabine. Previous studies have shown that indeed, other molecules containing fluorine substitutes

interact with UDG. For instance, 5-flurouridine is as substrate for UDG while gemcitabine (the hydrogens on the 2' carbons of deoxycytidine are substituted with fluorines) is able to inhibit the enzyme (33, 34).

Future studies involving crystal structure of human UDG bound to DNA containing F-ara-A will be focus on elucidating how UDG recognizes and removes fludarabine base and establish the role of the fluorine substitute in the biochemical mechanism of the enzymatic reaction. Also, considering that we did not test all eleven DNA N-glycosylases identified in mammalian cells, we could not rule out the possibility that other glycosylases may be capable to excise F-ara-A from DNA in cells.

In summary, our in vitro tests suggest that UDG is the major DNA glycosylase involved in excision of incorporated F-ara-A. In Chapter 4 of this material we present our *in vivo* experimental approach and results underlying the importance of UDG in response to fludarabine treatments.

3.5. References

1. Damia G, D'Incalci M. Targeting DNA repair as a promising approach in cancer therapy. European J of Cancer. 43: 1791-1801, 2007.
2. Trivedi RN, Almeida KH, Fornsaglio JL, Schamus S, Sobol RW. The role of base excision repair in the sensitivity and resistance to temozolomide-mediated cell death. Cancer Res 2005;65:6394-400.
3. Liu L, Gerson SL. Base excision repair as a therapeutic target in colon cancer. Clin Cancer Res 2002;8:2985-91.
4. Hoeijmakers JH. Genome maintenance mechanisms for preventing cancer. Nature 2001;411:366-74.
5. Wilson SH. Mammalian base excision repair and DNA polymerase beta. Mutat Res 1998;407:203-15.
6. Srivastava DK, Berg BJV, Prasad R, et al. Mammalian abasic site base excision repair. J Biol Chem 1998;273:21203-9.
7. Sokhansanj B, Rodrigue GR, Fitch JP, Wilson DM. A quantitative model of human DNA base excision repair. I. Mechanistic insights. Nucleic Acids Res 2002;30:1817-25.
8. Fortini P, Parlanti E, Sidorkina OM, Laval J, Dogliotti E. The type of DNA glycosylase determines the base excision repair pathway in mammalian cells. J Biol Chem 1999;274:15230-6.
9. Nilsen H, Krokan HE. Base excision repair in a network of defense and tolerance. Carcinogenesis 2001;22:987-98.
10. Sander M, Wilson S. Base excision repair, AP endonuclease and DNA glycosylases, Encyclopedia of Life Science, 2002.

11. Krohan H, Standal R, Slupphaung G. DNA glycosylases in the base excision repair of DNA. Biochem J, 325:1-16, 1997
12. Sharma R, Dianov G. Targeting base excision repair to improve cancer therapies. Molec Aspects of Medicine, 28:345-374, 2007.
13. Fromme JC, Banerjee A, Verdine GL. DNA glycosylase recognition and catalysis. Curr Opin Struct Biol. 2004 14(1):43-9
14. Ingraham HA, Tseng BY, Goulian M. Cancer Res, 40:998-1001, 1980
15. Zastawny TH, Doetsch PW, Dizdaroglu, FEBS Lett 364: 255-258, 1995
16. Hatahet Z, Kow YW, Purmal AA, Cunningham RP, Wallace SS. J Biol Chem, 269: 18814-20, 1994
17. Dizdaroglu M, Karakaya A, Jaruga P, Slupphaung G, Krokan HE. Nucleic Acid res, 24:418-422, 1994.
18. Nielsen H, Otterlei M, Haug T, Solum K, nagelhus T, Skorpen F, Krokan HE. Nucleic Acid Res 25: 750-755, 1997.
19. Aravind L, Koonin E. The α/β fold uracil DNA glycosylase: a common origin with diverse fates. Genome Biol, 1:0007.1-0007.8, 2000
20. Parikh SS, Mol CD, Slupphaug G, Bharati S, Krokan HE, Tainer JA. Base excision repair initiation revealed by crystal structures and binding kinetics of human uracil-DNA glycosylase with DNA. EMBO1998;17:5214-26.
21. Stivers J. Kinetic mechanism of damage site recognition and uracil flipping by E Coli Uracil DNA glycosylase. Biochem, 38: 952-963, 1999.
22. Pettitt AR. Mechanism of action of purine analogues in chronic lymphocytic leukemia. Br J Haematol 2003;121:692-702.

23. Iwasaki H, Huang P, Keating MJ, Plunkett W. Differential incorporation of ara-C, gemcitabine and fludarabine into replicating and repairing DNA in proliferating human leukemia cells. Blood 1997;90:270-8.

24. Kamiya K, Huang P, Plunkett W. Inhibition of the 3'-5' exonuclease of human DNA polymerase ε by fludarabine-terminated DNA. J Biol Chem 1996;271:19428-35.

25. Skalski V, Brown KR, Choi BY, Lin ZY, Chen S. A 3'-5' exonuclease in human leukemia cells: implications for resistance to 1-beta -D-arabinofuranosylcytosine and 9-beta-D-arabinofuranosyl-2-fluoroadenine 5'-monophosphate. J Biol Chem 2000;275:23814-19.

26. Yang SW, Huang P, Plunkett W, Becker F, Chan JYH. Dual mode of inhibition of purified DNA ligase I from human cells by 9-β-D-Arabinofuranosyl-2-fluoroadenine triphosphate. J Biol Chem 1992;267:2345-9.

27. Gandhi V, Plunkett W. Cellular and clinical pharmacology of fludarabine. Clin Pharmacokinet 2002;41:93-103.

28. Yan L, Bulgar A, Miao YL, et al. Combined treatment with temozolomide and methoxyamine: blocking apurinic/pyrimidinic site repair coupled with targeting topoisomerase IIα. Clin Cancer Res 2007;13:1532-9.

29. Nakamura J, Swenberg JA. Endogenous apurinic/apyrimidinic sites in genomic DNA of mammalian tissues. Cancer Res 1999;59:2522-6.

30. Nakamura J, Walker VE, Upton PB, Chiang SY, Kow YW, Swenberg JA. Highly sensitive apurinic/apyrimidinic site assay can detect spontaneous and chemically induced depurination under physiological conditions. Cancer Res 1998;58:222-5.

31. Cone R, Bonura T, Friedberg EC. Inhibitor of uracil-DNA glycosylase induced by bacteriophage PBS2. Purification and preliminary characterization. J Biol Chem 1980; 255:10354–58.
32. Mol CD, Arvai A, Sanderson R J et al. (1995). Crystal structure of the human Uracil-DNA glycosylase in complex with a protein inhibitor: protein mimicry of DNA. Cell 1995; 82: 701–708.
33. Mauro DJ, De Riel JK, tallarida RJ, Sirover MA. Mechanism of excision of 5-fluoruracil by uracil DNA glycosylase in normal human cells. Molec Pharma 1993; 43:854-57.
34. Liu L, Taverna P, Whitacre CM, Chatterjee S, Gerson SL. Pharmacological disruption of base excision repair sensitizes mismatch repair deficient and proficient colon cancer cells to methylating agents. Clin Cancer Res 1999;5:2908-17.

CHAPTER IV

TARGETING BASE EXCISION REPAIR BY METHOXYAMINE ENHANCES FLUDARABINE INDUCED CELL DEATH

Abstract

Fludarabine is a widely used anticancer drug. The inhibition of DNA replication via incorporation of F-ara-ATP into DNA and subsequent chain termination is thought to be its primary cytotoxic action. Here, AP (apurinic/apyrimidinic) site as a new target of fludarabine was identified and a novel therapeutic strategy combining fludarabine with methoxyamine (MX), an agent that blocks BER through its binding to AP site, was examined. This strategy rests on the hypothesis that the incorporation of fludarabine into DNA activates BER pathway to process F-ara-A as an abnormal base and to generate an ara-AP site, which is the target for MX. In cells, we found that formation of ara-AP sites was increased proportionally with concentrations and exposure time of fludarabine and that MX efficiently bound these ara-AP sites to form stable DNA lesions that have the

potential to interrupt BER mechanism, leading to cell death. Moreover, MX markedly enhanced fludarabine induced cytotoxic effect in tumor cells and therapeutic effect in human tumor xenografts. Taken together, our findings indicate for the first time that in cell BER can process incorporated fludarabine. They also provide insights into possible leads to new and promising therapeutic strategies to enhance the antineoplastic activity of fludarabine.

4.1. Introduction

Fludarabine (2-fluoroadenine 9-β-D-arabinofuranoside-monophosphate), a purine nucleoside analogue, is effective for the treatment of indolent lymphoproliferative disorders such as acute myelogenous leukemia, acute and chronic lymphocytic leukemia and low-grade non-Hodgkin's lymphoma (1-4).

In cell, fludarabine (F-ara-A) is rapidly converted to the triphosphate species (F-ara-ATP), which is the active form to incorporate into DNA and RNA strands (5). The incorporated F-ara-A serves as a poor substrate for DNA replication enzymes, leading to the inhibition of DNA replication. Several related molecular targets have been identified, including ribonucleotide reductase, DNA polymerases α, β, γ, and ε, DNA primase, and DNA ligase (6-8). Therefore, the primary action of fludarabine is thought to affect replicating cells (9, 10). In addition, fludarabine induced inhibition of ribonucleotide reductase results in depletion and imbalance of the deoxynucleotide pools required for DNA repair and synthesis, subsequently may favor itself and other mismatched nucleotides to incorporate into newly synthesized DNA strand. Collectively, stalling DNA

replication, chain termination and free DNA ends also trigger apoptosis, leading to cell death.

Given that the primary action of fludarabine is through its incorporation into DNA, we hypothesize that incorporated F-ara-A seen as an abnormal base in DNA activates base excision repair (BER). BER is the major DNA repair pathway to process small base modifications generated by mis-insertions from imbalanced nucleotide pool, deamination of cytosine to uracil, environmental mutagens, or anticancer agents (11). BER pathway is prototypically initiated by a DNA glycosylase to remove a specific base lesion and to generate an apurinic/apyrimidinic or abasic site (AP site) (12, 13). The AP endonuclease (APE) is responsible for repair of the resultant AP sites by incising the phosphodiester backbone of damaged DNA immediately 5' to an abasic site, leading to the formation of a 3'-hydroxyl residue and a 5'-deoxyribose phosphate (5'-dRP). In mammalian cells completion of BER occurs via two pathways, short-patch (single nucleotide) or long-patch (2-10 nucleotides) repair, depending on the ability to remove the 5'-dRP and to complete repair syntheses (14,15). In the short-patch pathway, DNA polymerase β removes the 5'-dRP residue and fills one nucleotide in the gap, which is then sealed by a DNA ligase III (16). In the alternative long patch BER process, the 5'-deoxyribosephosphate flap structure is excised by flap endonuclease (FEN1), DNA repair synthesis and strand displacement are done by polymerase β, δ/ε (17-20). BER is the most efficient repair mechanism to repair a variety of base lesions. Thus, while BER protects cell from DNA damage, it also causes cell resistance to anticancer agents that produce DNA lesions repaired by BER (21). To overcome BER conferred drug resistance, methoxyamine (MX) has been studied (22, 23) and developed as an active inhibitor of

BER. The specific action of MX is to specifically react with an aldehyde group in the sugar moiety left at an AP site and to form a MX-bound AP-site. This structural modified AP site is refractory to the repair activity of APE in BER pathway, resulting in the persistence of the DNA lesion (17). MX has been demonstrated to enhance therapeutic efficacy of different alkylating therapeutic agents (24-31) and currently is being evaluated in clinical trials for its therapeutic value.

4.1.1. Hypothesis and Rationale

Research focus: **To demonstrate BER involvement in fludarabine-induced damage and to investigate the effect of MX on blocking the repair process**

In this work BER response to fludarabine-induced DNA damage was determined. Based on the structural differences between fludarabine and adenosine (the normal nucleotide), we hypothesized that incorporated fludarabine in DNA triggers activation of BER pathway. This leads to the subsequent hypothesis that methoxyamine, a known inhibitor of BER, blocks fludarabine induced BER response and thus, enhances fludarabine cytotoxicity.

We examined whether incorporated fludarabine is a substrate for BER and tested whether blockage of BER by MX can potentiate fludarabine cytotoxicity *in vitro* and in human tumor xenografts. Our results support our hypotheses and reveal the role of BER activity in cellular sensitivity to fludarabine. These data provide a rationale for the clinical development of fludarabine and MX in the treatment of hematological malignancies.

Figure 4-1.

Working model: BER response to Fludarabine-induced DNA damage

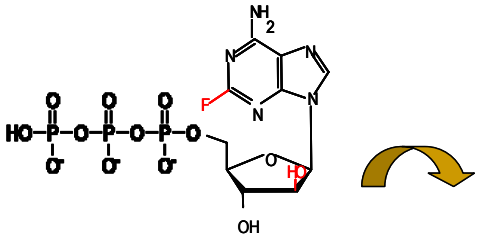

Fludarabine Triphosphate

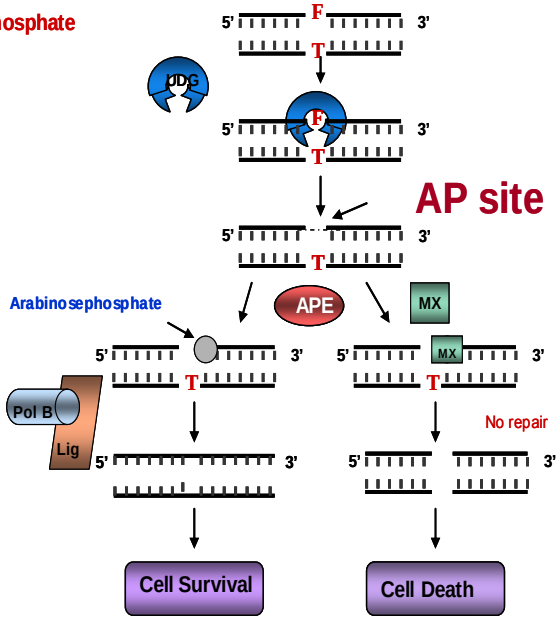

$MX = CH_3ONH_2$

4.2. Materials and Methods

4.2.1. Cells and reagents

Human tumor cell lines, Jurkat (lymphoblastic), HL60 (myelocitic leukemic), U937 (myelononocytic), SW480 and RKO (colon cancer) used in these studies were obtained from the American Type Culture Collection (Rockville, MD) and cultured in proper mediums. DLD1/UDG$^{-/-}$ cells were kindly provided by Dr. Sanford Markowitz. Fludarabine was obtained from Berlex Laboratories (Richmond, CA) and freshly prepared with mediums (containing alkaline phosphatase) for the treatment. Methoxyamine (MX) was purchased from Sigma Chemical Co (St. Louis, MO). MX was dissolved in sterilized water (pH 7.0) and stock solution (2.5 M) was stored at -20 ºC.

4.2.2. AP site assay

The AP sites were measured using ARP (aldehyde reactive probe) reagent that reacts with an aldehyde group at an AP sites and competes with MX to bind to AP sites. Therefore, this reagent only detects MX-free AP sites. The assay was performed as previously described with minor modifications (24, 32-34). Briefly, cells ($2x10^6$) were plated and exposed to fludarabine (0-20 μM) with or without MX (3 mM). Cells were collected at 24 hr after treatment and dose-dependent AP sites were measured. Alternatively, for the time-dependent assay, cells were exposed to 5 μM fludarabine with or without MX (3 mM) for a period of 72 hrs. Cells were harvested at 12, 24, 48 and 72 hr, respectively. After extracting by phenol (Fischer Scientific, Fair Lawn, NJ) and chloroform (Sigma-Aldrich, St Louis, MO), DNA (10 g) was incubated with 15 μL of 1 mM ARP (Dojindo Laboratories, Kumamoto, Japan) in 150 μL PBS solution at 37 ºC for 15 min. DNA was then precipitated with 400 μL ice-cold ethanol (100 %) at -20 ºC,

overnight and washed with 70% ethanol. DNA was dried at room temperature for 30 min and then resuspended in TE buffer to achieve a final concentration of 0.3 g/100 μL. The ARP-labeled DNA was then heat-denatured at 100 ºC for 5 min, quickly chilled on ice and mixed with an equal amount of 2 M ammonium acetate. The DNA was then immobilized on BAS 85 nitrocellulose membrane (Schleicher and Schuell, Dassel, Germany) using a minifold II vacuum filter device (Schleicher and Schuell, Dassel, Germany). The membrane was baked at 80 ºC for 1 hr and incubated with 0.25 % BSA/PBS containing streptavidin-conjugated horseradish peroxidase (BioGenex, SanRamon, CA) at room temperature for 40 min with gentle shaking. The nitrocellulose membrane was rinsed with washing buffer containing NaCl (0.26 M), EDTA (1 mM), Tris-HCl (20 mM) and Tween 20 (1 %) for 1 hr at room temperature. ARP-labeled AP sites were visualized by chemiluminescence (Amersham Corp, Piscataway, NJ) followed by quantitative densitometry analysis using NIH ImageJ software.

4.2.3. Cell Growth Assay

HL60 and Jurkat cells were seeded in complete growth medium in a 6-well plate (Falcon, Becton Dickinson) at a density of 5×10^{5} cells per well. Cells were treated with fludarabine or fludarabine plus MX and counted using a hemocytometer every 24 hr for 5 days.

4.2.4. Colony survival Assay

Tumor cells (2000/dish) were plated and treated with fludarabine (0-20 μM) or fludarabine plus MX (3 mM) for 24 hrs. After treatment the drugs were removed, fresh medium was added to the cells for 7 days. Survived colonies were stained with methylene

blue for 30 min at room temperature and the colonies containing more than 50 cells were counted to generate survival curves. To compare drug induced cytotoxicity DMF parameter was calculated. DMF is defined as the ratio of the IC50 of fludarabine alone to the IC50 obtained in the presence of the indicated modifier (DMF = IC50 for fludarabine alone / IC50 for fludarabine plus MX). DMF indicates the degree of potentiation of cytotoxicity by the modulator.

4.2.5. Comet assay

The single cell comet electrophoresis assay was performed using Comet Assay kit (Trevigen, Gaithersburg, MD). Approximately 5000 (in 50 µl) cells after exposure to drugs were mixed with 250 µl of 1 % low melting point agarose in 1x PBS at 37 ºC. The mixture (75 µl) was quickly pipetted onto a Comet slide (Trevigen, Gaithersburg, MD) and allowed to solidify at 4 ºC. Slides were immersed for 30 min in prechilled lysis buffer (2.5 mM sodium chloride, 100 mM EDTA pH 10, 10 mM Tris Base, 1 % sodium lauryl sarcosinate, 0.01 % Triton X-100) at 4 ºC. After lyses, slides were incubated for 20 min in alkali solution (0.3 M NaOH, 1 mM EDTA) at room temperature to allow unwinding of DNA and then subjected to both neutral and alkaline electrophoresis for the next 30 min. Comet in an individual cell was visualized by staining with Comet silver staining kit (Trevigen, Gaithersburg, MD). Fifty cells per treatment were analyzed using NIH ImageJ software to generate quantitative and statistical data. Cellular DNA damage was expressed as the tail "length" and the "tail moment" that combines a measurement of the length of the DNA migration and the relative DNA content therein (26, 35).

4.2.6. Western blot analysis

Cellular protein content was quantified spectrophotometrically using the Bio-Rad assay. Equal amounts of proteins (30 μg) were separated by SDS-PAGE and transferred to PVDF membrane (Millipore Cor., Bedford, MA). After blocking in 5 % non-fat dry milk in TBST for 40 min at room temperature the blots were incubated with primary antibody for 1 hour at room temperature. Sources of primary antibody were as follows: APE, FEN1, PCNA, polymerase β, TDG (Santa Cruz Biotechnology, CA), UDG, MPG, MBD4 (Abcam, Cambridge, MA), cleaved PARP (BD Pharmingen, San Jose, CA), γH2AX (Bethyl, Montgomery, Texas), α-Tubulin (Sigma-Aldrich, St Louis, MO), Ogg1 (Novus Biological, Littleton, CO). The primary antibody solutions were prepared in 1 % non-fat dry milk in TBST as followed: cleaved PARP 1: 1000 v/v dilution, APE 1:2000 v/v dilution, Fen1 1:200 v/v dilution, polymerase β 1:200 v/v dilution, UDG 1:500 v/v dilution, PCNA 1:200 v/v dilution, TDG 1:200 v/v dilution, MPG 1:500 v/v dilution, MBD4 1:500 v/v dilution, γH2AX 1:1000 v/v dilution, Ogg1 1:500 v/v dilution and Tubulin 1:500 v/v dilution. Blots were incubated with HRP-conjugated secondary antibody at room temperature for 1 hour. The blots were visualized by ECL (Amersham Corp, Piscataway, NJ) according to the manufacturer instructions.

4.2.7. RT-PCR assay

Total RNA was isolated from ~5 x 10^6 cells using RNAqueous-4PCR kit (Ambion, Austin, TX) according with the manufacturer's instructions. The extracted RNA was quantitated by measuring absorbance at 260 nm using NanoDrop100 spectrophotometer (Thermo Scientific, Wilmington, Delaware). Then cDNA was

synthesized from 5 μg of total RNA in a 20 μL reaction mixture according to the manufacturer's instructions using SuperScript III first strand kit (Invitrogen, Frederick, Maryland) with random hexamers. The thermal profile of the reaction was set for stage 1: 10 min at 25 ºC; stage 2: 50 min at 50 ºC and stage 3: 5 min at 85 ºC. TaqMan MGB probes (FAMTM dye labeled) for nuclear UDG (NM 080911.1) and β-actin (NM001101.2) were used. To amplify the cDNA, 0.25 μg of the reversed transcribed cDNA from cells were subjected to 40 cycles of PCR using TaqMan one-step RT-PCR master mixture reagent kit in a 96-well optical plate. The cycling parameters in an ABI 7500 Fast Real-Time PCR System (Applied Biosystem, Foster City, CA) were as follows: stage 1: 50 ºC for 2 min; stage 2: AmpliTaq activation 95 ºC for 10 min; stage 3: 40 cycles of amplification at 95 ºC for 15 s and stage 4: 60 ºC for 1 min. The amount of target was calculated after normalization to the β-actin as an endogenous control.

4.2.8. Immunofluorescence microscopy

Cells were grown on a 6 well plate and were treated with fludarabine and fludarabine plus methoxyamine for 24 and 48 hrs. At each time point, cells were washed with PBS and cytospin on a slide at 600 g for 8 min. Both treated and untreated cells were fixed in 2 % paraformaldehyde and permeabilized with 0.2 % Triton X-100. Cells were incubated with primary UDG antibody (Abcam, Cambridge, MA) for 1 hr at room temperature, followed by secondary antibody conjugated with Alexa 488 (green) (Molecular Probes, Carlsband, CA). Nucleus was stained using Hoersch dye, 2 mg/ml, for 30 min at room temperature. Images were digitally captured using an Olympus microscope equipped with a digital camera.

4.2.9. Xenograft tumors in nude mice

HL60, U937 and SW480 tumor cells (5×10^6) were injected into bilateral flanks of female athymic nude mice (6 weeks old). The tumors were measured with calipers and the tumor volume was calculated using the formula: $V = L \times I^2 / 2$, where V= tumor volume (mm^3), *L* is the largest diameter and *I* is the smallest diameter. When the tumor volumes reached 100-150 mm^3, mice were divided in control and treatment groups (6-9 mice/group).

Nude mice carrying tumors were treated with fludarabine alone (15 mg/kg), MX (2 mg/kg) alone and the combination of the two agents, by daily intraperitonial injection (i.p.) for 5 consecutive days. Tumor measurements were taken every 2 days. Tumor responses were quantified by tumor growth delay. Tumor growth delays were calculated using the formula: $T_{2x} - C_{2x,}$ where T_{2x}= the days to double tumor in size in drug treated tumor, C_{2x}= the days to double tumor in size in untreated tumor. Toxicity of the treatment was evaluated by measuring the body weight three times weekly from the first day of treatment until 2 weeks after the last treatment and also by analysis of whole blood counts (days 1, 5, 10 and 15 after treatment).

4.2.10. Statistical analyses

All results were expressed as mean ± SE. Statistical tests were performed using InStat3.06 (GraphPad). $P < 0.05$ was considered statistically significant.

4.3. Results

4.3.1. The formation of abasic sites of arabinosyl nucleotides (ara-AP site) in cells after exposure to fludarabine alone and in combination with MX

Studies *in vitro* and *ex vivo* using oligonucleotide demonstrated that F-ara-A residues in DNA were recognized and removed by UDG (presented in chapter 3). However, it is not clear whether the BER process of fludarabine occurs in cells. Thus, to detect the formation of ara-AP sites in cells after exposure to fludarabine is like confirming the initial step of BER in process of incorporated fludarabine in DNA. We have measured AP sites in cells induced by alkylating agents (24) using an aldehyde reactive probe reagent (ARP). ARP has been demonstrated to have similar chemical structures to MX that can specifically bind to an aldehyde group in an AP site of the natural deoxyribosyl sugar (23, 24). However, we do not know whether the AP site of an arabinosyl sugar can be detected by ARP in cells. Therefore, in this study, ARP was the first time used to measure ara-AP sites induced by fludarabine. Results showed that dose and time dependent formation of ara-AP sites were detected in three cancer cell lines, HL60, Jurkat and SW480 after fludarabine treatments (Figure 4-2. A & B) and that co-treatment with MX reduced detectable ara-AP sites. This reduction of ara-AP sites is presumably due to the binding of MX to the aldehyde group of the ara-AP site to form a MX-bound AP-site (24), making the ara-AP site unavailable for ARP. Importantly, these results indicate that MX is capable of blocking the repair of incorporated fludarabine. The ara-AP site assay was also performed in DLD1/UDG$^{+/+}$ and DLD1/UDG$^{-/-}$cells after fludarabine treatments. While the formation of ara-AP sites induced by fludarabine displayed a dose dependent effect in UDG$^{+/+}$ cells, no increased ara-AP sites were detected in UDG$^{-/-}$ cells (Figure 4-3. A) after exposure to increasing doses of fludarabine.

Thus, no detectable ara-AP sites in UDG-deficient cells were the results of the lack of UDG activity to recognize and remove incorporated F-ara-A, confirming that the activity of UDG plays the role in the initial repair-process of fludarabine in cells. Additionally, when genomic DNA extracted from these cells was incubated in vitro with purified UDG enzyme and then label with ARP, no significant increase in ara-AP sites formation was measured in $UDG^{+/+}$ cells. In contrast, considerable increase in ara-AP sites was detected in $UDG^{-/-}$ (Figure 4-3. B & C).

Figure 4-2

Fludarabine induces formation of ara-AP sites that are bound by MX

A, The dose-dependent relationship between the levels of ara-AP sites and the concentrations of fludarabine. The ara-AP sites in DNA were measured using ARP reagent after HL60, Jurkat and SW480 cells were treated with fludarabine alone (0-20 μM) or in combination with MX (3 mM) for 24 hrs (* $P<0.05$ compared to fludarabine alone). ***B***, The time-dependent relationship between the numbers of ara-AP sites and the length of time of exposure to fludarabine. The ara-AP sites were measured in Jurkat, HL60 and SW480 cells treated with fludarabine alone (5 μM) or fludarabine plus MX (3 mM) for 12, 24, 48 and 72 hr (* $P<0.05$ compared to fludarabine alone). Results represent the mean value of data from three independent experiments.

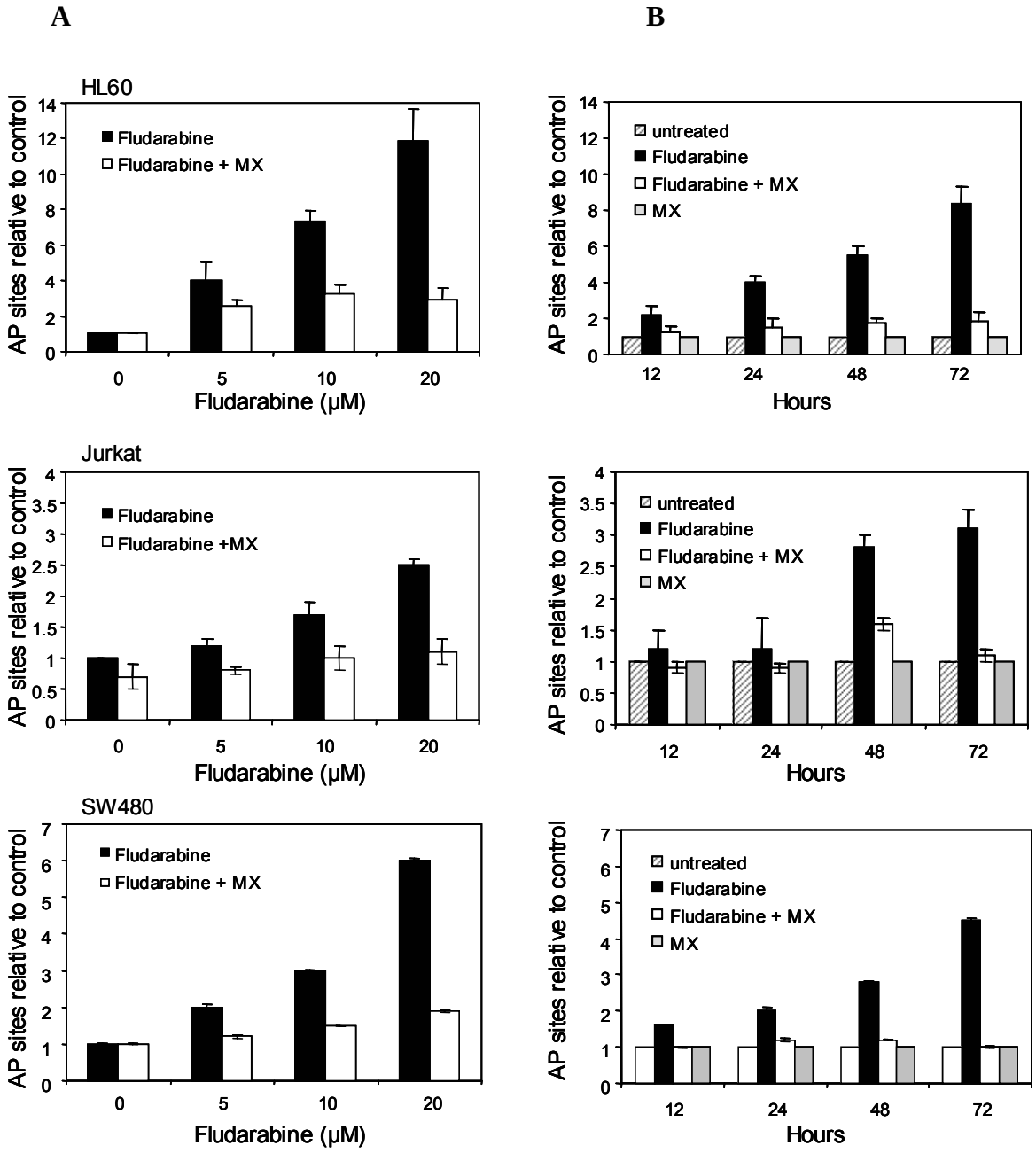
A
B
HL60
Fludarabine
Fludarabine + MX
AP sites relative to control
Fludarabine (μM)
untreated
MX
Hours
Jurkat
Fludarabine +MX
SW480

Figure 4-3

Fludarabine induces formation of ara-AP sites in UDG wild-type cells but not in $UDG^{-/-}$ cells

A, Comparison of the formation of ara-AP sites in colon cancer cells $DLD1/UDG^{+/+}$ versus $DLD1/UDG^{-/-}$ cells after exposure to fludarabine. $DLD1/UDG^{+/+}$ and $DLD1/UDG^{-/-}$ cells were treated with fludarabine (0-40 μM) for 24 hrs. DNA was extracted and ara-AP sites were measured using ARP. ***B,*** The formation of ara-AP sites in $DLD1/UDG^{+/+}$ cells after exposure to fludarabine (0-40 μM) for 24 hrs. DNA was extracted and divided in two samples. In one sample, ara-AP sites in 10 μg of DNA were measured using ARP. In the other sample, 10 μg of DNA were incubated with 5U of purified E. Coli UDG, for 2 hrs at 37 °C and subsequent ara-AP sites formed were labeled with ARP. ***C***, Ara-AP sites in $DLD1/UDG^{-/-}$ cells with or without incubation with purified UDG.

A

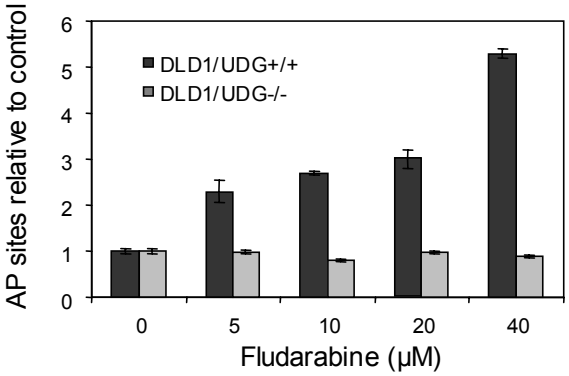
AP sites relative to control
DLD1/UDG+/+
DLD1/UDG-/-
0
1
2
3
4
5
6
0
5
10
20
40
Fludarabine (μM)

B

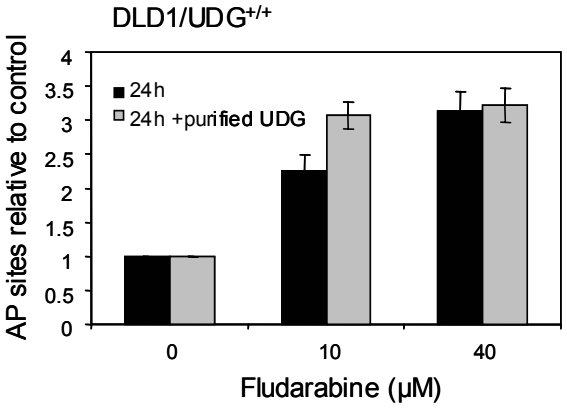
DLD1/UDG+/+
AP sites relative to control
24h
24h +purified UDG
0
0.5
1
1.5
2
2.5
3
3.5
4
0
10
40
Fludarabine (μM)

C

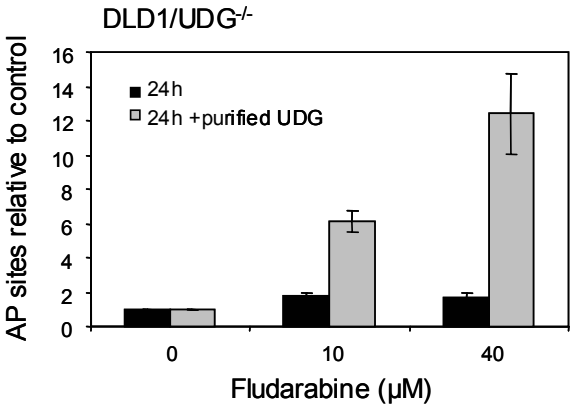
DLD1/UDG-/-
AP sites relative to control
24h
24h +purified UDG
0
2
4
6
8
10
12
14
16
0
10
40
Fludarabine (μM)

4.3.2. Up-regulation of cellular BER proteins after drug-treatments

In order to characterize the involvement of BER proteins in process of DNA damage induced by fludarabine alone or in combination with MX, we next evaluated the expression of BER proteins including UDG, APE, FEN1 and pol β in Jurkat and HL-60 cells before and after drug treatment. The altered expression of BER proteins displayed a similar pattern in response to the drug treatment in these two cell lines. UDG, FEN1 and pol β were up-regulated in varying degrees after exposure to either fludarabine alone or in combination with MX. As shown in Figure 4-4. A, a significant induction of UDG was seen in cells treated with the combination of fludarabine and MX when compared with cells treated with fludarabine alone (3 folds increase based on densitometric analysis) and the up-regulated UDG protein remained over a period of 72 hrs. It was noted that UDG was slightly induced by MX alone at 72 hr after treatment in these two cell lines. It is likely that the binding of MX to endogenous AP sites may stimulate UDG expression. APE expression remained unchanged before and after drug treatment in cells, indicating that either MX as a chemical compound or a MX-bond AP-site as a type of DNA damage has no direct effect on APE (24, 25) and thus are not accompanied by the upregulation of expression of this enzyme. APE can no longer recognize MX-bound AP site as a substrate, leading to further inhibition of BER process. The expressions of several other glycosylases, such as MPG, MBD4, TDG, AAG and Ogg1 were measured. No significant changes were observed in the expression levels of these glycosylases (Figure 4-4. B). These results, together with one obtained from the enzymatic activity assay (no cleavage activity observed, Chapter 3), suggest that the above mentioned glycosylase are not involved in the recognition and removal of incorporated fludarabine.

Moreover, to characterize the UNG gene transcript before and after the treatment with fludarabine alone and fludarabine plus MX, a real time RT-PCR assay was used. The values obtained for the target gene using TaqMan MGB probes were normalized to β-actin values (endogenous control) for each sample. As shown in Figure 4-4. C, a 2 fold increase in UNG transcript levels was observed for each time point, after fludarabine plus MX treatments. Similar up-regulation in the protein expression levels was measured using western blot analysis as described above, suggesting that MX-bound AP-sites may be able to trigger UNG transcription and translation, to overcome the repair inhibition. Furthermore, using immunofluorescence staining with UDG specific antibody, we confirm the up-regulation of UDG expression levels as well as nuclear localization of the protein after treatments with combined agents (Figure 4-4.D).

Although it is not clear yet for the exact mechanisms of induction of BER proteins, the results suggest that the expression of these BER proteins are up-regulated in response to the DNA damage formed by fludarabine and the combination of two drugs. It is apparent that up-regulation of UDG indicates the involvement of this DNA glycosylase in removing incorporated fludarabine as an aberrant base. Elevated poly β and FEN1 may suggest that MX-AP sites stall short patch BER process and simultaneously activate long patch BER, leading to upregulation of the key enzymes to pass through this blockage of repair pathway.

Figure 4-4

Induction of expression of some BER proteins and UNG mRNA levels

A, HL60 and Jurkat cells were continuously treated with drugs (5 μM fludarabine alone and fludarabine plus 3 mM MX) and collected at 24, 48 and 72 hrs. Cell lysates were subjected to western blot analysis with UDG, APE, FEN1, polymerase β, PCNA and tubulin specific antibodies. Control (lane 1), fludarabine alone (lanes 2,4,6), fludarabine plus MX lanes (3,5,7), MX alone (lane 8). ***B,*** No changes in the expression levels of other glycosylase before or after treatment of Jurkat cells with fludarabine and fludarabine plus MX. Cell lysates were subjected to western blot analysis with MPG, MBD4, Aag, TDG, OGG1 and tubulin specific antibodies. ***C,*** Folds increased relative to control of the UNG mRNA expression levels in Jurkat cells. ***D,*** Induction and localization of UDG in nucleus after treatment with fludarabine (5 μM) plus MX (3 mM) for 24 and 48 hrs. Cells were stained with UDG antibodies (green) and Hoersch dye (blue).

A

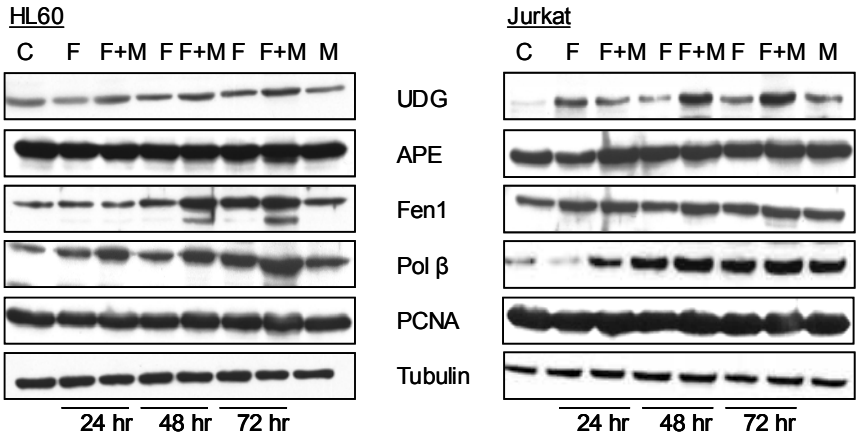
HL60
C F F+M F F+M F F+M M
Jurkat
C F F+M F F+M F F+M M
UDG
APE
Fen1
Pol β
PCNA
Tubulin
24 hr 48 hr 72 hr
24 hr 48 hr 72 hr

B

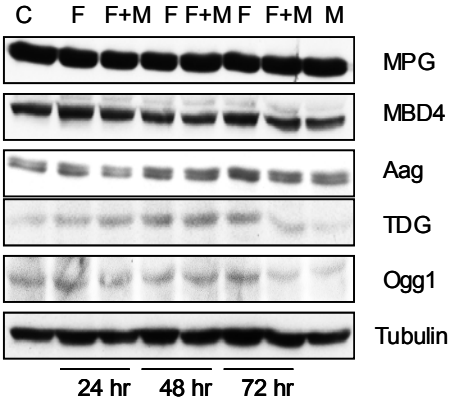
C F F+M F F+M F F+M M
MPG
MBD4
Aag
TDG
Ogg1
Tubulin
24 hr 48 hr 72 hr

C

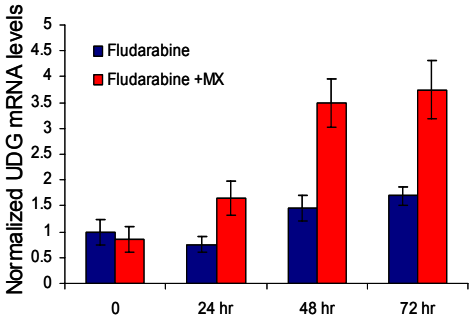
Normalized UDG mRNA levels
5
4.5
4
3.5
3
2.5
2
1.5
1
0.5
0
Fludarabine
Fludarabine +MX
0
24 hr
48 hr
72 hr

D

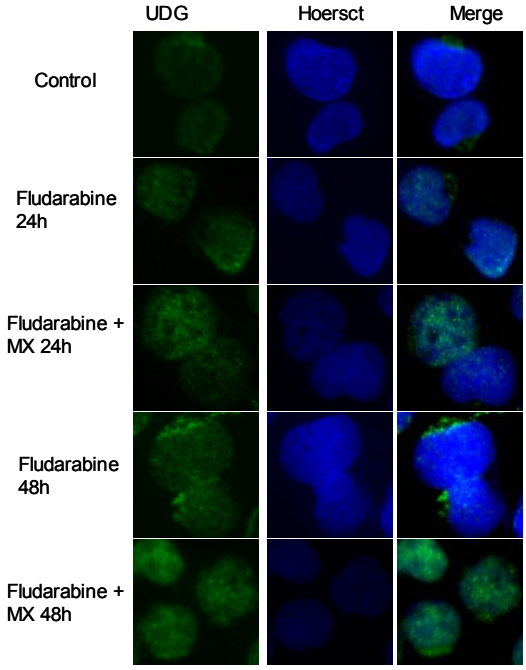
UDG
Hoersct
Merge
Control
Fludarabine 24h
Fludarabine + MX 24h
Fludarabine 48h
Fludarabine + MX 48h

4.3.3. MX enhances fludarabine-induced DNA strand breaks

Previous data showed that the combination of MX and alkylating agents, BCNU or TMZ, increased DNA strand breaks, leading to cell death (25, 26, 30, 36). To determine the induction of DNA damage induced by fludarabine alone or in combination with MX, the comet assay was introduced. Comet assay has been shown to be a sensitive and reliable measure of DNA strand breaks, AP sites, and incomplete excision repair sites. Comet images of Jurkat cells are presented in Figure 4-5. A. DNA damage in a single cell was assayed by both alkaline and neutral electrophoresis to detect single and double strand breaks, respectively. After treatment of Jurkat cells with fludarabine (0-20 μM) plus MX (3 mM) for 4 hrs, distinct comets were observed compared to fludarabine alone. Tail length determined by neutral comet assay (the appropriate parameter to quantitate DNA damage for this condition, as indicated by manufacturer's guidelines) was ~3-fold higher in cells treated with the combination of fludarabine and MX than that produced by fludarabine alone, $P< 0.05$ (Figure 4-5. B). The increased DNA double strand breaks were also observed with the duration of exposure to the combination of fludarabine (5 μM) and MX (3 mM). In contrast, tail moment determined by alkaline comet assay that measures DNA single strand breaks showed less differences in cells between the treatments with fludarabine alone and the combination in both dose and time dependent assays (Figure 4-5. C). Similar enhancement of fludarabine induced DNA strand breaks by MX was also observed in other three cancer cell lines, including HL60, U937 and SW480 (data not shown).

Figure 4-5

MX enhances single and double strand breaks in

lymphoma cells treated with fludarabine

A, Comet images assayed by neutral and alkaline electrophoresis. Jurkat cells were treated with fludarabine alone (5 μM) or fludarabine plus MX (3 mM) for 4 hrs. ***B***, Tail length of the comet detected by neutral electrophoresis in Jurkat cells after treatments with fludarabine alone (0-20 μM) and fludarabine plus MX (3 mM) and Tail length of comet detected by neutral electrophoresis at different times (4-24 hrs) after Jurkat cells treated with 5 μM fludarabine or fludarabine plus 3 mM MX (* $P<0.05$, compared with the treatment with fludarabine alone). ***C***, Tail moment of the comet detected by alkaline electrophoresis in Jurkat cells with the same treatments as described in B. Results represent the mean values of data from three independent experiments.

A

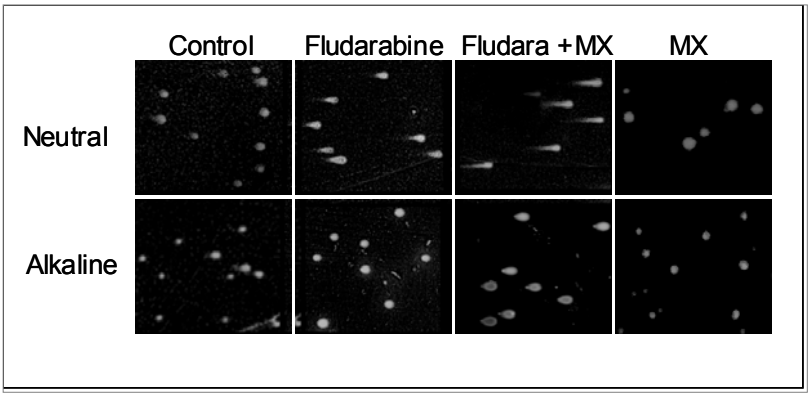
Control
Fludarabine
Fludara +MX
MX
Neutral
Alkaline

B

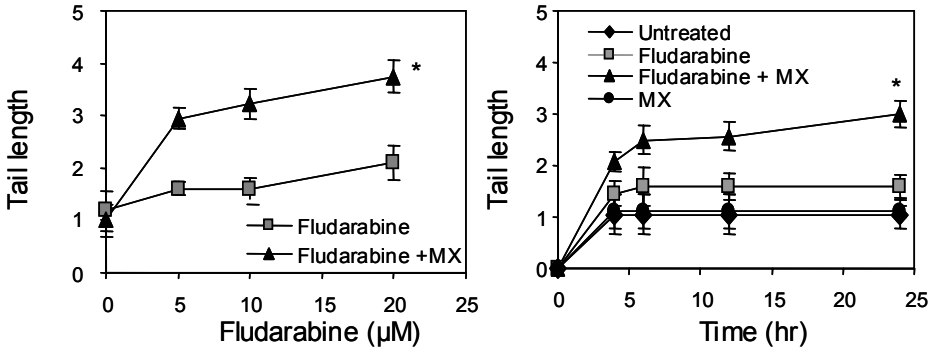
Tail length
Fludarabine (μM)
Fludarabine
Fludarabine +MX
*
Tail length
Time (hr)
Untreated
Fludarabine
Fludarabine + MX
MX
*

** p< 0.05*

C

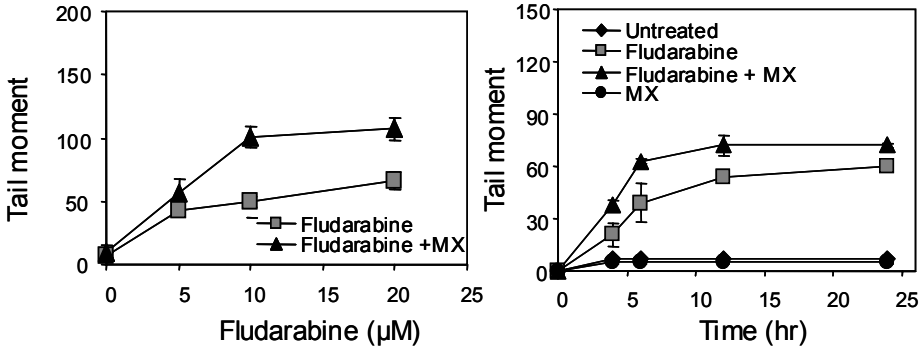
Tail moment
Fludarabine (μM)
Fludarabine
Fludarabine +MX
Tail moment
Time (hr)
Untreated
Fludarabine
Fludarabine + MX
MX

4.3.4. MX potentiates anti-tumor effect of fludarabine *in vitro*

To correlate DNA damage such as ara-AP sites and DNA strand breaks with the killing effect induced by the drug treatments, cell death was assayed. The potential of survival and cell growth were examined in cells treated with fludarabine in absence or presence of MX. Considering the fact that therapeutic efficacy of alkylating agents enhanced by MX was extensively studied in human colon tumor models, to establish the therapeutic strategy that allows for comparison between the combination of MX with alkylating agents and fludarabine, SW480 and RKO cells was selected and treated with fludarabine alone and the combination with MX. Clonogenic Survival assayed in SW480 cells (Figure 4-6. A) revealed that MX enhanced fludarabine-cytotoxicity, showing that the IC50 values for fludarabine was reduced from 13 μM to 6 μM by MX (DMF = 2.5, $p<0.05$). RKO cells were more sensitive to fludarabine alone (IC_{50} = 8 μM). Co-treatment with 3 mM MX sensitized cells to fludarabine with a dose modification factor (DMF) of 2 for RKO. HL60 and Jurkat cells were treated with fludarabine (5 μM) or fludarabine plus MX (3 mM) and the viable cells were counted using tryptan blue exclusion every 24 hrs for 5 days. Marked differences in cell growth were observed between the treatment of fludarabine in absence or presence of MX (Figure 4-6. B). At day 5, ~ 50 % HL60 cells and ~ 60 % of Jurkat cells remain viable after fludarabine alone, in contrast, the combining fludarabine and MX significantly decreased the survival of cells; only 13.3 % in HL60 and 24 % in Jurkat cells survived. The augment of cytotoxicity of fludarabine by MX in these leukemia cells was also about 2.5 – 3.0 folds ($p<0.02$).

Figure 4-6

MX potentiates therapeutic effect of fludarabine in tumors cells

A. Comparison of the cytotoxicity induced by fludarabine alone (0-20 μM) and the combination of fludarabine and MX (3 mM) in tumors cells assayed by clonogenic formation assay (SW480, RKO). ***B,*** Myeloid leukemia cells (HL60) and ***C,*** Lymphoma cells (Jurkat) were treated with 5 μM fludarabine and fludarabine plus 3 mM MX and cell viability was determined by tryptan blue exclusion. Cell viability is expressed as percentage of untreated control (growth inhibition assay).

A

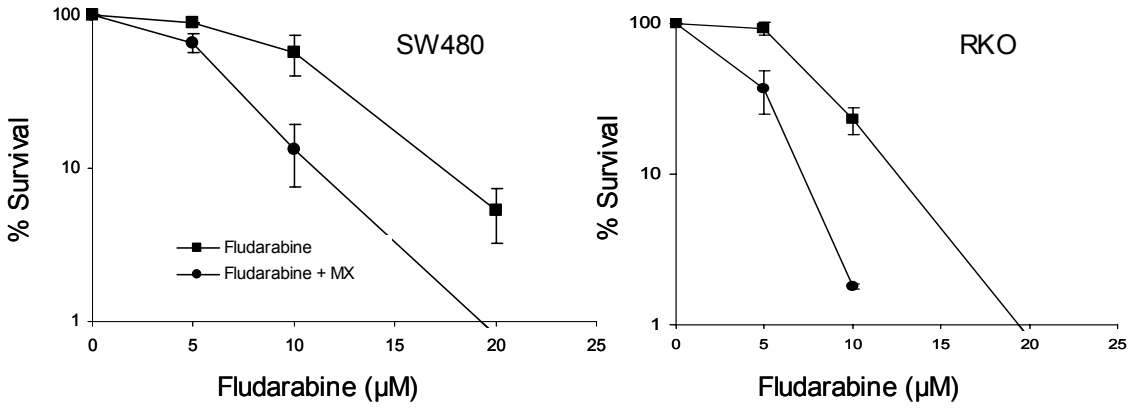
SW480
RKO
% Survival
Fludarabine (μM)
Fludarabine
Fludarabine + MX

B

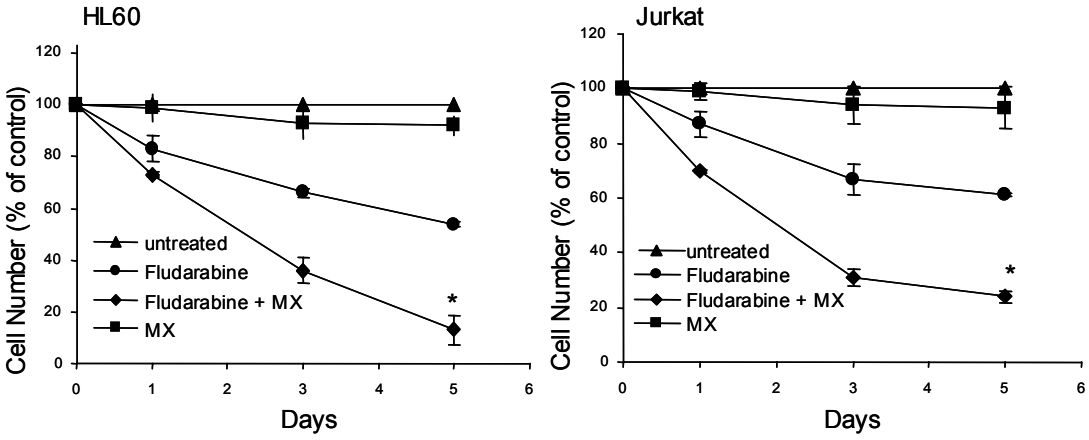
HL60
Jurkat
Cell Number (% of control)
Days
untreated
Fludarabine
Fludarabine + MX
MX
*

4.3.5. MX potentiates anti-tumor effect of fludarabine *in vivo*.

The therapeutic efficacy of this combination was further evaluated in xenografts of HL60, U937 and SW480 cells in nude mice. When the tumor volumes reached 100-150 mm^3 mice were divided into control and treatment groups (6-9 mice/group). Mice received a single i.p. daily injection of fludarabine alone (15 mg/kg), MX (2 mg/kg) alone or the combination of the two drugs (fludarabine 15 mg/kg and MX 2 mg/kg), for 5 consecutive days. Tumor responses were determined by tumor growth delay. As shown in Figure 4-7 , a moderate sensitivity to fludarabine was observed in both xenografts, but combined treatment significantly reduced tumor growth. HL60 xenograft treated with PBS for 17 days had a mean tumor volume of 2500±106 mm^3 compared with a mean tumor volume of 1456±76 mm^3 and 643±142 mm^3 ($P< 0.05$) in mice treated with fludarabine alone or in combination with MX, respectively. Similarly, MX enhanced the tumor inhibitory effect of fludarabine was observed in U973 and SW480 xenografts. The tumor growth delays were 11±0.6 days for HL60, 9±1.1 days for U973 and 10± 0.9 for SW480 ($P< 0.05$). At these doses, mice did not present any evidence of toxicity, evaluated by measurements of the body weight and whole blood toxicity analysis.

Figure 4-7

MX potentiates therapeutic effect of fludarabine in human xenografts

Methoxyamine enhanced antitumor effect of fludarabine in human xenografts (HL60, U937 and SW480). * $P<0.05$ compared with the treatment with fludarabine alone.

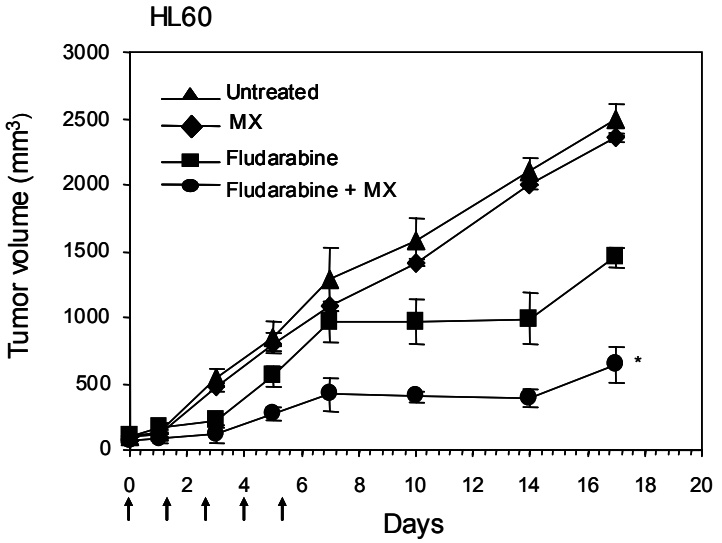
HL60
Untreated
MX
Fludarabine
Fludarabine + MX
Tumor volume (mm3)
Days
*

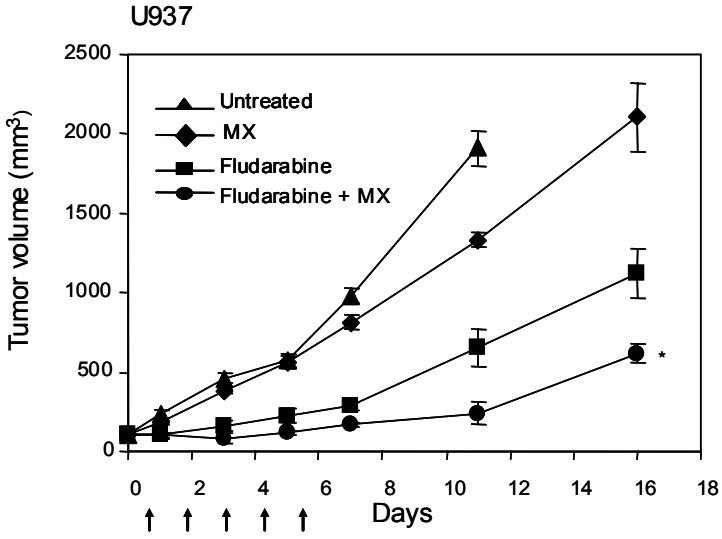
U937
Untreated
MX
Fludarabine
Fludarabine + MX
Tumor volume (mm3)
Days
*

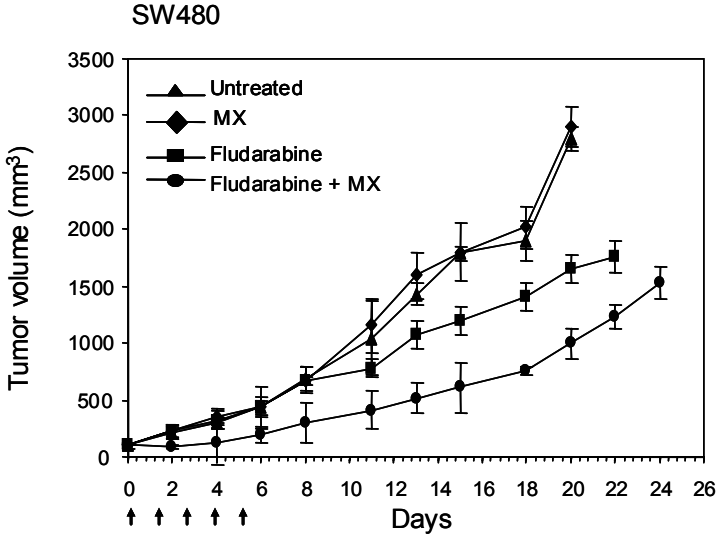
SW480
Untreated
MX
Fludarabine
Fludarabine + MX
Tumor volume (mm3)
Days

4.4. Discussion

We demonstrated that (*i*) the incorporation of fludarabine is processed by BER mechanism, resulting in formation of ara-AP sites (*ii*) MX-blocked repair of ara-AP-sites produced by fludarabine increases cell death through the blockage of BER, identifying a new mechanism for fludarabine; (*iii*) MX potentiates the therapeutic efficacy of fludarabine, developing a novel therapeutic strategy to combine inhibitor of BER with fludarabine for clinical treatment.

Incorporation of fludarabine into DNA initiates the process of BER. As presented in Chapter 3 by using oligonucleotide substrates containing F-ara-A residues, *in vitro and ex vivo* UDG excised incorporated F-ara-A from DNA. This enzymatic action by UDG will probably result in formation of an ara-AP-site in the DNA. Therefore, AP sites in DNA, as the intermediates generated during base excision repair of abnormal bases, are the indicators of activated BER pathway. In this study we demonstrated that ara-AP site formation is proportional with fludarabine dose and time-exposure, indicating that incorporated fludarabine is substrate of BER. This was further supported by studies demonstrating that a fludarabine dose dependent formation of ara-AP sites was detected in cells expressing UDG but not in their counterparts, in which expression of UDG has been genetically turned off through UNG gene knockout. When genomic DNA of these $UNG^{-/-}$ cells treated with fludarabine was in vitro reacted with purified UDG, a significant increase in AP sites was measured. These results provide further evidence of the role of UDG as well as the involvement of BER in processing incorporated fludarabine in cell. However, we can not rule out the possibility of other glycosylases that may also have the activity excising F-ara-A from DNA in cells, considering the fact that several DNA N-

glycosylases have been identified in mammalian cells and that each excises a specific damaged base with high specificity but allows some overlapping substrates (37).

MX binds to ara-AP sites to block BER. BER is the most pro-active repair pathway that corrects DNA modifications arisen either spontaneously or from attack by reactive chemicals and anticancer agents. BER is an essential repair pathway to maintain genome stability and normal development, and is quantitatively an important mechanism of DNA repair, by which drug resistance to variety of agents occurs. Thus, balanced expression of BER proteins is crucial for a proper repair activity.

MX has been developed as a blocker of BER to potentiate cytotoxicity of alkylating therapeutic agents such as TMZ and BCNU (24-27, 30). The action of MX to block BER pathway is through the binding of an aldehyde group in an AP site, the tautomeric open-ring form of deoxyribose. This biochemical reaction converts a repairable AP-site into MX-bound AP-site. This DNA lesion is refractory to the lyase activity of APE and poly β, consequently blocking the BER pathway. Our results presented in Figure 4-2. confirmed the role of MX in binding to ara-AP sites formed by fludarabine and the ability of MX-bound AP-sites to block repair of APE. Another important validation link of the involvement of BER in response to the DNA damage induced by the therapeutic treatment with fludarabine alone or in combination with MX was the findings of induction of several BER proteins, including UDG, poly β and FEN1 in cells. UDG was significantly up-regulated after drug treatments, especially in cells treated with combination of fludarabine and MX. Based on the observation that UDG has a higher affinity for the products of AP-site than the actual substrate itself (44), it has been proposed that subsequent to base release, UDG remains quickly rebound to the AP site to

protect the cell until the AP site was conveyed to APE and poly β, the next enzymes in the BER-pathway. Thus one possible explanation for induction of UDG by fludarabine and MX is that the persistence of MX-bound AP-sites results in the accumulation of UDG at un-repairable MX-bound AP-sites. DNA poly β is known to be the polymerase of choice and limiting factor for the short patch BER due to its dual enzymatic activity, and FEN1 recognizes and cleaves the single stranded DNA 'flap' structures during the long patch repair process. Thus, the elevated poly β and FEN1 suggest that MX-bound ara-AP-sites impact on both short and long patch BER (18). Although the mechanisms of regulation of BER proteins by the drug treatments are not clear yet, results suggest that BER proteins have an adaptive response to DNA damage that is exaggerated by the combination of fludarabine and MX. One possibility would be that the unrepaired damage, MX-bound AP-sites is recognized by protective proteins such as Akt which will lead to activation of several transcription factors. Another possible mechanism is again mediated by MX-bound AP sites that can not be further process by BER which will lead to increase transcription of the proteins involved in the repair process.

Lethal DNA lesions induced by the combination of fludarabine and MX contribute to cell death. Combining fludarabine with MX indeed increased lethal cytotoxicity in comparison with fludarabine alone. The combination produced higher levels of DNA strand breaks and more cell death that were related to the persistence of MX-bound AP-sites. We have previously demonstrated that MX-bound AP-sites are stable DNA lesions that can stall DNA synthesis, showing S phase arrest in cells after treatments. Cellular responses to the replication stalling by the combination of MX and alkylating agent such as TMZ (24) were accompanied by varying amounts of interphase nuclear DNA breaks

and associated metaphase chromosomal aberrations (i. e., chromosome fragmentation and sister chromatin exchange events). We have also reported that MX-bound AP-site acts as a topo II poison to trap topo II in DNA cleavage complex, resulting in topo II mediated DNA strand breaks and apoptosis (31). Thus, MX-bound AP-sites lethally cause cell death in many ways.

Although fludarabine is widely used to treat hematological malignancies, the therapeutic effect has been limited by several factors. For example, the major cytotoxic effect of fludarabine appears to be specific to replicating cells, which may result in less effective of fludarabine in indolent diseases because these tumor cells are usually quiescent (10,42). Fludarabine can induce cell cycle arrest and apoptosis that is thought to act primarily through the activation of p53. However, p53 is the most commonly mutated tumor suppressor gene in human cancer. Tumor cells carrying an inactivating mutation of p53 have been reported to be resistant to fludarabine (43, 44). Thus, MX enhanced-therapeutic efficacy of fludarabine by blocking BER should be promising with merits to overcome these resistant factors. Obviously, blocking BER induced cytotoxicity is non cell cycle specific, because BER mechanism is active throughout the entire cell cycle. Therefore, the potentiation of fludarabine by MX can be expected to be effective on both proliferating and resting tumor cells. Importantly, we demonstrated that MX enhanced fludarabine cytotoxicity in HL60 and Jurkat cells. These two cell lines are p53 deficient and Jurkat has the defect in function of mismatch repair (MMR). Thus, the potentiation by MX is independent of p53 and MMR status, which agrees with our previous observations (24, 26).

Implications of cancer treatment. The studies presented here suggest a viable synergistic approach for enhancing fludarabine cancer therapy involving disruption of base excision repair. Targeting BER-based therapeutic strategy can be extended to the combination of MX with any drugs that produce abnormal bases to incorporate into DNA either through acting as the nucleotide analogs or manipulating the nucleotide pools. Overall, this therapeutic strategy could improve both therapeutic index by decreasing the dose of anticancer drugs and therapeutic efficacy for the treatment of hematological malignancies.

4.5. References

1. Pettitt AR. Mechanism of action of purine analogues in chronic lymphocytic leukemia. Br J Haematol 2003;121:692-702.
2. Gandhi V, Plunkett W. Cellular and clinical pharmacology of fludarabine. Clin Pharmacokinet 2002;41:93-103.
3. Plunkett W, Kawai Y, Sandoval A, et al. Mechanism-based rationales for combination therapies of lymphoid malignancies. Haematologica 1999;84:73-77.
4. Mansson E, Spasokopukotskaja T, Sallstrom J, Eriksson S, Albertioni F. Molecular and biochemical mechanisms of fludarabine and cladribine resistance in a human promyelocytic cell line. Cancer Res 1999;59:5956-63.
5. Molina-Arcas M, Bellosillo B, Casado FJ, et al. Fludarabine uptake mechanisms in B-cell chronic lymphocytic leukemia. Blood 2003;101:2328-34.
6. Kamiya K, Huang P, Plunkett W. Inhibition of the 3'-5' exonuclease of human DNA polymerase ε by fludarabine-terminated DNA. J Biol Chem 1996;271:19428-35.
7. Skalski V, Brown KR, Choi BY, Lin ZY, Chen S. A 3'-5' exonuclease in human leukemia cells: implications for resistance to 1-beta -D-arabinofuranosylcytosine and 9-beta-D-arabinofuranosyl-2-fluoroadenine 5'-monophosphate. J Biol Chem 2000;275:23814-19.
8. Yang SW, Huang P, Plunkett W, Becker F, Chan JYH. Dual mode of inhibition of purified DNA ligase I from human cells by 9-β-D-Arabinofuranosyl-2-fluoroadenine triphosphate. J Biol Chem 1992;267:2345-9.
9. Huang P, Chubb S, Plunkett W. Termination of DNA synthesis by 9-β-D-Arabinofuranosyl-2-fluoroadenine. J Biol Chem 1990; 265:16617-25.

10. Iwasaki H, Huang P, Keating MJ, Plunkett W. Differential incorporation of ara-C, gemcitabine and fludarabine into replicating and repairing DNA in proliferating human leukemia cells. Blood 1997;90:270-8.
11. Rao VA, Plunkett W. Activation of a p53-mediated apoptotic pathway in quiescent lymphocytes after the inhibition of DNA repair by fludarabine. Clin Cancer Res 2003;9:3204-12.
12. Srivastava DK, Berg BJV, Prasad R, et al. Mammalian abasic site base excision repair. J Biol Chem 1998;273:21203-9.
13. Fortini P, Parlanti E, Sidorkina OM, Laval J, Dogliotti E. The type of DNA glycosylase determines the base excision repair pathway in mammalian cells. J Biol Chem 1999;274:15230-6.
14. Sokhansanj B, Rodrigue GR, Fitch JP, Wilson DM. A quantitative model of human DNA base excision repair. I. Mechanistic insights. Nucleic Acids Res 2002;30:1817-25.
15. Hoeijmakers JH. Genome maintenance mechanisms for preventing cancer. Nature 2001;411:366-74.
16. Matray TJ, Kool ET. A specific partner for abasic damage in DNA. Nature 1999;399:704-8.
17. Wilson SH. Mammalian base excision repair and DNA polymerase beta. Mutat Res 1998;407:203-15.
18. Horton JK, Prasad R, Hou E, Wilson SH. Protection against methylation-induced cytotoxicity by DNA polymerase β-dependent long patch base excision repair. J Biol Chem 2000;275:2211-18.

19. Prasad R, Dianov GL, Bohr VA, Wilson SH. FEN1 stimulation of DNA polymerase β mediates an excision step in mammalian long patch base excision repair. J Biol Chem 2000;275:4460-6.
20. Podlutsky AJ, Dianova Il, Podust VN, Bohr VA, Dianov GL. Human DNA polymerase beta initiates DNA synthesis during long-patch repair of reduced AP sites in DNA. EMBO J 2001;20:1477-82.
21. Chapados BR, Hosfield DJ, Han S, et al. Structural basis for FEN-1 substrate specificity and PCNA-mediate activation in DNA replication and repair. Cell 2004;116:39-50.
22. Trivedi RN, Almeida KH, Fornsaglio JL, Schamus S, Sobol RW. The role of base excision repair in the sensitivity and resistance to temozolomide-mediated cell death. Cancer Res 2005;65:6394-400.
23. Liuzzi M, Talpaert-Borle M. A new approach to study of the base excision repair pathway using methoxyamine. J Biol Chem 1985;260:5252-8.
24. Rosa S, Fortini P, Karran P, Bignami M, Dogliotti E. Processing in vitro of an abasic site reacted with methoxyamine: A new assay for the detection of abasic sites formed in vivo. Nucleic Acids Res 1991;19:5569-74.
25. Liu L, Taverna P, Whitacre CM, Chatterjee S, Gerson SL. Pharmacological disruption of base excision repair sensitizes mismatch repair deficient and proficient colon cancer cells to methylating agents. Clin Cancer Res 1999;5:2908-17.
26. Liu L, Gerson SL. Base excision repair as a therapeutic target in colon cancer. Clin Cancer Res 2002;8:2985-91.

27. Liu L, Yan L, Donze JR, Gerson SL. Blockage of abasic site repair enhances antitumor efficacy of 1,3-bis-(2-chloroethyl)-1-nitrosourea in colon tumor xenografts. Mol Cancer Ther 2003;2:1061-6.
28. Taverna P, Hwang HS, Schupp JE, et al. Inhibition of base excision repair potentiates iododeoxyuridine-induced cytotoxicity and radiosensitization. Cancer Res 2003;63:838-46.
29. Rinne M, Caldwell D, Kelley MR. Transient adenoviral N-methylpurine DNA glycosylase overexpression imparts chemotherapeutic sensitivity to human breast cancer cells. Mol Cancer Ther 2004;3:955-67.
30. Fishel ML, He Y, Smith ML, Kelley MR. Manipulation of base excision repair to sensitize ovarian cancer cells to alkylating agent temozolomide. Clin Cancer Res 2007;13:260-7.
31. Liu L, Gerson SL. Therapeutic impact of methoxyamine: Blocking repair of abasic sites in the base excision repair pathway. Curr Opin Investig Drugs 2004;5:623-7.
32. Yan L, Bulgar A, Miao YL, et al. Combined treatment with temozolomide and methoxyamine: blocking apurinic/pyrimidinic site repair coupled with targeting topoisomerase IIα. Clin Cancer Res 2007;13:1532-9.
33. Nakamura J, Swenberg JA. Endogenous apurinic/apyrimidinic sites in genomic DNA of mammalian tissues. Cancer Res 1999;59:2522-6.
34. Nakamura J, Walker VE, Upton PB, Chiang SY, Kow YW, Swenberg JA. Highly sensitive apurinic/apyrimidinic site assay can detect spontaneous and chemically induced depurination under physiological conditions. Cancer Res 1998;58:222-5.

35. Atamna H, Cheung I, Ames BN. A method for detecting abasic sites in living cells: age-dependent changes in base excision repair. Proc Natl Acad Sci U S A 2000;97:686-91.

36. Helma C, Uhl M. A public domain image-analysis program for the single cell-gel-electrophoresis (comet) assay. Mutat Res 2000;466:9-15.

37. Sharma R, Dianov G. Targeting base excision repair to improve cancer therapies. Mol Aspects of Med 2007; 28:345-74.

38. Cone R, Bonura T, Friedberg EC. Inhibitor of uracil-DNA glycosylase induced by bacteriophage PBS2. Purification and preliminary characterization. J Biol Chem 1980; 255:10354–58.

39. Mol CD, Arvai A, Sanderson R J et al. (1995). Crystal structure of the human Uracil-DNA glycosylase in complex with a protein inhibitor: protein mimicry of DNA. Cell 1995; 82: 701–708.

40. Taverna P, Liu L, Hwang HS, Hanson AJ, Kinsella TJ, Gerson SL. Methoxyamine potentiates DNA single strand breaks and double strand breaks induced by temozolomide in colon cancer cells. Mutat Res 2001;485:269-81.

41. Mauro DJ, De Riel JK, Tallarida RJ, Sirover MA. Mechanism of excision of 5-fluoruracil by uracil DNA glycosylase in normal human cells. Molec Pharma 1993; 43:854-57.

42. Nilsen H, Krokan HE. Base excision repair in a network of defense and tolerance. Carcinogenesis 2001;22:987-98.

43. Parikh SS, Mol CD, Slupphaug G, Bharati S, Krokan HE, Tainer JA. Base excision repair initiation revealed by crystal structures and binding kinetics of human uracil-DNA glycosylase with DNA. EMBO1998;17:5214-26.
44. Takagi K, Kawai Y, Yamauchi T, Ueda T. Inhibition of repair of carboplatin-induced DNA damage by 9-β-D-arabinofuranosyl-2-fluoroadenine in quiescent human lymphocytes. Biochem Pharmacol 2004;68:1757-66.
45. Faria JR, Yamamoto M, Faria RMD, Kerbauy J, Oliveira JSR. Fludarabine induces apoptosis in chronic lymphocytic leukemia- the role pf p53, Bcl-2, Bax, Mcl-1 and Bag-1 proteins. Braz J Med Biol Res 2006;39:327-33.
46. Sampath D, Rao VA, Plunkett W. Mechanism of apoptosis induction by nucleoside analogs. Oncogene 2003;22:9063-74.

CHAPTER V

MITOCHONDRIAL MEDIATED CELL DEATH INDUCED BY FLUDARABINE COMBINED WITH METHOXYAMINE DUE TO BLOCKAGE OF BASE EXCISION REPAIR PATHWAY

Abstract

Nuclear and mitochondrial DNA are constantly being exposed to damaging agents from endogenous and exogenous sources. To ensure viability of cells, elaborate mechanisms of DNA repair are essential for both nuclear and mitochondrial DNA (mtDNA). We have previously shown that base excision repair (BER) is activated by the fludarabine induced DNA damage. Methoxyamine (MX), an inhibitor of BER is able to enhance fludarabine cytotoxicity in cancer cell lines and human xenografts. The process of mitochondrial BER (mtBER) is very similar to that in nuclei, thus we hypothesize that mtDNA is also a target for fludarabine and MX and may represent an important aspect of cell death. We have demonstrated that dose dependent fludarabine treatments resulted in

proportional formation of mitochondrial AP sites, which are formed after the first step in mitochondrial BER. These mtAP-sites were efficiently bound by MX. MX-bound AP-sites may become stable DNA lesions that have the potential to interrupt mtBER mechanism, leading to apoptotic cell death. These events were accompanied by a concomitant increase cleavage of PARP and caspase 9, loss of mitochondrial membrane potential (JC-1 staining) and integrity and enhanced expression levels of proapoptotic mitochondrial proteins (e.g., Bax.). Together, our findings suggest a mitochondrial mediated apoptotic death after fludarabine and MX treatments.

5.1 Introduction

Many of the effective chemotherapeutic agents such as nucleoside analogues have mechanisms of action that target DNA. The ability of tumor cells to tolerate DNA damage and maintain their viability after treatments may contribute to reduce the desirable, cytotoxic outcome. Therefore, elucidating the mechanism that sense and repair DNA damage and targeting this mechanism is essential for development of more effective therapeutic strategies.

Fludarabine, an adenosine analogue, is effective in the treatment of the hematological malignancies such as chronic lymphocytic leukemia and non-Hodgkin's lymphoma (1, 2). Fludarabine is a potent inhibitor of DNA synthesis through the actions of its triphosphate metabolite, F-ara-ATP (3-8). F-ara-ATP incorporates into replicating strand causing reduced DNA synthesis. We have previously reported that a major DNA repair pathway, base excision repair, is involved in the cell response to fludarabine treatments, through the enzymatic activity of uracil-DNA glycosylase (9). Furthermore,

we have shown that methoxyamine (MX), a known inhibitor of BER, enhanced antitumor effect of fludarabine *in vitro* and in human tumor xenografts. MX binds to arabinosyl (ara)-AP sites formed by fludarabine and turn the repairable DNA damage into lethal lesion, leading to cell death. However, the molecular mechanism by which cells are killed by the combined treatment, fludarabine and MX is largely unknown.

Apoptosis, the most common form of cell death, is known to occur via an extrinsic (death receptor-ligand) or intrinsic (mitochondrial-centered) pathway (10). The apoptotic cascade is characterized by the activation of cysteine proteases called caspases, which cleave proteins essential for the survival of the cell. These caspases activate the endonucleases responsible for the internucleosomal cleavage of genomic DNA (11). Mitochondria play a key role in the events leading to caspases activation in cell undergoing apoptosis (12). Cell death at the mitochondrial level is initiated by alteration of the mitochondrial membrane which induce release of cytochrome c in cytosol where forms a complex with Apaf1 (apoptotic protease activating factor-1), ATP and inactive initiator procaspase-9, called the apoptosome (13-15). This complex is sufficient to recruit and activate caspase-9. Once activated, caspases-9 cleaves the downstream caspases (16,17). Death initiated by mitochondria is regulated by members of the Bcl-2 family (18).

In our studies, we note that treatments with fludarabine and MX resulted in a significant percentage of cells that undergo apoptosis. We propose that mitochondrial DNA (mtDNA) may also be an important target for fludarabine and MX, in addition to the conventional target, nuclear DNA (9) and together, these two DNA damage signals contribute to induction of mitochondrial mediated apoptosis.

Mt DNAs, 16.5 kb circular DNA molecules, have their own DNA repair systems (19). Mitochondrial BER (mtBER) pathway is very similar to the nuclear pathway and includes four distinct steps: lesion removal by a glycosylase, AP sites processing by an AP-endonuclease, insertion of a new nucleotide by polymerase γ and ligation by a DNA ligase (20-25). Thus, we propose that mtBER may be activated in response to fludarabine induced mtDNA damage. If MX binds mtAP-sites and thereby blocks the BER pathway in mitochondria, the level of damage induced by fludarabine will eventually become severe leading to lost of mitochondria ability to maintain their membrane potential and then activate apoptotic death pathway.

5.1.1. Hypothesis and Rationale

Research focus: To delineate the contribution of mitochondrial apoptotic pathway in cell death after fludarabine and MX exposure.

We hypothesized that cell death induced by fludarabine and MX is increased due to apoptotic signals emanating from mitochondrial DNA damage (Figure 5-1.).

We have examined whether fludarabine targets mtDNA and whether fludarabine is a substrate for mitochondrial BER. We also evaluated if MX is able to bind mitochondrial AP sites, thus blocking the repair pathway. Fludarabine and MX treatments resulted in a mitochondrial mediated apoptotic death.

Figure 5-1

Working model: mitochondrial BER response to Fludarabine-induced DNA damage which triggers mitochondrial mediated apoptotic cell death

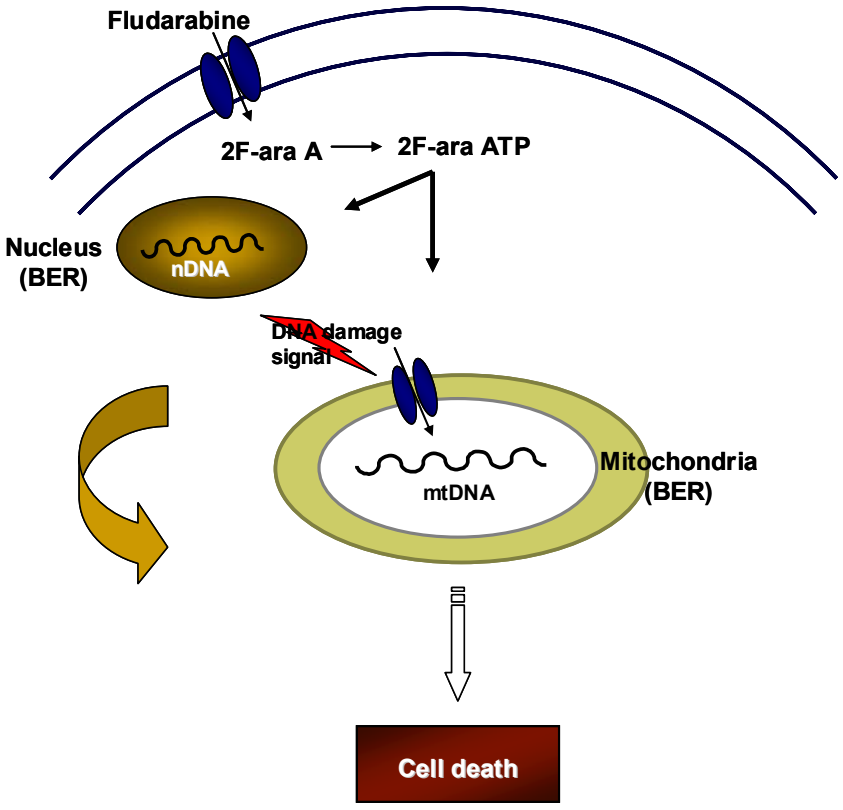
Fludarabine
2F-ara A
2F-ara ATP
Nucleus
(BER)
nDNA
DNA damage
signal
mtDNA
Mitochondria
(BER)
Cell death

5.2. Materials and Methods

5.2.1. Cells and reagents

Human tumor cell lines, Jurkat (lymphoblastic) and HL60 (myelocitic leukemic) used in these studies were obtained from the American Type Culture Collection (Rockville, MD) and cultured in proper mediums. Fludarabine was obtained from Berlex Laboratories (Richmond, CA) and freshly prepared with mediums (containing alkaline phosphatase) for the treatment. Methoxyamine (MX) was purchased from Sigma Chemical Co (St. Louis, MO). MX was dissolved in sterilized water (pH 7.0) and stock solution (2.5 M) was stored at -20 ºC.

5.2.2. Extraction of mitochondrial DNA

Mitochondrial DNA isolation was carried out as described previously (23) with some modifications. After treatments, cells were harvested and washed with PBS. The cell pellet was resuspended in 10 mM Tris- 10 mM EDTA buffer; 10 % SDS solution was added and incubated at room temperature for 10 min. RNase A was added for 15 min at 37 °C followed by incubation with Proteinase K for 15 min at 37 °C. 5 M NaCl was added to precipitate the high molecular DNA, overnight at 4 °C. The cell lysate was centrifuged at 12,000 rpms for 30 min at 4 °C. The supernatant was transferred to a new tube and the remaining cell lysate was centrifuged again for 10 min at same speed. The supernatants were combined and mtDNA was extracted once with phenol: chlorophorm (1:1 v/v) and 1:1 v/v to above lysate supernatants. The mixture was centrifuged at 6000 rpms for 10 min. The aqueous phase was transferred to a new tube and mtDNA was

precipitated by adding 2 x volume of cold 100 % ethanol. The mtDNA was washed once and resuspended in water.

5.2.3. AP site assay

The AP sites were measured using ARP (aldehyde reactive probe) reagent. ARP and MX have the same chemical reactivity; they competitively bind to an aldehyde group at an AP site. Therefore, ARP only detects MX-free AP sites. The assay was performed as previously described with minor modifications (26-29). Briefly, cells ($2x10^6$) were plated and exposed to fludarabine (0-20 μM) with or without MX (3 mM). Cells were collected at 24 hr after treatment and dose-dependent AP sites were measured. After extraction, mtDNA (10 μg) was incubated with 15 μl of 1 mM ARP (Dojindo Laboratories, Kumamoto, Japan) in 150 μl PBS solution at 37 ºC for 15 min. DNA was then precipitated with 400 μl ice-cold ethanol (100 %) at -20 ºC for 20 min and washed with 70 % ethanol. MtDNA was dried at room temperature for 30 min and then resuspended in TE buffer to achieve a final concentration of 0.3 μg/100 μl. The ARP-labeled mtDNA was then heat-denatured at 100 ºC for 5 min, quickly chilled on ice and mixed with an equal amount of 2 M ammonium acetate. The DNA was then immobilized on BA-S 85 nitrocellulose membrane (Schleicher and Schuell, Dassel, Germany) using a minifold II vacuum filter device (Schleicher and Schuell, Dassel, Germany). The membrane was baked at 80 ºC for 1 hr and incubated with 0.25 % BSA/PBS containing streptavidin-conjugated horseradish peroxidase (BioGenex, SanRamon, CA) at room temperature for 40 min with gentle shaking. ARP-labeled mtAP sites were visualized by

chemiluminescence (Amersham Corp, Piscataway, NJ) followed by quantitative densitometry using NIH ImageJ software.

5.2.4. Detection of mitochondrial DNA damage using PCR analysis

Amplification products were obtained by PCR of purified mitochondrial DNA. Primers pairs that target human mitochondrial genome were L-primer (5' - ^{15717} CTTTATTGACTCCTAGCCGCAGAC ^{15740} – 3') and H-primer (5'- ^{3590} CTGGTCAACCTCAACCTAGGCC ^{3611} -3'), which yield a product of 4467 bp (Figure 4-2 A). Template primers, 5 μL of 10 x buffer (without $MgCl_2$) and dH_2O were mixed in a 0.2 ml thin-walled PCR tube and heated for 5 min at 99.9 °C. The mixture was immediately placed on ice, at which time the remaining reagents were added. The final concentrations in the 50 μL amplification cocktail were 1x PCR buffer (Invitrogen), 300 nM each primers, 1.5 mM $MgCl_2$, 200 μM each dNTP and 2.6 U of Taq DNA polymerase. The PCR cycling profile used was: a pre-PCR incubation at 94 °C for 2 min, then 25 cycles of 94 °C for 15 sec, 50 °C for 30 sec and 68 °C for 4 min and then to 4 °C using the PCR system. Controls for the PCR were performed by amplification of GAPDH gene. The primers used for GAPDH were the following: GAPDH sense 5' GAGGGGCCATCCACAGTCTTCTG 3' and GAPDH antisense 5' CCCTTCATTGACCTCAACTACATGGT 3' (Sigma Genosys, Woodlands, TX). The PCR profile for the GAPDH gene amplification was the following: 24 cycles made up by 4 steps; *1*: 4 min at 95 °C, *2:* 55 s at 95 °C, *3:* 55 s at 65 °C and *4:* 30 s at 72 °C; followed by 6 min at 72 °C. An aliquot of each reaction mixture after PCR, in 6x loading buffer, was resolved by electrophoresis in TBE buffer at 90 V in a 0.5 % agarose gel.

5.2.5. Western blot analysis

Cellular protein content was quantified spectrophotometrically using the Bio-Rad assay. Equal amounts of proteins (30 μg) were separated by SDS-PAGE and transferred to PVDF membrane (Millipore Cor., Bedford, MA). After blocking in 5 % non-fat dry milk in TBST for 40 min at room temperature, the blots were incubated with primary antibody for 1 hour at room temperature. Sources of primary antibody were as follows: Bcl2, Bax (Santa Cruz Biotechnology, CA), cleaved caspase 9 (Cell Signaling, Danvers, MA), cleaved PARP (BD Pharmingen, San Jose, CA), γH2AX (Bethyl, Montgomery, Texas), α-Tubulin (Sigma-Aldrich, St Louis, MO). The primary antibody solutions were prepared in 1 % non-fat dry milk in TBST solution as followed: cleaved PARP 1: 1000 v/v dilution, Bcl2 1:200 v/v dilution, Bax 1:200 v/v dilution, cleaved caspases 9 1:500 v/v dilution, γH2AX 1:1000 v/v dilution, and Tubulin 1:500 v/v dilution. Blots were incubated with HRP-conjugated secondary antibody at room temperature for 1 hour. The blots were visualized by ECL (Amersham Corp, Piscataway, NJ) according to the manufacturer instructions.

5.2.6 Measurement of apoptosis by Annexin V staining

Cells were continuously treated with fludarabine (0-20 μM), MX (3 mM) or both drugs in combination and collected after 24, 48 and 72 hrs drug exposure. After two washes with PBS, cells were resuspended in 1 x binding buffer at a concentration of 1 x 10^6/mL. Cells were exposed at room temperature for 15 min to 5-μL Annexin V-FITC (BD Bioscience, San Jose, CA) following the instructions of the manufacturer. Analysis was carried out with FACSort (Becton Dickinson & Co., Mountain View, CA).

5.2.7. Cytofluorometric analysis of mitochondrial transmembrane potential (ΔΨm) by JC1

JC-1 (5,5',6,6'-tetrachloro-1,1',3,3'-tetraethylbenzimidazoyl carbocyanine iodide, Cell Technologies, Mountain View, Ca) is a lipophilic cationic dye that enters the inner mitochondrial matrix in its monomeric form when the mitochondrial membrane is polarized (Reers *et al*., 1991, 1995). Cells were treated with the indicated amounts of drugs either alone or in combination for 24 hrs. Cells were then washed with 1 x assay buffer and incubated for 15 min at 37 ºC with 1x JC1 reagent. In healthy cells the dye stains the mitochondria bright red. In the apoptotic cells, the mitochondrial membrane potential collapses and the JC1 reagent cannot accumulate within the mitochondria. In these cells JC1 remains in the cytoplasm in a green fluorescent monomeric form. The red form has absorption/emission maxima at 585/590 nm, while the green monomeric form has absorption/emission maxima at 510/527 nm. Cells were analyzed on FACSCalibur (Becton Dickinson, San Jose, CA) flow cytometer.

5.2.8. Immunofluorescence microscopy

Cells were grown on a 6 wells plate and were treated with fludarabine and fludarabine plus methoxyamine for 24 and 48 hrs. At each time point, cells were washed with PBS and incubated with 250 nM MitoTracker (Molecular Probes, Carlsband. CA) at 37 °C for 45 min. Then, cells were washed twice with PBS and cytospin on a slide at 600 g, for 8 min. Both treated and untreated cells were fixed in 2 % paraformaldehyde and permeabilized with 0.2 % Triton X-100. Cells were incubated with primary cytochrome C antibody (Santa Cruz) for 1 hrs at room temp, followed by secondary antibody

conjugated to Alexa 488 (green) (Molecular Probes, Carlsband, CA). Nuclei were stained using Hoersch dye, 2 mg/ml, for 30 min at room temperature. Images were digitally captured using an Olympus microscope equipped with a digital camera.

5.3. Results

5.3.1. Exposure to fludarabine alone and in combination with MX leads to mtDNA damage

Previous studies have reported that one class of nucleotide transporter (hENT1) is localized in the mitochondrial compartment (30). Several nucleotide analogues have been shown to use hENT1 transporter to target mtDNA (31). However, it is not clear whether fludarabine is actively transported into mitochondrial and subsequently induces mtDNA damage. In these studies we employed a PCR based method to measure the mtDNA damage after drug treatments. HL60 and Jurkat cells were treated with fludarabine alone (0-80 μM) or fludarabine plus MX (3 mM) and harvested at 24 hr. Total DNA and mtDNA was isolated and analyzed by PCR with primers that amplify a 4.4 kb segment of mitochondrial genome (Figure 5-1. A) or GAPDH primers (for control). As Figure 5-2. B shows, a substantial reduction in the 4.4-kb amplification product corresponding to the mitochondrial genome was detected with DNA isolated from Jurkat cells treated with increase concentration of H_2O_2. H_2O_2 is a known agent proved to induce extensive mitochondrial DNA damage. We used this treatment as a positive control to validate our method. We use GAPDH as a control for our PCR reactions.

When the same cells were treated with fludarabine for 24 hr, a decrease of 30 % in amplification signal was observed at the highest concentration of fludarabine, while a

more significant decrease in amplification was measured when cells were treated with the combination of fludarabine and MX. A 30 % decrease was observed at 10 μM fludarabine plus 3 mM MX which reached 54 % decrease at the concentration of 40 μM (Figure 5-2. C). Similar results were obtained when HL60 were incubated with fludarabine or fludarabine plus MX and assessed for mtDNA damage. Fludarabine alone, at very high concentration (100 μM) resulted in a 50 % reduction in amplification signal, while the same concentration of fludarabine plus 3 mM MX resulted in a very significant decrease in the amplification rate (76 %) (Figure 5-2. D). These results prove that the combination of fludarabine and MX targets mtDNA resulting in overall reduced amplification suggesting the presence of mtDNA damage that cannot be overcome by the polymerase employed in the PCR reaction.

Figure 5-2

Detection of mitochondrial DNA damage induced in the presence of fludarabine plus MX

A*,** The length and localization of the PCR amplification product in the human mitochondrial genome ***B, PCR amplification products were resolved in 0.5 % agarose gel and visualized by ethidium bromide staining. A representative picture shows a reduction in the 4.4 kb product corresponding to the mitochondrial genome. Amplification was done with DNA from Jurkat cells incubated with H_2O_2 (0-800 μM) for 1 hr and collected 24 hr after treatment. Amplification of the GAPDH served as a control for the PCR. ***C*,** Jurkat cells were treated with fludarabine (0-80 μM) or fludarabine plus 3 mM MX for 24 hr and mtDNA damage was measured. Vertical bars measure relative amplification based on the density of the bands that is inversely proportional to the extent of DNA damage ***D,*** HL60 cells were treated with fludarabine (0-100 μM) or fludarabine plus 3 mM MX for 24 hr and mtDNA damage was measured.

A

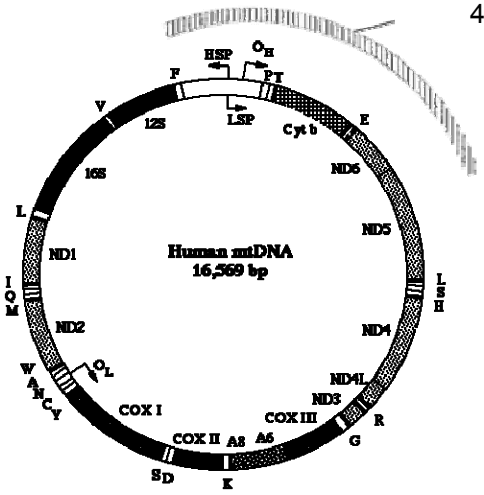
4467 bp PCR product
HSP
O_H
F
P_T
V
12S
LSP
Cyt b
E
16S
ND6
L
ND5
ND1
Human mtDNA
16,569 bp
I
Q
M
L
S
H
ND2
ND4
O_L
W
A
N
C_Y
ND4L
ND3
COX I
COX III
R
COX II
A8
A6
G
S_D
K

B

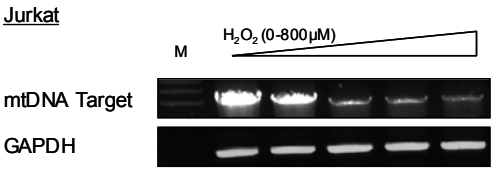
Jurkat
M
H_2O_2 (0-800μM)
mtDNA Target
GAPDH

C

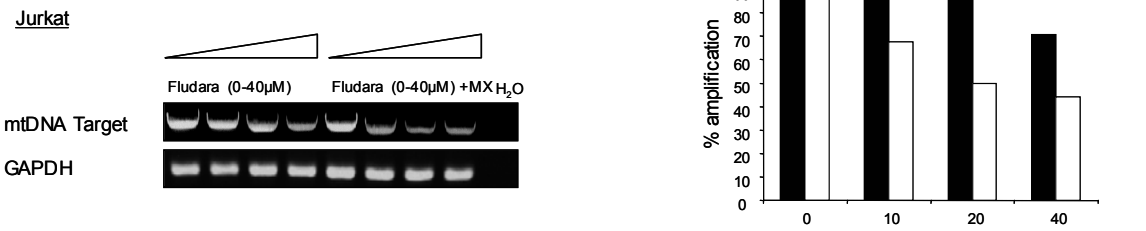
Jurkat
Fludara (0-40μM)
Fludara (0-40μM) +MX
H_2O
mtDNA Target
GAPDH
% amplification
Fludarabine
Fludarabine + MX
0
10
20
40

D

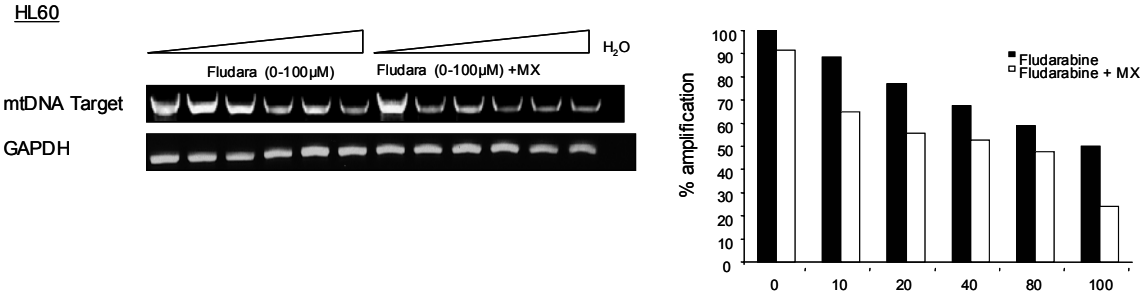
HL60
Fludara (0-100μM)
Fludara (0-100μM) +MX
H_2O
mtDNA Target
GAPDH
% amplification
Fludarabine
Fludarabine + MX
0
10
20
40
80
100

5.3.2. Formation of ara-AP sites in mitochondrial DNA after exposure to fludarabine alone and in combination with MX

The above experiments confirm that the combination of fludarabine and MX targets mtDNA and determines mtDNA damage. Our previous studies showed that the MX enhancement of fludarabine-induced nuclear damage is due to binding of MX to the ara-AP sites formed by fludarabine and subsequent interrupts BER pathway. Considering that fludarabine action is mediated by the incorporation of the nucleotide analog into DNA strand, we hypothesize that fludarabine is incorporated into mtDNA and mitochondrial (mt) BER pathway is activated. Therefore, a direct assay was used to measure the mtBER response after fludarabine, by measuring mitochondrial ara-AP sites using ARP. ARP has been demonstrated to have similar chemical structures to MX and can specifically bind to an aldehyde group in an AP site (27, 32). Tumor cells were treated with fludarabine alone (0-20 μM) or fludarabine plus MX (3 mM) and harvested at 24 hr. MtDNA was extracted and mtAP-sites were measured. Results showed formation of that mtAP-sites proportional with fludarabine concentrations, in the two cancer cell lines used HL60 and Jurkat (Figure 5-3. A & B). Co-treatment with 3 mM MX reduced by 2-4 folds the detectable mtAP-sites (Figure 5-3. A & B). This reduction of mtAP-sites is presumably due to the binding of MX to the aldehyde group of the mtAP-sites to form MX-bound AP-sites, making the mtAP-sites unavailable for ARP. Importantly, these results indicate that MX is capable of blocking mitochondrial repair of fludarabine-induced damage. These results are also in agreement with our PCR analysis results of mtDNA damage which showed increased damaged when cells were treated with the combination of the two drugs.

Figure 5-3

Fludarabine induces formation of mitochondrial ara-AP sites that are bound by MX

A, The dose-dependent relationship between the levels of mtAP-sites and the concentrations of fludarabine. The ara-AP sites in mtDNA were measured using ARP reagent after Jurkat cells were treated with fludarabine alone (0-20 μM) or in combination with MX (3 mM) for 24 hrs (* $P<0.05$ compared to fludarabine alone). ***B***, The dose-dependent relationship between the levels of mtAP-sites and the concentrations of fludarabine (0-20 μM) or fludarabine plus MX (3 mM) for 24 hr in HL60 (* $P<0.05$ compared to fludarabine alone). Results represent the mean value of data from three independent experiments.

A. HL60 cells

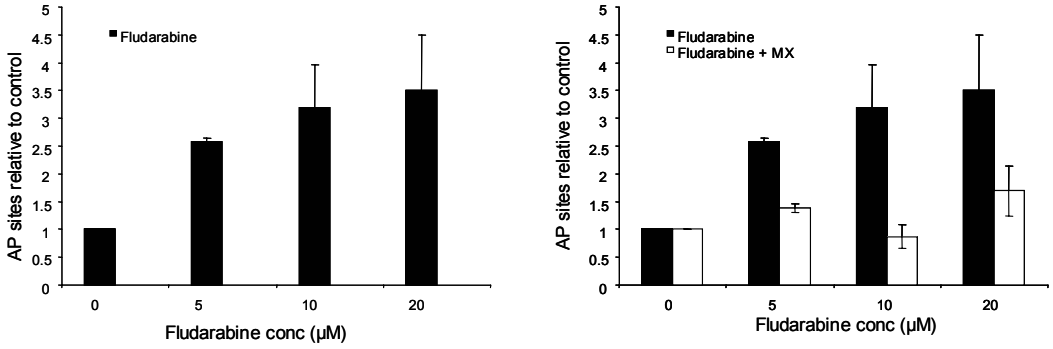

B. Jurkat cells

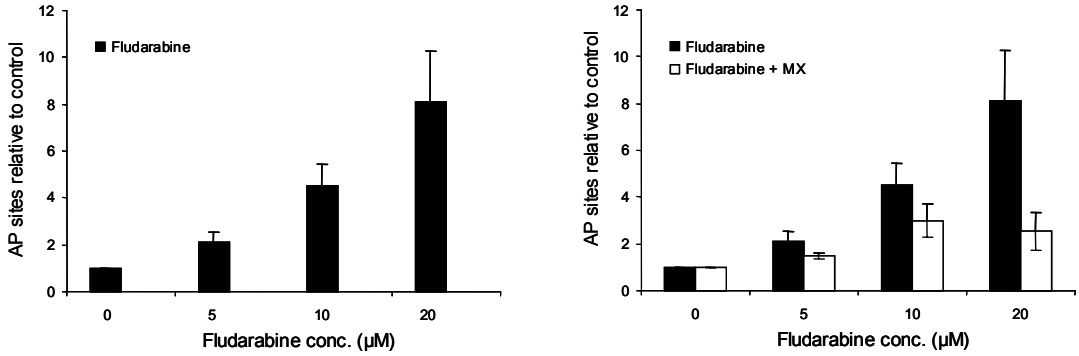

5.3.3. MX enhances fludarabine induced apoptosis

To correlate mtDNA damage such MX-bound mtAP-sites with the killing effect induced by the drug treatments, apoptotic cell death was assayed. HL60 and Jurkat cells were treated with fludarabine (5 μM) in the absence and presence of MX (3 mM) and collected at 24, 48 and 72 hr after treatments. Each sample was subjected to analysis of apoptosis by stained with Annexin V and detection of expression levels of apoptotic proteins by western blotting assay. The results showed that fludarabine alone produced low percentage of apoptotic cells in HL60 and Jurkat cell lines (Figure 5-4. A) and co-treatment of fludarabine with MX significantly increased Annexin V-positive cells. At 72 hr the combination-treatment induced 60-70 % of cells undergoing to apoptosis, which was 3 to 7-fold higher than that induced by fludarabine alone in HL60 and Jurkat cells respectively. We next examined proteolytic cleavage of PARP by caspases, which is a hallmark of apoptosis. As shown in Figure 5-4. B, time-dependent PARP cleavage was seen in HL60 and Jurkat cells after drug treatment. In HL60 cells, cleaved PARP was detected by 48 and 72 hr of treatments with either fludarabine alone or in combination with MX. In Jurkat cells, cleaved PARP was significantly induced by the combination of fludarabine and MX. The enhanced PARP cleavage appeared to continue to accumulate even as late as 72 hr, suggesting that this process of caspase activation was more specifically activated by the combination treatment in Jurkat cells. Moreover, γH2AX, the marker of DNA strand break, was also remarkably induced by the combined treatment in both cell lines, which was consistent with the cleaved PARP, suggesting that DNA strand breaks produced by the combination of fludarabine and MX may signal for cell death. Further, we monitored the expression of several apoptotic proteins after

fludarabine alone or combined treatments (Figure 5-4 B) in a time dependent fashion. Treatment of HL60 and Jurkat cells with MX, fludarabine alone, or in combination, exerted little effect on expression of Bcl2, an antiapoptotic protein. In contrast, the levels of proapoptotic protein Bax were induced. In HL60 cells, at 24 and 72 hr, there was a slightly induction of Bax by fludarabine or the combination. A peak level in Bax expression was observed at 48 hr after combined treatments. Similarly, expression levels of Bax were up-regulated after treatment of Jurkat cells with fludarabine plus MX starting at 24 hr and persisted over 72 hr. Finally, the expression levels of procaspase/caspases 9, an important mitochondrial related apoptotic protein were determined. Treatments of HL60 cells with fludarabine alone resulted in minimal cleavage/ activation of procaspase 9 at 24 and 48 hr and a slightly increased effect at 72 hr. However, the exposure of cells to fludarabine and MX resulted in marked induction of caspases activation. In Jurkat cells, more modest effects are measured even after the exposure of cells to combined treatments.

Figure 5-4

MX potentiates fludarabine induced mitochondrial mediated apoptotic cell death

A, The percentage of Annexin V-positive cells produced by fludarabine alone and fludarabine plus MX at 24, 48 and 72 hr (*P<0.05 compared with the treatment with fludarabine alone). ***B***, Induction of the cleaved form of PARP, γH2AX, Bcl-2, Bax and caspases 9 proteins was detected by western blotting in cells after treatments with fludarabine alone and in combination with MX. Control (lane 1), fludarabine alone (lanes 2,4,6), fludarabine plus MX (lanes 3,5,7), MX alone (lane 8). Results are representative of at least three experiments.

A

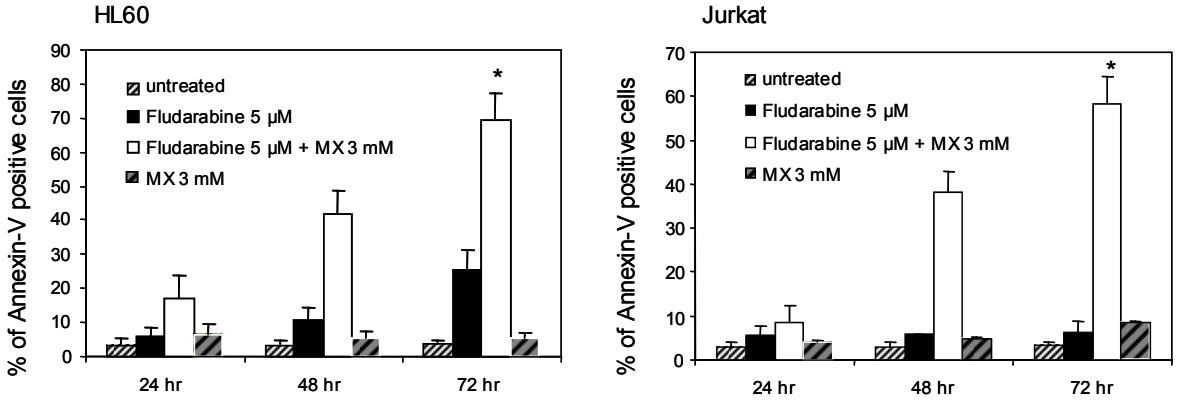
HL60
% of Annexin-V positive cells
untreated
Fludarabine 5 μM
Fludarabine 5 μM + MX 3 mM
MX 3 mM
24 hr
48 hr
72 hr
Jurkat
% of Annexin-V positive cells
untreated
Fludarabine 5 μM
Fludarabine 5 μM + MX 3 mM
MX 3 mM
24 hr
48 hr
72 hr

B

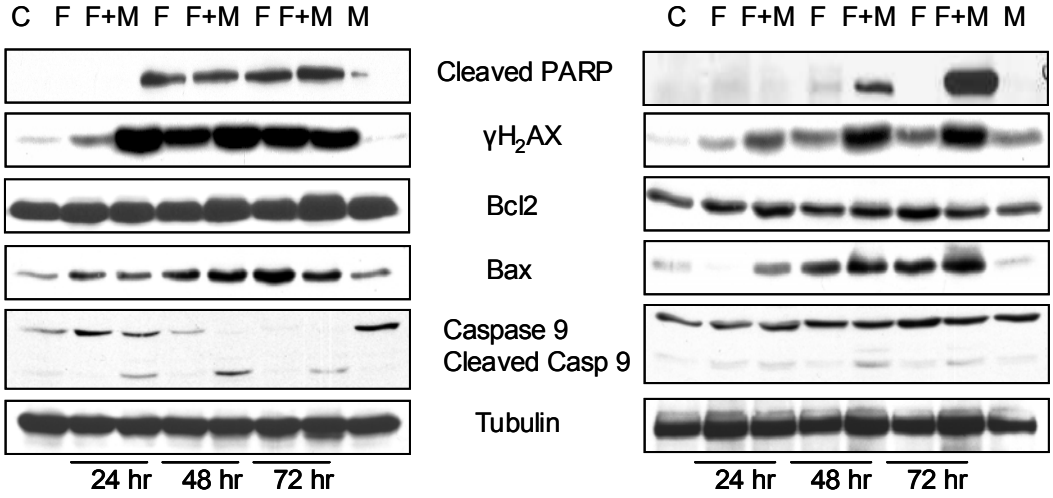
HL-60
Jurkat
C F F+M F F+M F F+M M
Cleaved PARP
γH2AX
Bcl2
Bax
Caspase 9
Cleaved Casp 9
Tubulin
24 hr
48 hr
72 hr

5.3.4. Loss of mitochondrial membrane potential as a result of mitochondrial DNA damage induced by combined treatment

Induction of apoptosis, particularly by cytotoxic drugs, is intimately related to mitochondrial dysfunction [33]. Consequently, the effects of combined exposure to fludarabine and MX on mitochondrial integrity were examined. Mitochondrial membrane potential is a key indicator of cellular viability, as it reflects the pumping of hydrogen ions across the inner membrane during the process of electron transport and oxidative phosphorylation, the driving force behind ATP production (Figure. 5-5 A). The lipophilic mitochondrial probe JC-1 was used to estimate changes in membrane potential ($\Delta\psi m$). Cells were treated with fludarabine and fludarabine plus MX for 24, 48 and 72 hr. At each time point, JC-1 reagent was added and cells were analyzed by flow cytometry for polymeric (intramitochondrial) and monomeric (cytosolic) forms of JC-1. As shown in Figure 5-5. B exposure to fludarabine had minimally affected the transmembrane potential. In contrast, combined exposure MX/fludarabine resulted in a 6-fold increase in the fluorescence intensity for the monomeric form of the dye at 24 hr. This significant increase in the percentage of cells that lost their mitochondrial membrane potential after combined treatments lasted over 72 hr (Figure 5-5 C).

These results are consistent with the preceding measurements of apoptotic cells and they indicate that exposure of leukemic cells to fludarabine and MX results in a marked potentiation of mitochondrial dysfunction and activation of apoptotic pathway.

Figure 5-5

Fludarabine plus MX induced mitochondrial membrane potential collapse

A*,** mtDNA damage can lead to decrease in electron transport and subsequent to loss of mitochondrial membrane potential. ***B, An example of the flow cytometer data for the drug-induced loss of mitochondrial membrane potential in Jurkat cells as determined with JC-1 dye. The polymeric form (intramitochondrial) is found in the top quadrant while the monomeric form of the dye (cytosolic) is found in the bottom quadrant. ***C***, Jurkat cells were treated with 5 μM fludarabine or fludarabine plus 3 mM MX for 24, 48 and 72 hr. The percentage of cells that lost their mitochondrial membrane potential was determined using JC-1 staining and flow cytometer as described in ***B*.**

A

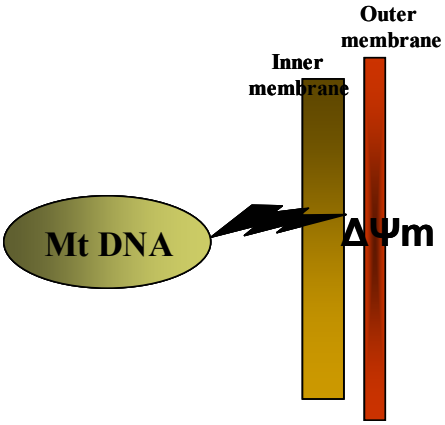
Outer membrane
Inner membrane
Mt DNA
ΔΨm

B

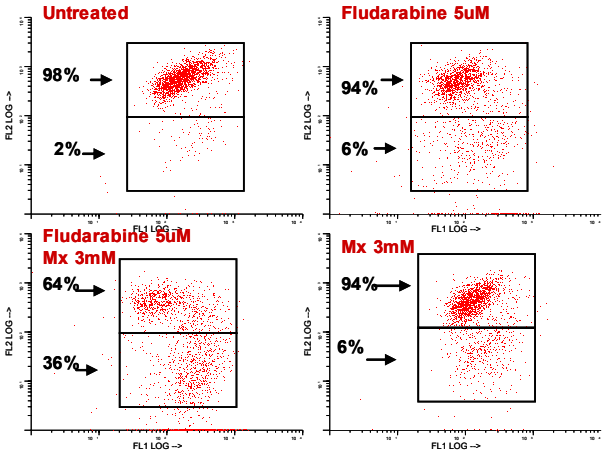
Untreated
98%
2%
Fludarabine 5uM
94%
6%
Fludarabine 5uM
Mx 3mM
64%
36%
Mx 3mM
94%
6%
FL1 LOG -->
FL2 LOG -->

C

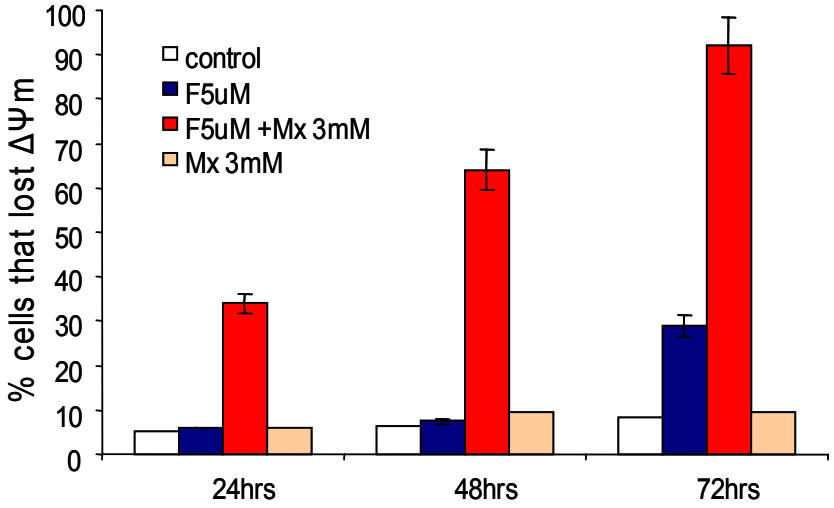
% cells that lost ΔΨm
100
90
80
70
60
50
40
30
20
10
0
control
F5uM
F5uM +Mx 3mM
Mx 3mM
24hrs
48hrs
72hrs

5.3.5. Loss of mitochondrial integrity induced by combined treatment

Parallel studies were carried out using Jurkat cells treated fludarabine or fludarabine plus MX which at 24 hr after treatment were cytospin on a slide and immunofluorescence stained for mitochondria with MitoTracker (MT) and cytochrome C. In the control cells, cytochrome C and MT co-localized in the mitochondria (Figure 5-6). After treatments with either fludarabine or MX alone, no visible effect was observed, which correlated with previous published data [34]. However, when cell were treated with 5 μM fludarabine plus 3 mM MX for 24 hr, both cytochrome C and MT fluorescence signals were reduced and accompanied by disruption of the arranged organization of mitochondria in cytoplasm. These data are in agreement with our mitochondrial membrane potential data. The combination of fludarabine plus MX induces mtDNA damage presumably through the inhibition of mtBER that will eventually lead to loss of mitochondrial membrane potential and mitochondrial collapse. As an end point, mitochondrial-mediated apoptosis will be triggered.

Figure 5-6

Immunocytochemistry of mitochondrial damaged caused by fludarabine plus MX treatments

Jurkat cells were treated with indicated drugs for 24 hr. Cells were stained for mitochondria with MitoTracker (red) for 30 min , pelleted on a slide at 600 g for 8 min, fixed in 2 % paraformaldehyde, and stained for cytochrome C (green) with monoclonal antibody (Santa Cruz) and secondary antibody Alexa 488. DNA was visualized with Hoersch (blue). The very right panel represents the composed images.

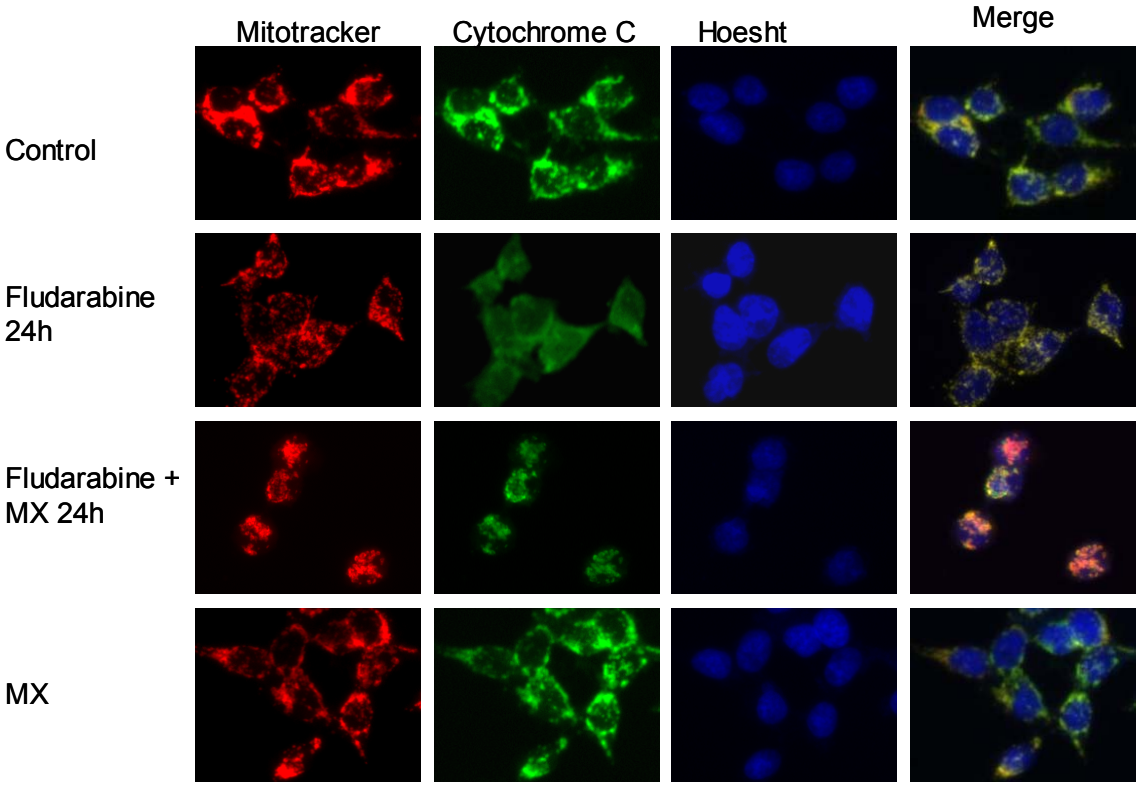
Mitotracker
Cytochrome C
Hoesht
Merge
Control
Fludarabine 24h
Fludarabine + MX 24h
MX

5.4. Discussion

In addition to the nuclear genome, cells harbor a mitochondrial genome. Mitochondrial DNA exists as a 16.6 kb circular structure and contains 13 oxidative phosphorylation genes, two rRNAs, and 22 tRNAs. The increased susceptibility of the mtDNA to drug-induced damage, as compared with the nDNA, has been previously documented (35); however, the specific molecular causes of these phenomena are not well understood. It has been hypothesized that a combination of biological determinants, such as the proximity of the mtDNA to ROS, the lack of a compact nucleosome structure to protect the genome, and a paucity of mtDNA damage-processing pathways relative to those present in the nucleus play a role (36). Moreover, the susceptibility of mtDNA and the role of mitochondrial repair pathways to the damage induced by specific class of chemotherapeutic agents such as nucleotide analogs have been poorly investigated.

Previous data (chapter 3 and chapter 4) have shown that fludarabine-induced nuclear DNA damage activates BER. Combining fludarabine with MX, an agent that blocks BER, led to significant cell death. In the present study we prove that mtDNA is a site for fludarabine and MX actions and we elucidated the mechanism of cell death induced by the combination of the two agents along with the role of mitochondria in this process.

Mitochondrial BER system is activated as response to fludarabine damage. It has been shown that several types of mtDNA damage are repaired by a short-patch mtBER process (21). Here, we report for the first time that fludarabine and fludarabine combined with MX induced mtDNA damage. At low fludarabine concentration, the global assessment of mtDNA damage using PCR amplification showed minimal effects. In

contrast, when fludarabine was combined with MX, low amplification was measured, suggesting the presence of significant mtDNA damage. Also, we considered measuring a more specific type of mtDNA damage and that was the mtAP-site formation. Our results showed for the first time that fludarabine induces formation of mtAP-sites which are bound by MX resulting in inhibition of further mtBER. These MX-bound AP-sites refractory to BER will result in global mtDNA damage.

Interruption of BER by MX results in induction of mitochondrial mediated apoptosis. Measurements of apoptotic cell death revealed that the combination of fludarabine plus MX resulted in more than additive apoptotic cell death. To determine the prevalence of intrinsic (mitochondrial-mediated) over extrinsic (death receptor) pathway in execution of apoptotic cell death, several approaches were used.

(i) Time course analyses of mitochondrial membrane potential in whole cells demonstrated that fludarabine alone had minimal effect on mitochondrial integrity, as previously reported (37). In contrast, fludarabine plus MX treatments lead to a significant percentage of cells that lost their mitochondrial membrane potential. To explain this observation, we propose that mitochondrial MX-bound AP–sites block mtBER leading to accumulation of mtDNA damage. Accumulation of unrepaired mtDNA damage will eventually become severe, impairing the electron transport machinery along the inner membrane that will lead to collapse of the mitochondrial membrane potential.

(ii) Immunofluorescence microscopy using Mitotracker, a mitochondrial staining, and cytochrome c antibody were conducted. The immunofluorescence images confirmed these results, showing a disrupted arrangement of mitochondria.

(iii) These events were accompanied by cleavage and activation of PARP and caspase 9. Also, the expression levels of proapoptotic protein Bax are up-regulated, suggesting that Bax is translocated to the outer mitochondrial membrane. Bax translocation to the mitochondria has been shown to reduce mitochondrial membrane potential, enhance cytochrome c release from mitochondria and activate caspases (37).

Together, our results point out for the first time that the combination of fludarabine and MX targets mtDNA. Interruption of mtBER pathway along with nuclear BER induces severe damage, leading to lost of mitochondria ability to maintain the membrane potential and subsequent activation of mitochondrial mediated apoptotic death.

5.5. References

1. Keating MJ, O'Brien S, Lerner S, Koller C, Beran M, Robertson et all. Long-term follow-up of patients with chronic lymphocytic leukemia (CLL) receiving fludarabine regimens as initial therapy. Blood, 92:1165-1171, 1998.

2. Laughlin P, Hagemeister FB, Romaguera JE, Sarris AH, Pate O, Younes A et all. Fludarabine, mitotraxone and dexamethasone: an effective new regimen for indolent lymphoma. J Clinic Oncol, 14: 1262-1268, 1996.

3. Huang P, Plunkett W. Fludarabine and gemcitabine induced apoptosis: incorporation of analogs into DNA is a critical event. Cancer Chem Pharmacol 36: 181-188, 1995

4. Kamiya K, Huang P, Plunkett W. Inhibition of the 3'-5' exonuclease of human DNA polymerase ε by fludarabine-terminated DNA. J Biol Chem 1996;271:19428-35.

5. Skalski V, Brown KR, Choi BY, Lin ZY, Chen S. A 3'-5' exonuclease in human leukemia cells: implications for resistance to 1-beta -D-arabinofuranosylcytosine and 9-beta-D-arabinofuranosyl-2-fluoroadenine 5'-monophosphate. J Biol Chem 2000;275:23814-19.

6. Yang SW, Huang P, Plunkett W, Becker F, Chan JYH. Dual mode of inhibition of purified DNA ligase I from human cells by 9-β-D-Arabinofuranosyl-2-fluoroadenine triphosphate. J Biol Chem 1992;267:2345-9.

7. Huang P, Chubb S, Plunkett W. Termination of DNA synthesis by 9-β-D-Arabinofuranosyl-2-fluoroadenine. J Biol Chem 1990; 265:16617-25.\

8. Iwasaki H, Huang P, Keating MJ, Plunkett W. Differential incorporation of ara-C, gemcitabine and fludarabine into replicating and repairing DNA in proliferating human leukemia cells. Blood 1997;90:270-8.

9. Bulgar A, Snell M, Donze JR, Kirkland E, Li L, Xu Y, Gerson SL, Liu L. UDG is a major DNA glycosylase having activity on F:T mispairs: Identifying a new target for fludarabine. Cancer Res, 2008

10. Elmore S. Apoptosis: A review of programmed cell death. Toxicol Pathol, 35: 495-516, 2007.

11. Salvesen GS, Dixit DM. Caspases: intracellular signaling by proteolysis. Cell. 1997, 91: 443-446.

12. Kroemer G, Zamzami N, Susin SA. Mitochondrial control of apoptosis. Immunol today. 1997, 18: 44-51.

13. Li P, Nijhawan D, Budihardijo I et al. Cytochrome c and ATP-dependent formation of Apaf1/caspases-9 complex initiates an apoptotic protease cascade. Cell. 1997. 91: 479-489.

14. Petit PX, Zamzami N, Vayssiere JL, Mignotte B, Kroemer G, Castedo M. Implication of mitochondria in apoptosis. Mol Cell Biochem, 1997. 174: 185-188.

15. Zxens X, Festjens N, Vandle Walle L, van Gurp M, van Loo G, Vandenebeele P. Toxic proteins released from mitochondria in cell death. Oncogene, 23: 2861-74, 2004.

16. Zou H, Li Y, Liu X Wang X. An Apaf1-cytochrome c multimeric complex is a functional apoptosome that activates procaspase-9. J Biol Chem. 1999, 274:11549-11556.

17. Chinnaiyan AM. The apoptosome: heart and soul of the cell death machine. Neoplasia, 1:5-15, 1999.

18. Joza N, Susin SA, Daugas E, Stanford WL, Cho SK, Li CY, et al. Essential role of the mitochondrial apoptosis-inducing factor in programmed cell death. Nature, 410:549-54, 2001.

19. Pinz, K. G., and Bogenhagen, D. F. Efficient repair of abasic sites in DNA by mitochondrial enzymes. Mol. Cell. Biol., 18: 1257–1265, 1998.

20. Tomkinson, A. E., Bonk, R. T., and Linn, S. Mitochondrial endonuclease activities specific for apurinic/apyrimidinic sites in DNA from mouse cells. J. Biol. Chem., 263: 12532–12537, 1988.

21. Nilsen, H., Otterlei, M., Haug, T., Solum, K., Nagelhus, T. A., Skorpen, F., and Krokan, H. E. Nuclear and mitochondrial uracil-DNA glycosylases are generated by alternative splicing and transcription from different positions in the UNG gene. Nucleic Acids Res., 25: 750–755, 1997.

22. Bohr,V.A. Repair of oxidative DNA damage in nuclear and mitochondrial DNA and some changes with aging in mammalian cells. Free Radic. Biol. Med., 32, 804–812, 2002.

23. Stuart JA, Mayard S, Hashiguchi K, Souza-Pinto, Bohr VA. Localization of mitochondrial DNA base excision repair to an inner membrane-associated particulate fraction. Nucleic Acid Res, 33: 3722-3732, 2005.

24. Liu, L. Qian, J.-S. Sung, N. C. de Souza-Pinto, L. Zheng, D. F. Bogenhagen, V. A. Bohr, D.M.Wilson III, B. Shen, and B. Demple. Removal of Oxidative DNA Damage via FEN1-Dependent Long-Patch Base Excision Repairin Human Cell Mitochondria. Mol. Cell. Biol. 2008; 28(16): 4975 - 4987.

25. Karahalil B., Hogue B.A., Souza-Pinto N.C. and Bohr V.A Base excision repair capacity in mitochondria and nuclei: tissue-specific variations. FASEB J., 16, 1895–190,2002

26. Rosa S, Fortini P, Karran P, Bignami M, Dogliotti E. Processing in vitro of an abasic site reacted with methoxyamine: A new assay for the detection of abasic sites formed in vivo. Nucleic Acids Res 1991;19:5569-74.

27. Yan L, Bulgar A, Miao YL, et al. Combined treatment with temozolomide and methoxyamine: blocking apurinic/pyrimidinic site repair coupled with targeting topoisomerase IIα. Clin Cancer Res 2007;13:1532-9.

28. Nakamura J, Swenberg JA. Endogenous apurinic/apyrimidinic sites in genomic DNA of mammalian tissues. Cancer Res 1999;59:2522-6.

29. Nakamura J, Walker VE, Upton PB, Chiang SY, Kow YW, Swenberg JA. Highly sensitive apurinic/apyrimidinic site assay can detect spontaneous and chemically induced depurination under physiological conditions. Cancer Res 1998;58:222-5.

30. Yurong Lai, Chung-Ming Tse, and Jashvant D. Unadkak. Mitochondrial Expression of the Human Equilibrative Nucleoside Transporter 1 (hENT1) Results in Enhanced Mitochondrial Toxicity of Antiviral Drugs. J. Biol. Chem., Vol. 279, Issue 6, 4490-4497, 2004

31. Fernández Calotti P, Galmarini CM, Cañones C, Gamberale R, Saénz D, Avalos JS, Chianelli M, Rosenstein R, Giordano M. Modulation of the human equilibrative nucleoside transporter1 (hENT1) activity by IL-4 and PMA in B cells from chronic lymphocytic leukemia. Biochem Pharmacol. 2008 75(4):857-65. Epub 2007

32. Liu L, Taverna P, Whitacre CM, Chatterjee S, Gerson SL. Pharmacological disruption of base excision repair sensitizes mismatch repair deficient and proficient colon cancer cells to methylating agents. Clin Cancer Res 1999;5:2908-17.

33. Fulda S, Meyer E, Friesen C, Susin SA, Kroemer G, Debatin KM Cell type specific involvement of death receptor and mitochondrial pathways in drug-induced apoptosis. Oncogene, 20: 1063-75, 2001.

34. Davide Genini, Souichi Adachi, Qi Chao, David W. Rose, Carlos J. Carrera, Howard B. Cottam, Dennis A. Carson, and Lorenzo M. Leoni. Deoxyadenosine analogs induce programmed cell death in chronic lymphocytic leukemia cells by damaging the DNA and by directly affecting the mitochondria. Blood, 15 Vol. 96, No. 10, pp. 3537-3543.

35. Janine Hertzog Santos L'uba Hunakova, Yiming Chen, Carl Bortner and Bennett Van Houten. Cell Sorting Experiments Link Persistent Mitochondrial DNA Damage with

Loss of Mitochondrial Membrane Potential and Apoptotic Cell Death. J. Biol. Chem., Vol. 278, Issue 3, 1728-1734, 2003

36. Sawyer DE, Van Houten B. Repair of DNA damage in mitochondria. Mutat Res. 1999 434(3):161-76

37. Zhang L, Yu J, Park B, Kinzler KW and Volelstein B. Role of Bax in the apoptotic response to anticancer agents. Science, 290: 989-992, 2000.

CHAPTER VI

DISRUPTION OF BASE EXCISION REPAIR BY METHOXYAMINE SENSITIZIES CHRONIC LYMPHOCYTIC LEUKEMIA CELLS TO FLUDARABINE

Abstract

We have applied our findings on biochemical mechanisms governing fludarabine-induced cytotoxic effects (Chapter 3-5) to test if fludarabine plus MX combination can improve the treatment of chronic lymphocytic leukemia (CLL). More specifically, we are investigating how blockage of the DNA base excision repair (BER) pathway via BER inhibitor, methoxyamine affects the action of the nucleotide analog fludarabine. In this study, we used primary CLL cells and similar experimental approach, as employed in previous chapters. Enhancement of fludarabine toxicity by methoxyamine was analyzed using *in vitro* assays, including AP sites assay, Comet assay to quantitate DNA damage, apoptosis via Annexin staining, mitochondrial membrane potential via JC1 staining and Western Blotting and RT-PCR analysis for protein expressions and transcript levels of key BER enzymes as well as apoptotic proteins. Data showed that activity of fludarabine

was effectively modulated by methoxyamine in CLL cells. Enhancement of fludarabine-induced cytotoxicity was dependent on formation of nuclear and mitochondrial ara-AP sites by fludarabine which are bound by MX. Primary CLL lymphocytes exhibited intrinsically higher BER expression and activity when compared with normal lymphocytes. CLL cells were significantly more sensitive to the fludarabine in combination with methoxyamine as assayed by cytotoxicity, apoptosis, and levels of DNA damage. Exposure of CLL lymphocytes to fludarabine plus MX treatments resulted in mitochondrial-mediated apoptosis with loss of mitochondrial membrane potential and enhanced cytosolic release of proapoptotic mitochondrial proteins.

This study shows that through manipulation of the BER pathway, an increase in response to fludarabine is achieved in CLL lymphocytes. Thus, the combination of fludarabine plus methoxyamine has potential for further clinical targeted therapy, with lower toxicity to normal cells.

6.1. Introduction

Chronic lymphocytic leukemia (CLL) is the most common form of lymphoid malignancies with a variable clinical course (1). It is manifested by progressive accumulation of morphological mature but immunological dysfunctional B lymphocytes. Outcome for advanced-stage CLL patient is poor, with an expected median survival of three years (2). Although the introduction of purine nucleoside analogues (3) and monoclonal antibody therapies such as alemtuzumab and rituximab (4,5), either as single or in combination regimens (6), have led to improved significant response rates, none of these options are curative. Consequently, there is a need for novel therapeutic strategies in

the treatment of CLL.

Fludarabine is a synthetic adenine nucleoside analog approved as the first-line treatment in CLL. Fludarabine is used, as a stand-alone drug, as well as in combination with chemotherapeutic agents such as cyclophosphamide (7,8), cytararabine (9,10) or cisplatin (11,12). While it has been shown to be effective in inducing complete remission, many patients eventually develop drug resistance leading to disease progression. Fludarabine is an inhibitor of DNA synthesis through the actions of its triphosphate metabolite, F-ara-ATP (13-19). F-ara-ATP incorporates into replicating strand causing reduced DNA synthesis. Although the relative contributions of diverse molecular actions of fludarabine to cell death remain unknown, its incorporation in the DNA strand appears to be required for lethality (20). We have previously shown that incorporated F-ara-A acts as an abnormal base in DNA and initiates base excision repair (BER) through the enzymatic activity of uracil DNA glycosylase (21), using tumor cell lines (Chapter 3, Chapter 4).

BER is initiated by a DNA glycosylase that recognizes and removes the inappropriate base with the formation of a potentially cytotoxic abasic (AP) site that is processed by an AP endonuclease (APE). APE incises the phosphodiester backbone immediate at the 5' position to the lesion, leaving behind a strand break. Replacement of the damaged base and religation of the DNA involves recruitment of DNA polymerase β and ligase III (22-27). BER is the most efficient repair mechanism to repair a variety of base lesions, contributing to cells resistance to anticancer agents that produce DNA lesions. Thus, expression and activity of BER key proteins in CLL lymphocytes may play a role in development of resistance to fludarabine treatments. It also may be an important

factor for the development of new combinatory therapeutic strategy to target BER, with high selectivity toward tumors cells by exploiting the biological differences between normal and cancer cells. Methoxyamine (MX), an inhibitor of BER, specifically binds to AP sites (28-39) preventing their processing by APE and leading to accumulation of these cytotoxic sites in DNA. Recently, we have shown that MX improves the therapeutic efficacy of fludarabine *in vitro* and in human tumor xenografts (21). Exploring the combination of fludarabine and MX in the treatment of CLL is a first step toward developing future targeted combinatory treatment regimens.

An important feature of CLL cells that contributes to failure of the treatments is their resistance to apoptosis due to several factors such as Bcl2 overexpression or increase production of anti-apoptotic cytokines (40). Apoptosis, the most common form of cell death, is known to occur via an extrinsic (death receptor-ligand) or intrinsic (mitochondrial-centered) pathway, in which mitochondria play a key role in the events leading to caspase activation. Mitochondrial DNA is a target for damage induced by a variety of therapeutic agents (41-43). Even though mitochondrial DNA (mtDNA) lacks efficient repair systems, a simplified BER pathway have been established that is similar with the one in nuclei (42). Thus, in addition to nuclear DNA (the conventional target of fludarabine) mtDNA may also be targeted and perhaps an important mediator of apoptosis during mtBER disruption by MX in CLL lymphocytes.

The present work was designed to show for the first time that MX enhances fludarabine cytotoxicity in CLL. We studied the intrinsic BER expression and activity of CLL lymphocytes and the response to fludarabine and MX treatments. We quantified ara-AP site formation, monitored expression levels of relevant proteins and measured

production of DNA strand breaks after combined treatments. We also characterized the nature of the cell death induced in CLL by fludarabine and MX combination. Our data showed that fludarabine treatment has generated dose- and time-dependent formation of nuclear and mitochondrial ara-AP sites in CLL cells which were bound by MX. MX-bound AP-sites were resistant to BER and eventually led to enhanced single and double DNA strand breaks triggering mitochondrial mediated apoptosis. Taken together, these results established for the first time the basis for a possible clinical therapeutic strategy.

6.2. Materials and Methods

6.2.1. Reagents and enzymes

Fludarabine was obtained from Berlex Laboratories (Richmond, CA) and freshly prepared when used. Methoxyamine was purchased from Sigma Chemical CO (St. Louis, MO), dissolved in sterilized water (pH 7.0) at a concentration of 2.5 M (stock solution) and stored at -20 ºC. E. Coli Uracil DNA glycosylase (UDG) and human AP endonuclease (APE) were purchased from Trevigen (Gaithersburg, MD).

6.2.2. Isolation and culture of primary cells

Peripheral blood was obtained from CLL patients and healthy donors who have provided written informed consent. The clinical characteristics of the patient cohort is summarized in Table 5-I. Heparinized peripheral blood samples were fractioned by Ficoll-Paques sedimentation (Sigma Chemicals, St Louis, MO). Freshly isolated peripheral blood lymphocytes were cultured in RPMI medium (HyClone, Logan, Utah) supplemented with 10 % fetal bovine serum and 1 % L-Glutamine at a density of 1 x

10^6/ml. Lymphocytes were incubated at 37 ºC in a humidified 5 % carbon dioxide atmosphere in the presence of fludarabine (0-20 μM), MX (3 mM) or both drugs in combination. In addition, control cultures with no drug added were carried out. All experiments were performed in duplicates.

Tabel 6-I. Characteristics of the 47 patients

Characteristics	CLL patients	Normal donor
Sex		
Male	15	9
Female	18	6
Age (years)		
Median	58	41
Range	44 - 78	30-67
Lymphocytes counts (per µl)		
Median	69 x $10^{3/}$/ µL	8 x $10^{3/}$/ µL
Range	11 – 365 x $10^{3/}$/ µL	5- 11 x $10^{3/}$/ µL

6.2.3. DNA glycosylase/APE assay

The fluorescent HEX labeled 40-mer oligonucleotide containing a deoxyuridine residue at position 19 and its complement strand labeled with Cy5 were synthesized by Operon Biotechnologies (Huntsville, Alabama). The sequences of the top and bottom strands were: 5'[HEX]GTAAAACGACGGCCAGTG**U**ATTCGAGCTCGGTACCCGG GG (top) and 5'-[Cy5]CCCCGGGTACCGAGCTCGAATGCACTGGCCGTCGTTTT AC (bottom). Duplex oligonucleotides were generated by annealing the two complementary strands in a reaction buffer containing 10 mM Tris-HCl, 50 mM KCl, and 1 mm EDTA, by incubation at 95 ºC for 5 min followed by slow cooling at room temperature for 1 hour. The standard assay mixture for DNA glycosylase activity, containing 4 pmols of the fluorescent labeled duplex oligonucleotides in 20 μL buffer [1 mM EDTA, 1 mM dithiothreitol (DTT), and 20 mM Tris-HCl (pH 8.0)] was incubated with purified DNA glycosylase (UDG) for 1 hr at 37 ºC. The reaction was stopped at 95 °C for 5 min. After excising the misincorporated base by DNA glycosylase, abasic sites were incised by 1 unit of purified APE at 37 °C for 1 hr. Similar procedure was used to measure glycosylase activity of cell extracts. Substrate was incubated with cell extracts for 30 min, at 37 °C. The reaction was stopped at 95 °C. Ten ml of loading buffer (300 mmol/L NaOH, 97 % formamide and 0.2 % bromophenol blue) were added and reaction mixtures were heated to 95 ºC for 5 min, then cooled at 4 ºC on ice. Reaction products were resolved by electrophoresis through denaturing 19 % polyacrylamide gels (7 M urea, 1x Tris-borate-EDTA) and visualized by using a Typhoon 9200 fluorescent Imager (Amersham BioScience, Piscarawat, NJ). Fluorescent densities were quantified using ImageQuant software.

6.2.4. AP site assay

The AP sites were measured using ARP (aldehyde reactive probe) reagent that reacts with an aldehyde group at an AP sites. MX binds to the AP site at the same aldehyde group. Therefore, the ARP reagent only detects MX-free AP sites. The assay was performed as previously described (34, 44-46) with minor modifications. Briefly, cells ($2x10^6$) were plated and exposed to fludarabine (0-20 μM) with or without MX (3 mM). Cells were collected at 24 hrs after treatment and dose-dependent AP sites were measured. Alternatively, for the time-dependent assay, cells were exposed to 5 μM fludarabine with or without MX (3 mM) up to 72 hrs. Cells were harvested at 12, 24, 48 and 72 hrs, respectively. After extraction with phenol (Fischer Scientific, Fair Lawn, NJ) and chloroform (Sigma-Aldrich, St Louis, MO), DNA (10 g) was incubated with 15 μL of 1 mM ARP (Dojindo Laboratories, Kumamoto, Japan) in 150 μL PBS solution at 37 ºC for 15 min. DNA was then overnight precipitated with 400 μL ice-cold ethanol (100 %) at -20 ºC and washed with 70 % ethanol. DNA was dried at room temperature for 30 min and then resuspended in TE buffer to achieve a final concentration of 0.3 g/100 μL. The ARP-labeled DNA was then heat-denatured at 100 ºC for 5 min, quickly chilled on ice and mixed with an equal amount of 2 M ammonium acetate. The DNA was then immobilized on BAS 85 nitrocellulose membrane (Schleicher and Schuell, Dassel, Germany) using a minifold II vacuum filter device (Schleicher and Schuell, Dassel, Germany). The membrane was baked at 80 ºC for 1 hr and incubated with 0.25 % BSA/PBS containing streptavidin-conjugated horseradish peroxidase (BioGenex, SanRamon, CA) at room temperature for 40 min with gentle shaking. The nitrocellulose membrane was rinsed with washing buffer containing NaCl (0.26 M), EDTA (1 mM),

Tris-HCl (20 mM) and Tween 20 (1 %) for 1 hr at room temperature. ARP-labeled AP sites were visualized by chemiluminescence (Amersham Corp, Piscataway, NJ) followed by quantitative densitometry analysis using NIH ImageJ software.

6.2.5. Western blot analysis

Cellular protein content was quantified spectrophotometrically using the Bio-Rad assay. Equal amounts of proteins (30 μg) were separated by SDS-PAGE and transferred to PVDF membrane (Millipore Cor., Bedford, MA). After blocking in 5 % non-fat dry milk in TBST for 40 min at room temperature the blots were incubated with primary antibody for 1 hr at room temperature. Sources of primary antibody were as follows: cleaved PARP (BD Pharmingen, San Jose, CA), APE, Fen1, polymerase β, PCNA (Santa Cruz Biotechnology, CA), UDG (Abcam, Cambridge, MA), cleaved caspase 9, Bax, Bcl2, topoisomerase IIα (Cell Signaling, Danvers, MA), and Tubulin (Sigma-Aldrich, St Louis, MO). The primary antibody solutions were prepared in 1 % non-fat dry milk in TBST as followed: cleaved PARP 1: 1000 v/v dilution, APE 1:2000 v/v dilution, Fen1 1:200 v/v dilution, polymerase β 1:200 v/v dilution, UDG 1:500 v/v dilution, PCNA 1:200 v/v dilution, Bcl2 1:200 v/v dilution, Bax 1:200 v/v dilution, cleaved caspases 9 1:500 v/v dilution, γH2AX 1:1000 v/v dilution, topoisomerase IIα 1:500 v/v dilution and Tubulin 1:500 v/v dilution. Blots were incubated with horseradish peroxidase-conjugated secondary antibody (1:1000 v/v dilutions in 1 % non-fat dry milk in TBST) for 1 hr. The blots were visualized by ECL (Amersham Corp, Piscataway, NJ) according with the manufacturer's instructions.

6.2.6. RT-PCR assay

Total RNA was isolated from ~5 x 10^6 lymphocytes using RNAqueous-4PCR kit (Ambion, Austin, TX) according with the manufacturer's instructions. The extracted RNA was quantitated by measuring absorbance at 260 nm using NanoDrop100 spectrophotometer (Thermo Scientific, Wilmington, Delaware). Then cDNA was synthesized from 5 μg of total RNA in a 20 μL reaction mixture according to the manufacturer's instructions using SuperScript III first strand kit (Invitrogen, Frederick, Maryland) with random hexamers. The thermal profile of the reaction was set for stage 1: 10 min at 25 ºC; stage 2: 50 min at 50 ºC and stage 3: 5 min at 85 ºC. TaqMan MGB probes (FAMTM dye labeled) for nuclear UDG (NM 080911.1), topoisomerase IIα (NM001067.2) and β-actin (NM001101.2) were used. To amplify the cDNA, 0.25 μg of the reversed transcribed cDNA from cells were subjected to 40 cycles of PCR using TaqMan one-step RT-PCR master mixture reagent kit in a 96-well optical plate. The cycling parameters in an ABI 7500 Fast Real-Time PCR System (Applied Biosystem, Foster City, CA) were as follows: stage 1: 50 ºC for 2 min; stage 2: AmpliTaq activation 95 ºC for 10 min; stage 3: 40 cycles of amplification at 95 ºC for 15 s and stage 4: 60 ºC for 1 min. The amount of target was calculated after normalization to the β-actin as an endogenous control.

6.2.7. Measurement of Cell Growth

Lymphoma cells were seeded at a density of 5×10^5 cells/well in 6-well plates in the presence of 10 % (v/v) fetal bovine serum. Cells were treated with various concentrations of fludarabine (5-20 μM) or fludarabine plus MX (3 mM). Viable

cells were counted daily, for 5 days, in a hemocytometer (10 μL of cell suspension), using tryptan blue exclusion.

6.2.8. The alkaline and neutral single cell gel electrophoresis (Comet) assay

The single cell comet electrophoresis assay was performed using Comet Assay kit (Trevigen, Gaithersburg, MD). Approximately 5000 (in 50 μL) cells after the treatment were mixed with 250 μL of 1 % low melting point agarose in 1x PBS at 37 ºC. The mixture (75 μL) was quickly pipetted onto a Comet slide (Trevigen, Gaithersburg, MD) and allowed to solidify at 4 ºC. Slides were immersed for 30 min in prechilled lysis buffer (2.5 mM sodium chloride, 100 mM EDTA pH 10, 10 mM Tris Base, 1 % sodium lauryl sarcosinate, 0.01 % Triton X-100) at 4 ºC. After lysis, slides were incubated for 20 min in alkali solution (0.3 M NaOH, 1 mM EDTA) at room temperature to allow unwinding of DNA and then subjected to both neutral and alkaline electrophoresis for the next 20- 30 min. Comet in an individual cell was stained with Comet silver staining kit (Trevigen, Gaithersburg, MD) and visualized using an online CCD camera. Fifty cells per treatment were analyzed using NIH ImageJ software to generate quantitative and statistical data. Cellular DNA damage was expressed as the “tail length” for neutral conditions and “tail moment” that combines a measurement of the length of the DNA migration and the relative DNA content therein, for the alkaline conditions (47).

6.2.9. Measurement of apoptosis by Annexin V staining

Cells were continuously treated with fludarabine (0-20 μM), MX (3 mM) or both drugs in combination At 24 hrs after exposure to drugs, cells were harvested by

centrifugation. After two washes with PBS, cells were resuspended in 1 x binding buffer at a concentration of 1 x 10^6/mL. Cells were exposed at room temperature for 15 min to 5-µL Annexin V-FITC (BD Bioscience, San Jose, CA) following the instructions of the manufacturer. Analysis was carried out with FACSort (Becton Dickinson & Co., Mountain View, CA).

6.2.10. Cytofluorometric analysis of mitochondrial transmembrane potential (ΔΨm) by JC1

JC-1 (5,5',6,6'-tetrachloro-1,1',3,3'-tetraethylbenzimidazoyl carbocyanine iodide, Cell Technologies, Mountain View, Ca) is a lipophilic cationic dye that enters the inner mitochondrial matrix in its monomeric form when the mitochondrial membrane is polarized (Reers *et al*., 1991, 1995). Cells were treated with the indicated amounts of drugs either alone or in combination for 24 hrs. Cells were then washed with 1 x assay buffer and incubated for 15 min at 37 ºC with 1x JC1 reagent. In healthy cells the dye stains the mitochondria bright red. In the apoptotic cells, the mitochondrial membrane potential collapses and the JC1 reagent cannot accumulate within the mitochondria. In these cells JC1 remains in the cytoplasm in a green fluorescent monomeric form. The red form has absorption/emission maxima at 585/590 nm, while the green monomeric form has absorption/emission maxima at 510/527 nm. Cells were analyzed on FACSCalibur (Becton Dickinson, San Jose, CA) flow cytometer.

6.3. Results

6.3.1. Higher BER activity and proteins expression are intrinsic properties of CLL

Based on our previous studies showing that BER pathway is involved in response to fludarabine damage, we characterize the repair properties of CLL lymphocytes. The repair capacity of human CLL lymphocytes was evaluated in comparison with the activity of the normal lymphocytes or the activity of several types of human cancer cell lines. The enzymatic activity was determined by incubation of a specific BER substrate (synthetic 40 mer double-stranded oligonucleotide containing a deoxyuridine at the position 19) with cell extracts from these cells. Each sample was also subjected to western blot analysis and RT-PCR for protein expression and mRNA expression levels, respectively. As shown in Figure 6-1. A, the cell extracts from three different representative CLL samples had increased repair activity when compared with similar cell extracts from normal lymphocytes. The repair enzymatic activity was measured by incubation of the 40 mer double stranded oligonucleotide with 5 μg cell extracts for 30 min at 37 ºC, which resulted in a cleaved fragment visualized by 19 % polyacrylamide denaturing gel. In contrast, when the enzymatic activity of CLL cell extracts was evaluated in comparison with extracts from other human cancer cell lines (Figure 6-1. A), similar levels were observed by in vitro enzymatic assays. Moreover, western blot analysis for endogenous expression levels of UDG and APE, enzymes responsible for enzymatic activity shown, were used to determine whether the increased enzymatic activity correlates to increased protein expression. Untreated CLL or normal cells were lysate and subjected for western blot analysis for UDG. The protein levels were quantitated based on densitometric analysis and normalized to the β-actin levels. As

shown in Figure 6-1. B, primary CLL cells exhibited a significant higher UDG expression levels compared with normal lymphocytes. An example of the blots used in these studies is also presented. Further analysis revealed that elevated UDG in CLL cells was accompanied by less dramatic elevation in APE levels when compared with normal cells (Figure 6-1. C). Additionally, we determined the basal expression levels of nuclear transcript of UNG by RT-PCR analysis. As Figure 6-1. D shows, the transcript levels in primary CLL samples were more heterogeneous, the majority of the samples expressed higher levels of UNG transcripts, while few had lower expression when compared with normal lymphocytes. Among the population of normal cells, the expression of the transcripts was has uniform and low.

Figure 6-1

Higher BER proteins expression levels and activity in CLL samples

A, Cleavage of BER substrate (40 mer double-stranded oligonucleotide containing a deoxyuridine at the 19 position) by cell extracts from untreated CLL or normal donor lymphocytes. 5'-end labeled 40 mer oligonucleotides were incubated for 30 min, at 37 ºC with 5 μg of several cell extracts. The products of reaction were analyzed by electrophoresis on 19 % denaturating polyacrylamide gels. Comparison of BER enzymatic activities of tumor cells, CLL and normal lymphocytes. The cleaved products were obtained after oligonucleotide substrates were incubated with 5 μg cell extracts. ***B,*** Same cell lysates were subjected to Western blot analysis with UDG and APE specific antibodies. Elevated levels of both UDG and APE enzymes in lymphocytes from CLL samples compared with lymphocytes from healthy donors. ***C***, Quantification of UDG and APE basal protein expression levels in CLL samples versus normal samples. ***D***, Quantification of UNG mRNA basal levels in CLL versus ND samples, using RT-PCR analysis. Representative of three independent experiments.

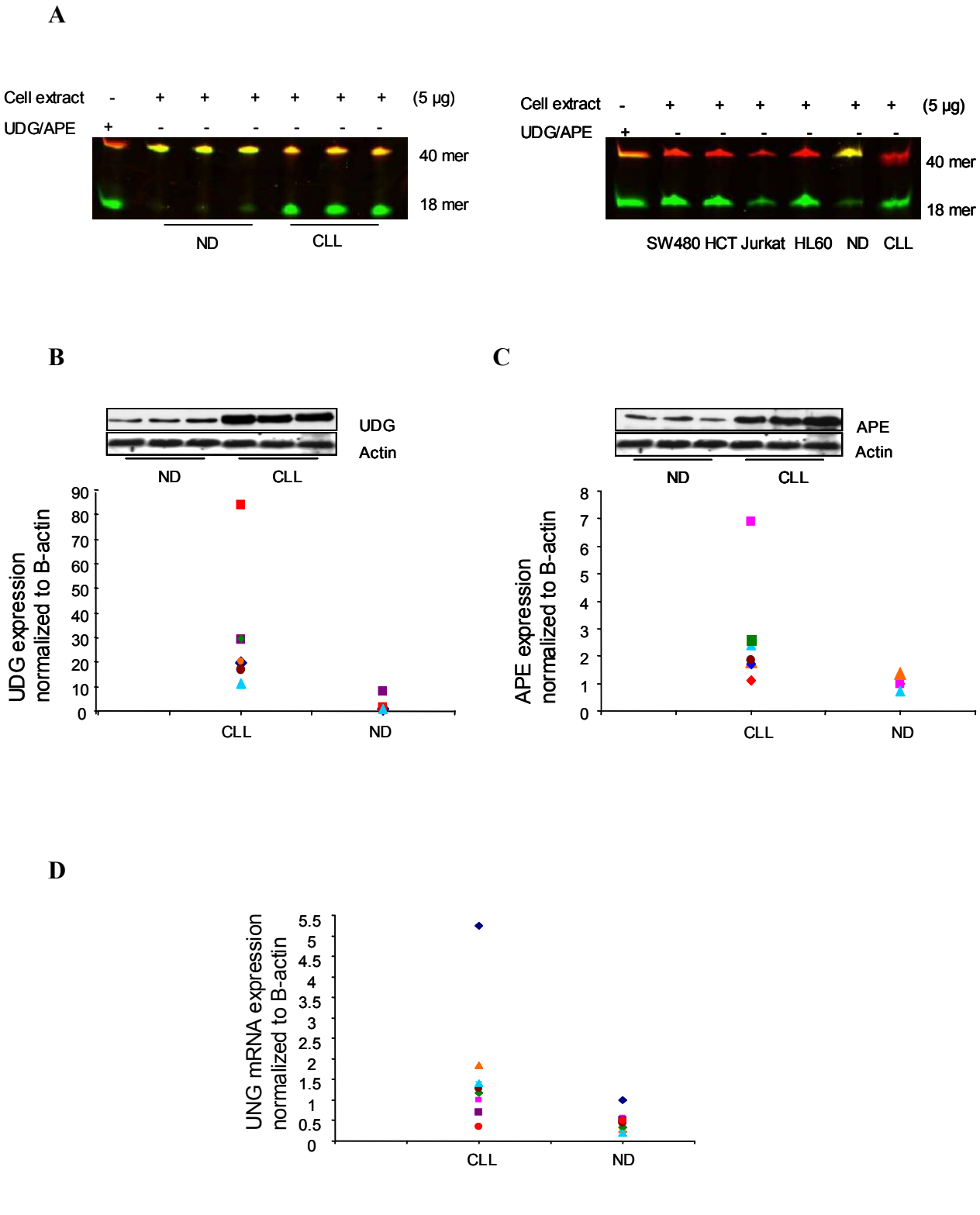
A
Cell extract - + + + + + + (5 µg)
UDG/APE + - - - - - -
40 mer
18 mer
ND CLL
Cell extract - + + + + + + (5 µg)
UDG/APE + - - - - - -
40 mer
18 mer
SW480 HCT Jurkat HL60 ND CLL
B
UDG
Actin
ND CLL
UDG expression normalized to B-actin
90 80 70 60 50 40 30 20 10 0
CLL ND
C
APE
Actin
ND CLL
APE expression normalized to B-actin
8 7 6 5 4 3 2 1 0
CLL ND
D
UNG mRNA expression normalized to B-actin
5.5 5 4.5 4 3.5 3 2.5 2 1.5 1 0.5 0
CLL ND

6.3.2. In fludarabine treatment of CLL lymphocytes, ara-AP sites are formed following BER activation and are bound by MX.

The promising observed difference in repair activity between CLL and normal lymphocytes led us to evaluate BER response in processing fludarabine residues by measuring the formation of arabinosyl (ara)-AP sites in CLL lymphocytes after drug treatments. We measured the ara-AP sites formed in cells using AP site assay based on the capacity of the aldehyde reactive probe reagent (ARP) to bind to the aldehyde free moiety of the AP site. Human lymphocytes were incubated with fludarabine in the presence or absence of MX. Total genomic DNA was isolated, labeled with ARP and analyzed. As shown in Figure 6-2. A, the number of ara-AP sites in DNA proportionally increased with the concentration and with the duration of exposure to fludarabine (Figure 6-2. B). Co-treatment with MX reduced detectable ara-AP sites generated by fludarabine. This reduction of ara-AP sites is presumably due to the binding of MX to the aldehyde group of the ara-AP site to form a MX-bound AP-sites (31, 36), thereby making the ara-AP sites unavailable for ARP. These results demonstrate that lymphocyte exposure to fludarabine initiates BER response.

Figure 6-2

Fludarabine induces ara-AP sites formation due to the presence of active BER pathway in CLL lymphocytes

A, The dose-dependent relationship between the numbers of ara-AP sites and the concentrations of fludarabine. CLL lymphocytes were treated with fludarabine alone (0-20 μM) or fludarabine plus MX (3 mM) for 24 hrs. Genomic DNA was extracted and ara-AP sites were measured using aldehyde reactive probe reagent (*, $p<0.05$). ***B***, The time-dependent relationship between the number of ara-AP sites and the time of exposure to fludarabine. CLL lymphocytes were treated with fludarabine alone (5 μM) or fludarabine plus MX (3 mM). Cells were collected at 24, 48 and 72 hrs treatments and ara-AP sites were measured using ARP. Data represents the mean of at least triplicate experiments.

A

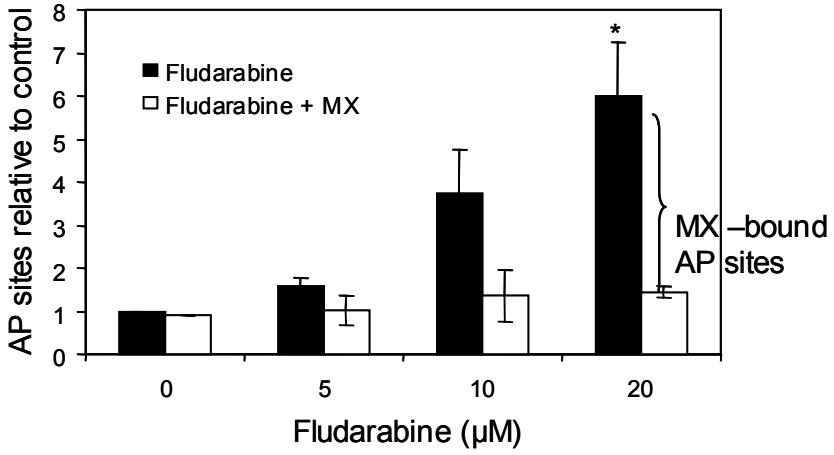
AP sites relative to control
8
7
6
5
4
3
2
1
0
Fludarabine
Fludarabine + MX
*
MX –bound
AP sites
0
5
10
20
Fludarabine (μM)

B

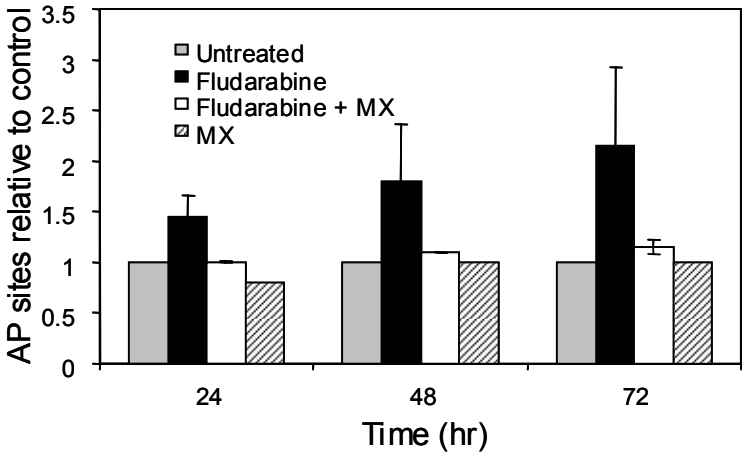
AP sites relative to control
3.5
3
2.5
2
1.5
1
0.5
0
Untreated
Fludarabine
Fludarabine + MX
MX
24
48
72
Time (hr)

6.3.3. BER proteins UDG and pol β are upregulated in CLL cells co-treated with fludarabine and MX

To further characterize the involvement of BER in the process of DNA damage induced by fludarabine or by the combination of fludarabine with MX, we subsequently evaluated the expression of BER proteins: UDG, APE, FEN1, pol β and PCNA in lymphocytes before and after drug treatment. UDG and pol β were up-regulated after exposure to either fludarabine alone or the combination. Still, a more significant elevation of these two proteins was observed in cells treated with fludarabine plus MX (Figure 6-3. A) and their up-regulation persisted over a period of 72 hrs. In contrast, APE levels did not change before and after drug treatment indicating that MX and MX-bond AP sites have no direct effect on APE. To investigate whether the induction of UDG protein levels is regulated at the transcriptional levels, a real time RT-PCR assay was used. CLL lymphocytes were treated with fludarabine alone (10 μM) or fludarabine plus MX (3 mM) for 24 hr. The RNA was isolated, cDNA was prepared and analyzed using TagMan MGB probes and RT-PCR amplification. The values obtained for the target gene were normalized to β-actin values (endogenous control) for each sample. Results presented in Figure 6-4 showed that at 24 hr, the UNG transcript levels were 2-3 folds increased after exposure of cells to combined treatments, when compared to fludarabine alone. The mechanism of BER proteins induction remains to be further elucidated; these results indicate that the BER pathway is targeted and activated as an adaptive response to the DNA damage formed by fludarabine and the combination in human CLL lymphocytes.

Figure 6-3

Induction of protein and mRNA expression of BER related enzymes as a response to fludarabine and MX combined treatment

CLL lymphocytes were continuously treated with fludarabine alone (5 μM) or fludarabine plus MX (3 mM) and collected at 24, 48 and 72 hrs. Cell lysates were subjected to Western blot analysis with UDG, polymerase β, APE1, Fen1, PCNA and tubulin specific antibodies. C = control, F = Fludarabine alone, F + M = Fludarabine plus MX; M = MX.

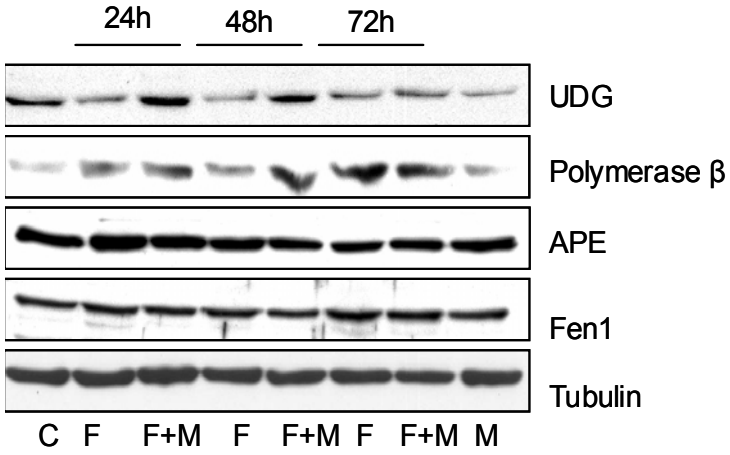
24h
48h
72h
UDG
Polymerase β
APE
Fen1
Tubulin
C F F+M F F+M F F+M M

Figure 6-4.

Induction of mRNA levels of nuclear isoform of UNG

A, CLL lymphocytes were continuously treated with fludarabine alone (10 μM) or fludarabine plus MX (3 mM) and collected at 24 hr. The RNA was isolated; cDNA was prepared and analyzed using TagMan MGB probes and RT-PCR amplification. The values obtained for the target gene were normalized to β-actin values (endogenous control) for each sample. UDG transcript level for each individual patient is presented. ***B,*** Average values.

A

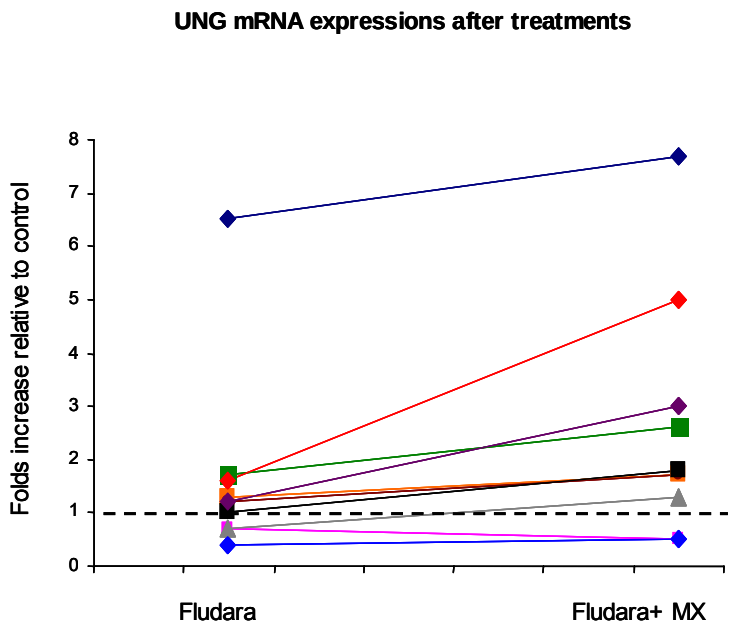
UNG mRNA expressions after treatments
Folds increase relative to control
8
7
6
5
4
3
2
1
0
Fludara
Fludara+ MX

B

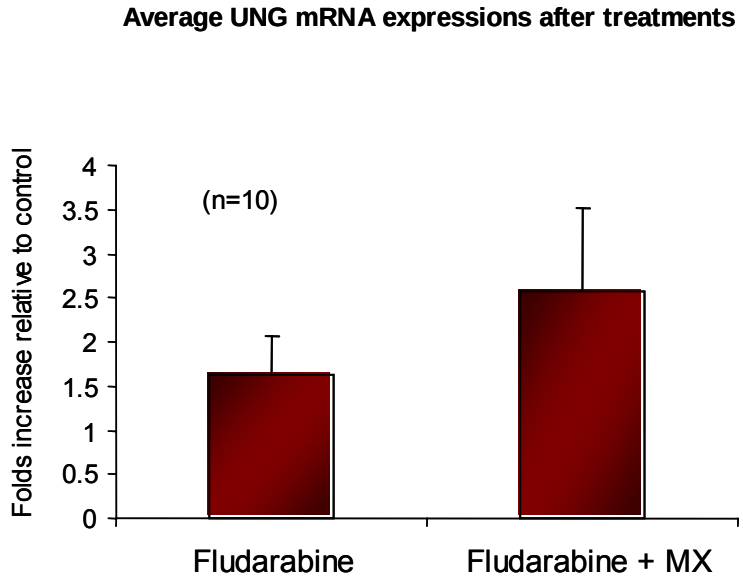
Average UNG mRNA expressions after treatments
Folds increase relative to control
4
3.5
3
2.5
2
1.5
1
0.5
0
(n=10)
Fludarabine
Fludarabine + MX

6.3.4. MX combined with fludarabine generates DNA strands breaks

We have shown previously that the combination of MX and fludarabine or alkylating agents such as BCNU or TMZ, increased DNA strand breaks in cancer cell lines, leading to cell death (31, 42-44). We used comet assay to asses the induction of DNA strand breaks by fludarabine or the combination with MX in CLL lymphocytes. DNA damage in a single cell was assayed by neutral electrophoresis to detect double strand breaks and representative Comet images are shown in Figure 6-5. A. When quiescent human lymphocytes were incubated for 24 hrs in the presence of various concentrations of fludarabine plus 3 mM MX, a dose dependent increase in the tail length was observed. In contrast, fludarabine alone at the same concentrations range (0-20 μM) had no significant effect on comet formation and tail length. The levels of strand breaks were evaluated by assessing tail lengths of at least 50 comets for each experimental regimen. Results showed that MX enhanced 2-4 folds the tail length when combined with fludarabine (Figure 6-5. B). In addition, time course treatments in the same experimental conditions were used to determine the persistence or the repair of strand breaks after either single agent (5 μM fludarabine, 3 mM MX) or combined treatments. As illustrated in Figure 6-5. C, the DNA damage induced by 5 μM fludarabine was minimal over a 72 hrs period. However, when cells were treated with fludarabine combined with MX, the comet tail length was significantly increased and it failed to recover (to control values) over 72 hr which suggests that MX suppressed any repair process of the fludarabine-induced DNA damage.

Figure 6-5

MX enhances fludarabine-induced DNA single and double strand breaks in CLL

***A*,** Comet images, neutral conditions. CLL lymphocytes were treated continuously with 5-20 μM fludarabine and /or fludarabine plus 3 mM MX for 24 hrs**. *B*,** Tail length of the comet formed in neutral electrophoresis after dose-dependent treatments with fludarabine alone (0-20 μM) and fludarabine plus MX (3 mM) ***C*,** Tail length of comet formed after continuously treatments with 5 μM fludarabine or fludarabine plus 3 mM MX for 24, 48 and 72 hrs. Data represent the mean of at least triplicate experiments, * $p<0.05$.

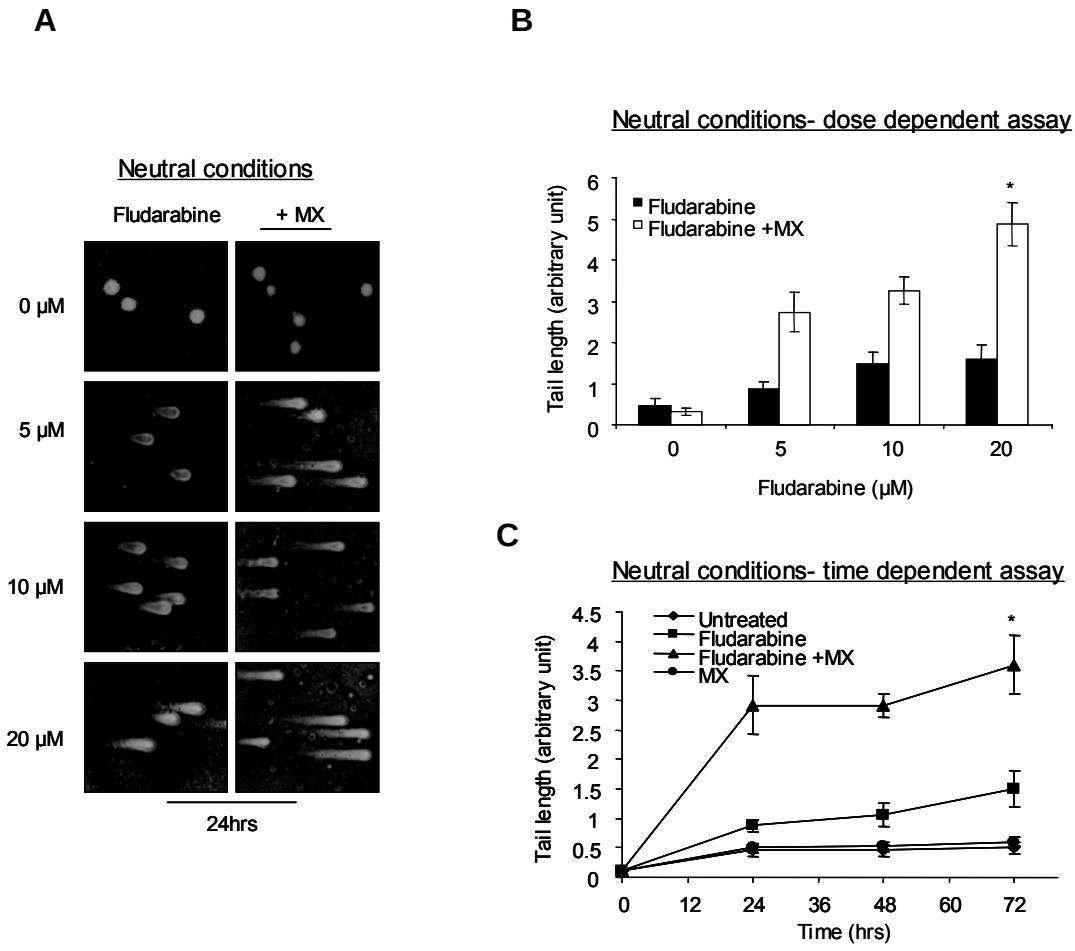
A
Neutral conditions
Fludarabine
+ MX
0 µM
5 µM
10 µM
20 µM
24hrs
B
Neutral conditions- dose dependent assay
Fludarabine
Fludarabine +MX
Tail length (arbitrary unit)
Fludarabine (µM)
C
Neutral conditions- time dependent assay
Untreated
Fludarabine
Fludarabine +MX
MX
Tail length (arbitrary unit)
Time (hrs)

6.3.5. Induction of Topoisomerase IIα levels correlates with CLL sensitivity to the combined treatments

One mechanism involved in the generation of double-strand breaks relies on the formation of MX-bound ara-AP sites refractory to BER that can act as topoisomerase poisons to stabilize the DNA-topoisomerase IIα cleavable complex. Thus, the endogenous and drug-related topoisomerase IIα (topo II) levels were measured. We compared the basal levels of protein expression and transcript in fresh CLL cells with that of normal lymphocytes obtained from healthy donors. As shown in Figure 6-6 A, the protein expression in all CLL lymphocytes was higher compared with normal cells. Moreover, analysis of the topo II transcript levels by RT-PCR revealed that higher protein expression is due to higher transcript levels, when compared with normal cells (Figure 6-6. B). These results are in agreement with our previously published data that there is a difference of 20 fold in topo II expression between primary cells and tumor cell lines. Next, the drug-related induction of topo II at the levels of protein expression and transcript were measured by Western Blot and RT-PCR analysis, respectively. As shown in Figure 6-6. C, prolong induction of topo II was seen in CLL lymphocytes over a period of 72 hr after exposure of cells with fludarabine plus MX, compared with treatment with fludarabine alone. We then examined the relationship between induced protein expression and the transcript levels in lymphocyte cells before and after drug treatments. The total RNA was extracted from CLL lymphocytes treated with either fludarabine alone or in combination with MX and topo II transcript levels were assayed by RT-PCR analysis. Results showed a 2-3 fold increase in topo II transcript levels after fludarabine plus MX treatments (Figure 6-7) in each sample tested.

To correlate the DNA strand breaks accompanied by induction of topo II with the killing effect determined by the drug treatments, cell death was assayed. Lymphocytes from CLL were treated with 5 μM fludarabine or fludarabine plus 3 mM MX and cells were counted every day using triptan blue exclusion. As shown in Figure 6-6. D, lymphocyte cells were sensitive to the combination of fludarabine and MX, MX enhancing fludarabine cytotoxicity by 2 fold.

Figure 6-6

MX enhances fludarabine induced cell death in CLL due to induction of Topoisomerase IIα levels

A, Comparison of the mRNA levels of topoisomerase IIα between human CLL lymphocytes and human normal lymphocytes, assayed by RT-PCR***. B,*** CLL lymphocytes were continuously treated with fludarabine alone (5 μM) or fludarabine plus MX (3 mM) and collected at 24, 48 and 72 hrs. Cell lysates were subjected to Western blot analysis with topoisomerase IIα and tubulin specific antibodies. C = control, F = Fludarabine alone, F + M = Fludarabine plus MX; M = MX. ***C,*** Comparison of the levels of topoisomerase IIα between human CLL lymphocytes and human normal lymphocytes, assayed by western bloting. Representative of three independent experiments. ***D,*** The CLL lymphocytes were treated with fludarabine (5 μM) and fludarabine plus MX (3 mM). Cell viability was determined by tryptan blue exclusion. Cell viability is expressed as percentage of untreated control. (* $p<0.05$).

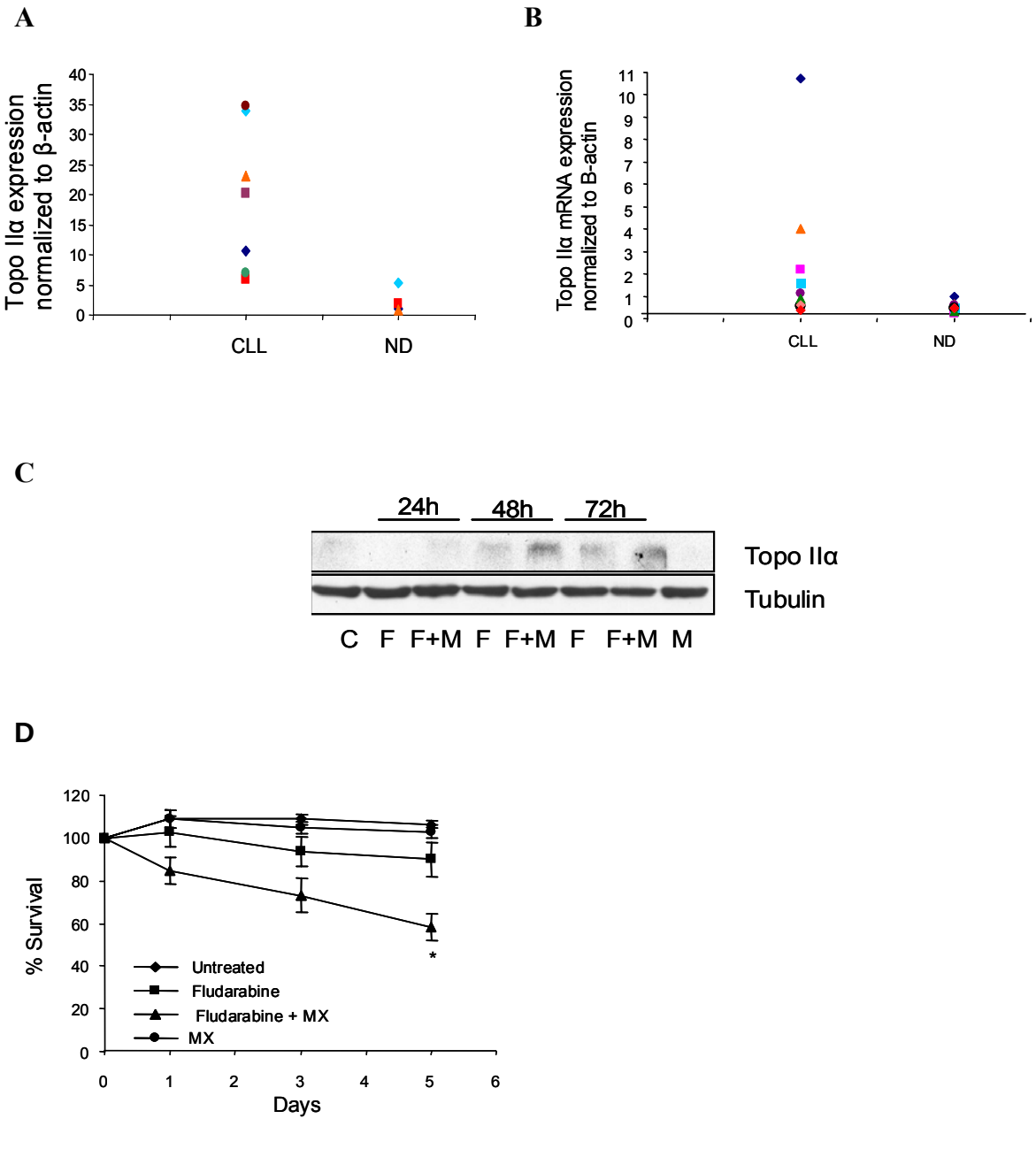
A
Topo IIα expression normalized to β-actin
40
35
30
25
20
15
10
5
0
CLL
ND
B
Topo IIα mRNA expression normalized to B-actin
11
10
9
8
7
6
5
4
3
2
1
0
CLL
ND
C
24h
48h
72h
Topo IIα
Tubulin
C F F+M F F+M F F+M M
D
% Survival
120
100
80
60
40
20
0
Untreated
Fludarabine
Fludarabine + MX
MX
*
0 1 2 3 4 5 6
Days

Figure 6-7. The Topo II mRNA expression after treatments.

A, CLL lymphocytes were continuously treated with fludarabine alone (10 μM) or fludarabine plus MX (3 mM) and collected at 24 hr. The RNA was isolated, cDNA was prepared and analyzed using TagMan MGB probes and RT-PCR amplification. The values obtained for the target gene were normalized to β-actin values (endogenous control) for each sample. Topo IIα transcript level for each individual patient is presented. ***B,*** Average values.

A

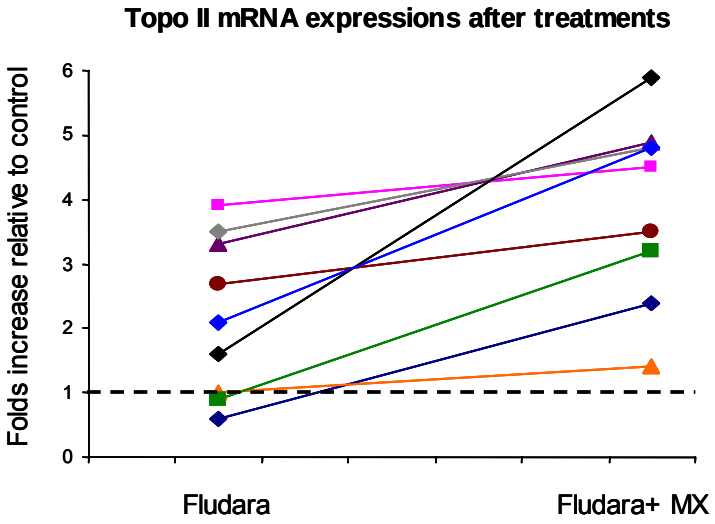
Topo II mRNA expressions after treatments
Folds increase relative to control
0
1
2
3
4
5
6
Fludara
Fludara+ MX

B

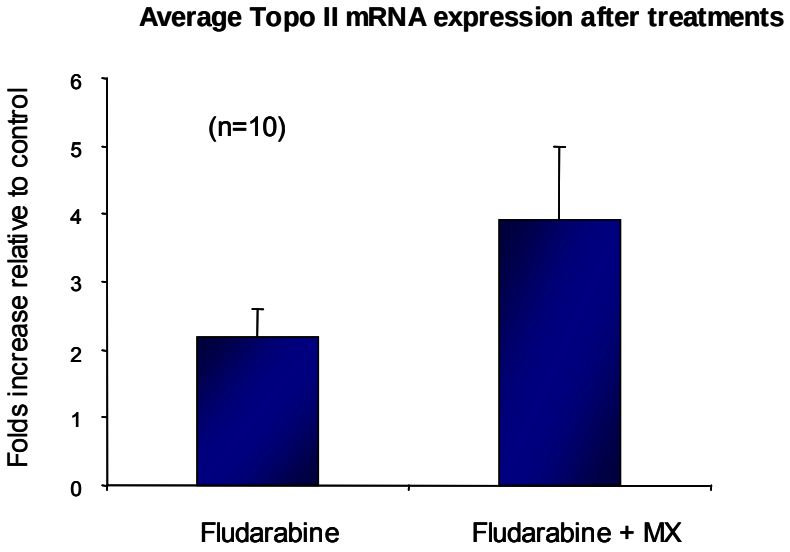
Average Topo II mRNA expression after treatments
Folds increase relative to control
(n=10)
0
1
2
3
4
5
6
Fludarabine
Fludarabine + MX

6.3.6. MX blocks the repair of Fludarabine-induced mitochondrial DNA damage and leads to mitochondrial mediated apoptosis

Since mitochondrial DNA (mtDNA) is potentially targeted by fludarabine, the effects of fludarabine alone and the combination with MX were determined at the levels of mtDNA. CLL lymphocytes were exposed to increased fludarabine concentrations, ranging from 0 to 20 μM for 24 hrs. MtDNA was extracted and mtAP-sites were quantitated using ARP reagent. As shown in Figure 6-8. A, increased drug concentrations resulted in proportionally higher levels of mtAP-sites ($r = 0.971$). This suggests that fludarabine targets mtDNA and that the induced damage is processed by the mitochondrial repair pathway. However, when cells were treated with fludarabine and methoxyamine (3 mM) detectable AP sites were reduced almost to the control levels due to binding of MX. This suggests that MX is able to bind not only nuclear, but also mitochondrial AP sites. The large extent of persistent fludarabine-induced nuclear and mitochondrial DNA damage due to MX suggests that MX-AP sites are key DNA lesions which potentiate the apoptotic death of fludarabine. Thus, apoptosis was assayed. Exposure of cells to fludarabine alone (0- 20 μM) for 24 hrs resulted in a modest degree of apoptosis (6 % increase over control values at 20 μM). However, combination of fludarabine with MX for 24 hrs resulted in a 2-fold increase in apoptosis (14 % at 20 μM) (Figure 6-8. B). Similar potentiation of apoptosis by MX was seen in a time course analysis (data not shown). To further determine the role of mitochondria in apoptosis mechanism, we measured treatment-mediated changes in mitochondrial membrane $\Delta\Psi m$ using fluorescent mitochondrial probe JC-1. Time course response analysis of CLL lymphocytes treated with 5 μM fludarabine revealed that the percentage of cells which

lost their mitochondrial membrane integrity and, subsequently, their ability to accumulate JC1 dye increased from 7 % at 24 hrs to 30 % at 72 hrs (Figure 6-8. C). When cells were co-treated with MX the percentage of cells with damaged mitochondria increased to 29 % at 24 hrs and to 42 % at 72 hrs, respectively. Moreover, the results were confirmed by western blot analysis for mitochondrial related apoptotic proteins. As shown in Figure 6-6. D, combined treatment resulted in a very clear induction of pro-apoptotic protein Bax at 24 hrs and lasted for at least 72 hrs. Since a key marker of mitochondrial apoptotic cascade is the activation of caspase 9 by proteolytic cleavage, we examined the levels of the cleaved fragment (Figure 6-8. D). Cleaved caspase 9 was observed at 48 hrs and 72 hrs after treatment with fludarabine alone or fludarabine plus MX. However, in fludarabine plus MX treatments caspase 9 cleavage was ~2-fold greater than in cells treated with fludarabine alone. Similar results were obtained for another marker of the apoptotic cascade, the proteolytic cleavage of PARP by caspases (Figure 6-6. D). No changes were observed in the expression levels of Bcl2, an anti-apoptotic molecule. Together, these results demonstrate that MX potentiates fludarabine *in vitro*. Results also demonstrate that fludarabine induced ara-AP sites in mitochondrial DNA and they suggest that the mtDNA damage could play a significant role in mediating activation of apoptosis and cell death following fludarabine treatments.

Figure 6-8

Mitochondrial DNA damage and activation of mitochondrial-mediated cell death

A, The dose–dependent relationship between the numbers of mitochondrial ara-AP sites and the concentrations of fludarabine. CLL cells were continuously treated with fludarabine alone (0-20 μM) or fludarabine plus MX (3 mM). Mitochondrial DNA was extracted and ara-AP sites were measured using aldehyde reactive probe reagent. (*, $p<0.05$). ***B***, Induction of apoptosis by the combined treatment fludarabine and methoxyamine. CLL lymphocytes were continuously treated with fludarabine alone (5 μM) or fludarabine plus MX (3 mM), collected at 24 hrs and assayed for apoptosis by Annexin V staining and flow cytometry analysis. ***C,*** Increased mitochondrial membrane potential loss measured in cells treated with combined agents for 24 hrs. ***D***, Aliquots of the samples used in ***B*** were subjected to Western blot analysis with Bcl2, Bax, Cleaved caspases 9, Cleaved PARP and tubulin specific antibodies. Control (lane 1), fludarabine alone (lane 2,4,6) and fludarabine plus MX lanes (3,5.7), MX alone (lane 8). Representative of three independent experiments.

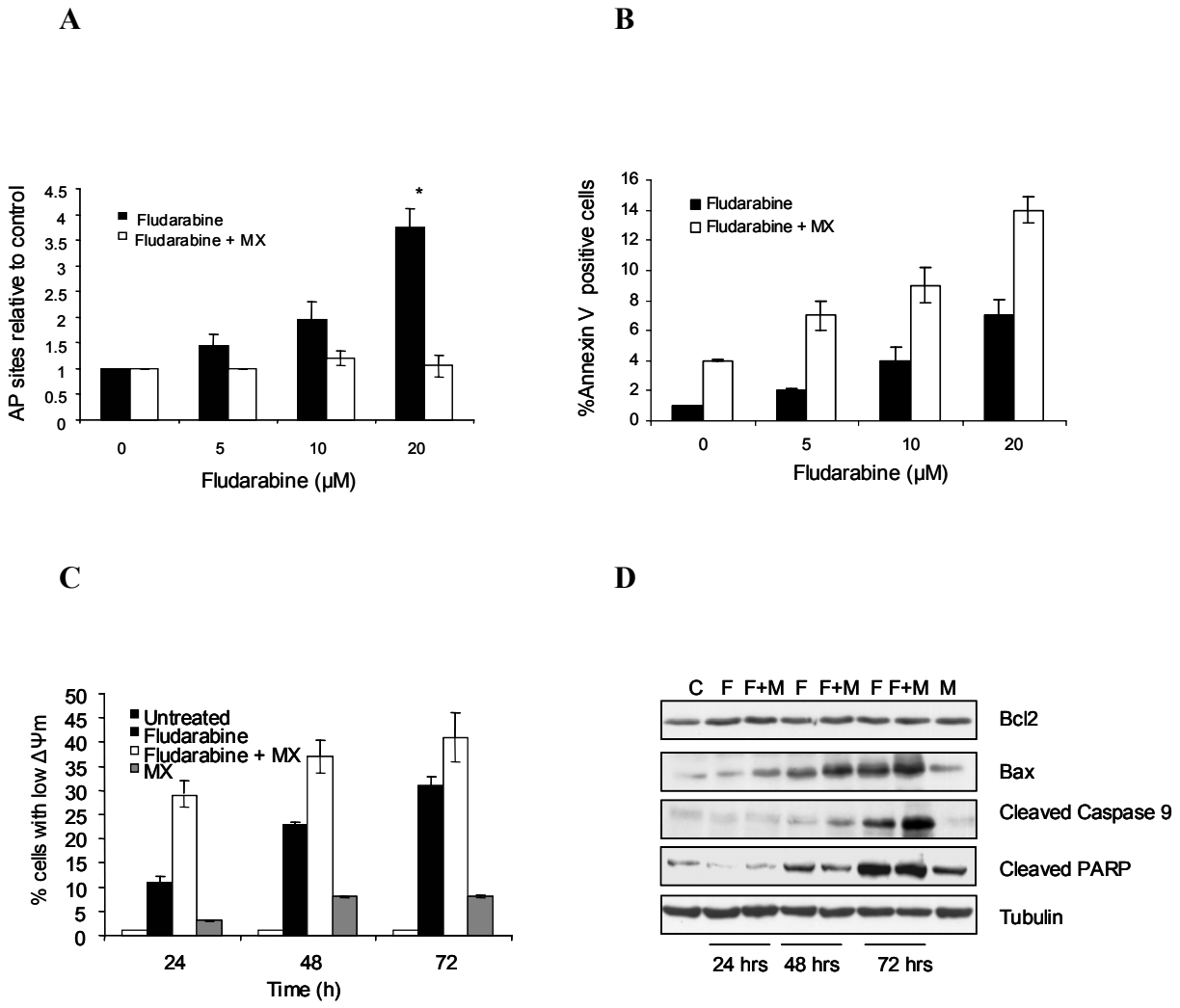
A
B
AP sites relative to control
Fludarabine
Fludarabine + MX
*
Fludarabine (μM)
%Annexin V positive cells
C
D
% cells with low ΔΨm
Untreated
Fludarabine
Fludarabine + MX
MX
Time (h)
C F F+M F F+M F F+M M
Bcl2
Bax
Cleaved Caspase 9
Cleaved PARP
Tubulin
24 hrs
48 hrs
72 hrs

6.4. Discussion

Base excision repair is a major repair pathway that corrects DNA modifications arising either spontaneously or after attack by exogenous DNA damaging factors, such as certain cancer therapies. An efficient BER can reverse the DNA damage caused by therapeutic agents leading to development of resistance. However, BER therapeutic implications have been evaluated by several targeted approaches, such as blocking of the repair pathway by methoxyamine (MX) or PARP-inhibitors (48). In this study we underlined the possibility of exploiting BER pathway in primary CLL lymphocytes as a basis for targeted combinatory therapy involving standard therapeutic agent, fludarabine. This conclusion is based on several lines of evidence. (i) The primary lymphocytes isolated from CLL patients exhibited higher BER proteins expressions and increased BER activity when compared to normal lymphocytes. (ii) BER involvement in response to fludarabine-induced damage was confirmed by generation of ara-AP sites. (iii) Ara-AP sites formed by fludarabine were bound by MX leading to induction of protein levels of key BER proteins and resulted in DNA strand beaks and cell death. (iv) Mitochondrial DNA was found to be a target of fludarabine and MX that triggers mitochondrial mediated apoptosis following disruption of mitochondrial BER.

Fludarabine-induced cytotoxicity is enhanced when active BER pathway in primary CLL is inhibited by MX.

BER is more active in CLL compared with normal lymphocytes. BER is an important factor in cancer treatment based on several considerations: drug efficacy is influenced by the efficiency of repair pathway, increased levels of DNA repair proteins have been correlated with resistance to anticancer agents acting as DNA-damaging agents and

understanding the repair pathway have made it potentially 'druggable' target for the enhanced anti-tumor activity of DNA-damaging agents (48). Based on our previous studies (Chapter 3, Chapter 4), two BER proteins have been shown to play an important role in response to fludarabine induced damage: UDG and APE. When comparing the basal levels of these proteins along with their activity on specific BER substrates, the results showed a clear, significant difference: both proteins have higher expression levels and activity in CLL cells, compared with normal lymphocytes. In contrast, the protein expression pattern in CLL samples is similar with the ones measured in other human cancer cells. Although more studies are needed, these findings suggest a possible mechanism of resistance of CLL lymphocytes toward fludarabine and set the stage for potential combinatory therapy to reduce the development of resistance to fludarabine. Additionally, based on this difference between the normal and tumor primary cells, targeting BER may be a selective approach to enhance fludarabine potency with lower toxicity toward normal tissue. Furthermore, the intrinsic higher level of expression of BER proteins may play a role in the limited sensitivity of CLL for fludarabine.

MX stabilizes ara-AP sites induced by fludarabine. Intermediates in BER, AP-sites are formed as a consequence of the removal of modified bases by DNA glycosylases, the first step in BER pathway. We have previously identified (Chapter 3 and Chapter 4) that uracil DNA glycosylase plays a role in processing of incorporated fludarabine leading to formation of ara-AP sites (21). In the present study, we report that fludarabine treatment of lymphocytes from CLL samples resulted in a dose- and time- dependent formation of ara-AP sites, suggesting that the repair pathway is involved in response of lymphocytes to fludarabine-induced DNA damage. Also, our results confirmed that non-toxic doses of

MX are sufficient for effective binding of the ara-AP sites formed by fludarabine. BER involvement in response to MX plus fludarabine treatments of CLL was also confirmed by increased expression levels of UDG and polymerase β.

MX-bound AP-sites generate double strand breaks and cell death. Formation of MX-bound AP-sites following treatment with fludarabine and MX resulted in double strand breaks and cell death. This increase in double stranded breaks can be explained by previous data from our laboratory demonstrating that AP sites can act as topoisomerase II poisons, trapping the protein into stabilized cleavable complexes (31). Indeed, formation of MX-bound AP-sites was accompanied by higher expression levels of topo II in CLL cells supporting the above mentioned scenario.

Fludarabine and MX treatment triggers mitochondrial mediated apoptotic cell death in CLL cells. To determine the mechanism of apoptotic cell death, we focused on mitochondrial involvement in this process. MtDNA is more prone to cytotoxic damage due to several factors such as lack of protective histone, production of reactive oxygen species and limited repair capacities (41,43). Recent studies showed that BER pathway is the predominant repair pathway in mitochondria (42). Thus, we measured the formation of ara-AP sites in mtDNA after exposure to fludarabine. Data have shown that mitochondrial ara-AP sites formation is in dose dependent fashion and that MX binds these ara-AP sites, thereby blocking the BER pathway in mitochondria. The level of mtDNA damage eventually becomes severe, mitochondria lose their ability to maintain the membrane potential and activate mitochondrial apoptotic death pathway.

These results suggest a possible synergistic approach for enhancing fludarabine cancer therapy that involves disruption of base excision repair in CLL lymphocytes. This

therapeutic strategy could improve both therapeutic index by decreasing the dose of anticancer drugs and therapeutic efficacy for the treatment of hematological malignancies.

6.5. References

1. Bosch F, Montserrat E. Refining prognostic factors in chronic lymphocytic leukemia. Rev Clin Exp Hematol, 6:335-349, 2002.

2. Lee JS, Dixon DO, Kantarjian HM, Keating MJ, Talpaz M. Prognosis of chronic lymphocytic leukemia: a multivariante regression analysis of 325 untreated patients. Blood 69: 929-936, 1987.

3. Byrd JC, Murphy T, Howard RS Lucas MS, Goodrich A, Park K, Pearson M, Waselenko JK, Ling G, Grever MR, Grillo-Lopez AJ, Rosenberg J, Kunkel L, Flinn IW. Rituximab using a thrice weekly dosing schedule in B-cell chronic lymphocytic leukemia and small lymphocytic lymphoma demonstrates clinical activity and acceptable toxicity. J Clin Oncol 19: 2153-2164, 2001.Zhu Q, Tan DC, Samuel M, Chan ES, Linn YC. Fludarabine in comparison to alkylator-based regimen as induction therapy for chronic lymphocytic leukemia: a systematic review and meta-analysis. Leuk Lymphoma 45: 2239-2245, 2004.

4. Keating MJ, Flinn I, Jain V, Binnet JL, Hillmen P, Byrd J, Albitar M, Brettman L, Snatabarbara P, Wacker B, Rai KR. Therapeutic role of alemtuzumab (Campath-1H) in patients who have failed fludarabine: results of a large International Study. Blood 99: 3554-3561, 2002.

5. Kay NE. Purine analogue-based chemotherapy regimens for patients with previously untreated B-chronic lymphocytic leukemia. Semin Hematol, 43: S50-S54, 2006.

6. Bellosillo B, Villamor N, Colomer D, Pons G, Monsserrat E, Gil J. In vitro evaluation of fludarabine in combination with cyclophosphamide and/or mitoxantrone in B-cell chronic lymphocytic leukemia . Blood 94: 2836-2843, 1999.

7. Koehl U, Li L, Nowak B. Fludarabine and cyclophosphamide:synergistic cytotoxicity associated with inhibition of interstrand crosslink removal. Proc Am Assoc Cancer Res 38:2, 1997.

8. Seymour JF, Huang P, Plunkett W, Gandhi V. Influence of fludarabine on pharmacokinetics and pharmacodynamics of cytarabine: implication for continuous infusion schedule. Clin Cancer Res 2: 653-658, 1996.

9. Rayappa C, McCulloch EA. A cell culture model for the treatment of acute myeloblastic leukemia with fludarabine and cytosine arabinose. Leukemia 7: 992-999, 1993.

10. Yang LY, Li L, Keating MJ, Plunkett W. Arabinosyl-2-fluoroadenine augments cisplatin cytotoxicity and inhibits cisplatin –DNA cross-link repair. Mol Pharmacol, 47: 1072-1079, 1995.

11. Zaffaroni N, Orladi L, Gornati D, De Marco C, Vaglini M, Silvestrini R. Fludarabine as a modulator of cisplatin activity in human tumor primary cultures and established cell line. Eur J Cancer 32A: 1766-1773, 1996.

12. Ross SR, McTavish D, Faulds D. Fludarabine: a review of its pharmacological properties and therapeutic potential in malignancies. Drugs 45: 737-759, 1993.

13. Plunkett W, Gandhi V, Huang P, Robertson LE, Yang LY, Gregoire V et al. Fludarabine: pharmacokinetics, mechanism of action and rationales for combination therapy. Semin Oncol 20: 2-12, 1993.

14. Gandhi V, Plunkett W. Cellular and clinical pharmacology of Fludarabine. Clin Pharmacokinet; 41:93-103, 2002.

15. Gandhi V, Huang P, Chapman AJ, Chen F, Plunkett W. Incorporation of fludarabine and 1-beta-D-arabinofuranosylcytosine 5'-triphosphates by DNA polymerase alpha: affinity, interaction, and consequences. Clin Cancer Res.3(8):1347-551997

16. Kamiya K, Huang P, Plunkett W. Inhibition of the 3'-5' exonuclease of human DNA polymerase ε by fludarabine-terminated DNA. J of Biolog Chemistry; 271:19428-35, 1996.

17. Skalski V, Brown KR, Choi BY, Lin ZY, Chen S. A 3'-5' exonuclease in human leukemia cells. J Biol Chem; 275:23814-19, 2000.

18. Yang SW, Huang P, Plunkett W, Becker F, Chan JYH. Dual mode of inhibition of purified DNA ligase I from human cells by 9-β-D-Arabinofuranosyl-2-fluoroadenine triphosphate. J Biol Chem; 267:2345-9, 1992.

19. Huang P, Plunkett W. Fludarabine and gemcitabine induced apoptosis: incorporation of analogs into DNA is a critical event. Cancer Chem Pharmacol 36: 181-188, 1995.

20. Bulgar A, Snell M, Donze JR, Kirkland E, Li L, Xu Y, Gerson SL, Liu L. UDG is a major DNA glycosylase having activity on F:T mispairs: Identifying a new target for fludarabine. Cancer Res, 2008

21. Srivastava DK, Berg BJV, Prasad R, et al. Mammalian abasic site base excision repair. J Biol Chem; 273:21203-9, 1998.

22. Fortini P, Parlanti E, Sidorkina OM, Laval J, Dogliotti E. The type of DNA glycosylase determines the base excision repair pathway in mammalian cells. J Biol Chem; 274:15230-6, 1999.

23. Sokhansanj B, Rodigue GR, Fitch JP, Wilson DM. A quantitative model of human DNA base excision repair. I. mechanistic insights. Nucleic Acids Research; 30:1817-25, 2002.

24. Hoeijmakers. Genome maintenance mechanisms for preventing cancer. JNJ Nature; 411:366-74, 2001.

25. Matray T and Kool ET. A specific partner for abasic damage in DNA. Nature; 399:7047, 1999.

26. Wilson SH. Mammalian base excision repair and DNA polymerase beta. Mutation Res; 407:203-15, 1998.

27. Liuzzi M, Talpeart-Borle, M. A new approach to study of the base excision repair pathway using methoxyamine. J Biolg Chem; 260:5252-58, 1985.

28. Rosa S, Fortini P, Bignami M, Dogliotti E. Processing in vitro of an abasic site reacted with methoxyamine: A new assay for the detection of abasic sites formed in vivo. Nucleic Acids Res; 19:5569-74, 1991.

29. Liu L, Gerson SL. Therapeutic impact of methoxyamine: Blocking repair of abasic sites in the base excision repair pathway. Current Opinion in investigational Drug; 5:623-7, 2004.

30. Ling Y, Bulgar A, Miao YL, et al. Combined treatment with temozolomide and methoxyamine: blocking apurinic/pyrimidinic site repair coupled with targeting topoisomerase IIα. Clin Cancer Res; 13:1532-9, 2007.

31. Liu L, Gerson SL. Base excision repair as a therapeutic target in colon cancer. Clin CancerRes; 8:2985-91, 2002.

32. Liu L, Taverna P, Whitacre CM, Chatterjee S, Gerson SL. Pharmacological disruption of base excision repair sensitizes mismatch repair deficient and proficient colon cancer cells to methylating agents. Clin Cancer Res; 5:2908-17, 1999.

33. Liu L, Yan L, Donze JR, Gerson SL. Blockage of abasic site repair enhances antitumor efficacy of 1,3-bis-(2-chloroethyl)-1-nitrosourea in colon tumor xenografts. Mol Cancer Ther; 2:1061-6, 2003.

34. Taverna P, Hwang HS, Schupp JE, et al. Inhibition of base excision repair potentiates iododeoxyuridine cytotoxicity and radiosensitization. Cancer Res; 63:838-46, 2003.

35. Yan T, Seo Y, Schupp JE, Zeng X, Desai A, Kinsella T. Methoxyamine potentiates iododeoxyuridine-induced radiosensitization by altering cell cycle kinetics and enhancing senescence. Molec Cancer Therap 5: 893-902, 2006.

36. Taverna P, Liu L, Hwang HS, Hanson A, Kinsella T, Gerson SL. Methoxyamine potentiates DNA single strand breaks and double strand breaks induced by temozolomide in colon cancer cells. Mutation Res; 485:269-81, 2001.

37. Fishel ML, He Y, Smith ML, Kelley MR. Manipulation of base excision repair to sensitize ovarian cancer cells to alkylating agent temozolomide. Clin cancer Res; 13:260-7, 2007.

38. Rinne M, Cladwell D, Kelley MR. Transient adenoviral N-methylpurine DNA glycosylase overexpression imparts chemotherapeutic sensitivity to human breast cancer cells. Mol Cancer Ther 3:955-67, 2004;.

39. De Totero D, Tazzari PL, Capaia M, Montera MP, Clavio M, Balleari E, Foa R, Gobbi M CD40 triggering enhances fludarabine-induced apoptosis of chronic lymphocytic leukemia B-cells through autocrine release of tumor necrosis factor-alpha and interferon-

gama and tumor necrosis factor receptor-I-II upregulation. Haematologica, 88:142-158, 2003.

40. Yakes F. M.a.B. V. H. Mitochondrial DNA damage is more extensive and persists longer than nuclear DNA damage in human cells following oxidative stress.. Proc. Natl. Acad. Sci. USA, *94:* 514-519, 1997.

41. LeDoux S. P., Wilson G. L., Beecham E. J., Stevnsner T., Wassermann K., Bohr V. A. Repair of mitochondrial DNA after various types of DNA damage in Chinese hamster ovary cells. Carcinogenesis (Lond.), 13*:* 1967-1973, 1992.

42. Zastawny T. H., Dabrowska M., Jaskolski T., Klimarczyk M., Kulinski L., Koszela A., Szczesniewicz M., Sliwinska M., Witkowski P., Olinski R. Comparison of oxidative base damage in mitochondrial and nuclear DNA. Free Radic. Biol. Med., 24*:* 722-725, 1998.

43. Nakamura J, Swenberg JA. Endogenous apurinic/apyrimidinic sites in genomic DNA of mammalian tissues. Cancer Res; 59:2522-6, 1999.

44. Nakamura J, Walker VE, Upton PB, Chiang SY, Kow YW, Swenberg JA. Highly sensitive apurinic/apyrimidinic site assay can detect spontaneous and chemically induced depurination under physiological conditions. Cancer Res; 58:222-5, 1998.

45. Atamna H, Cheung I, Ames BN. A method for detecting abasic sites in living cells: agedependent changes in base excision repair. Proc Natl Acad Sci U S A; 97:686-92, 2000.

46. Helma, C. Uhl M. A public domain image-analysis program for the single cell-gel-electrophoresis (comet) assay. Mutat Res; 66:9-15, 2004.

47. Damia G, D'Incalci M. Targeting DNA repair as a promising approach in cancer therapy. European J of Cancer. 43: 1791-1801, 2007.

48. Durig J, Ebeling P, Grabellus F at el. A novel nonobese diabetic/severe combined immunodeficient xenograft model for chronic lymphocytic leukemia reflects important clinical characteristics of the disease. Cancer Res. 2007, 67: 8653-8661.

CHAPTER VII

SUMMARY AND FUTURE DIRECTIONS

The work presented here focused on investigating the involvement of BER pathway in the response to fludarabine induced DNA damage and the possibility of enhancing antineoplastic activity of fludarabine by inhibition of BER (e.g. methoxyamine). Key findings of this research include:

(i) Uracil DNA glycosylase is the BER enzyme responsible for recognition and removal of fludarabine incorporated into DNA strand, triggering activation of BER pathway and subsequent formation of ara-AP sites.

(ii) By completion of BER, the cytotoxic potential of fludarabine is diminished, suggesting a possible mechanism of resistance.

(iii) MX, an inhibitor of BER, enhances fludarabine cytotoxicity through its ability to bind to fludarabine-induced ara-AP sites; new MX-bound AP-sites formed are resistant to BER action and the blockage of BER increases cell death in vitro and in human xenografts.

(iv) Mitochondrial DNA is a target of fludarabine plus MX; inhibition of mtBER leads to accumulation of mtDNA damage that will eventually result in mitochondrial mediated apoptotic cell death.

(v) MX potentiates the antineoplastic activity of fludarabine in primary CLL lymphocytes, setting the stage for the development a novel therapeutic strategy by combining the inhibitor of BER (MX) with fludarabine.

The chart in next page outlines the connection between the main results presented in this thesis, results which also set up the basis for future investigations.

Figure 7-1. Conclusions

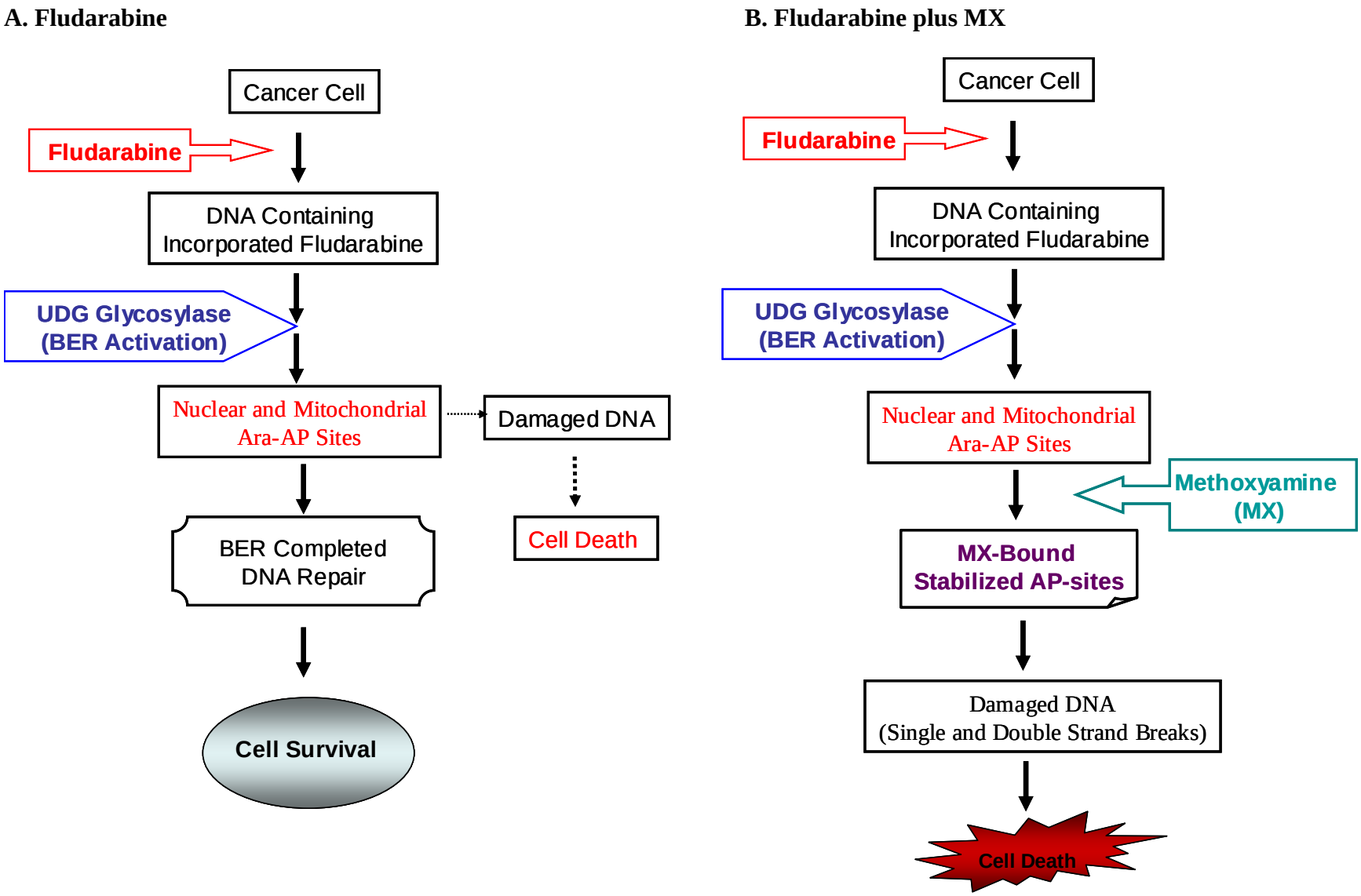

Future efforts will be directed toward three main focus areas:

(i) Uracil DNA glycosylase and other BER glycosylases.

Investigations involving crystal structure of human UDG bound to DNA containing F-ara-A should help elucidating the mechanism by which UDG recognizes and removes fludarabine base from DNA helix and establishing the specific role of the fluorine substitute in the biochemical mechanism of the enzymatic reaction.

Studies aimed to understand "if and how" the localization of incorporated fludarabine (in-DNA-strand vs. at-3'-DNA-end) is important for UDG activity will be carried out, starting with oligonucleotide substrates containing fludarabine at different positions and *in vitro* tests.

(ii) Mitochondrial involvement in the apoptotic cell death.

Detection of early apoptotic events is of crucial importance. To understand more precisely the sequential steps in fludarabine-induced apoptosis, we will continue the studies presented in Chapter 5, where we have shown that not only nuclear DNA, but also mtDNA is a target for fludarabine. Next question: Is the mitochondrial DNA damage prevailing in signaling for apoptosis?

iii) Translating the preclinical data into clinical use.

As underlined in Chapter 6, preliminary studies using primary CLL cells have shown promising results regarding the therapeutic potential of the combination fludarabine plus MX. Thus, we will aim to include this combination into clinical application. While the path toward implementing a new therapy is a very long and complex endeavor, small but well coordinated steps and perseverance are some of the necessary ingredients for success.